

AN ASSESSMENT OF MICROCLIMATES IN SOUTHERN ONTARIO: THE
APPLICATION OF THE LOCAL CLIMATE ZONE METHOD IN TORONTO AND THE
SURROUNDING REGION.

By

E. Jerome Price-Todd, Hon BSc, University of Toronto, 2013

A thesis presented to Ryerson University

in partial fulfillment of the

requirements for the degree of

Master of Applied Science

in the program of

Environmental Applied Science and Management

Toronto, Ontario, Canada, 2015

© E. Jerome Price-Todd 2015

AUTHOR'S DECLARATION FOR ELECTRONIC SUBMISSION OF A THESIS

I hereby declare that I am the sole author of this thesis. This is a true copy of the thesis, including any required final revisions, as accepted by my examiners.

I authorize Ryerson University to lend this thesis to other institutions or individuals for the purpose of scholarly research.

I further authorize Ryerson University to reproduce this thesis by photocopying or by other means, in total or in part, at the request of other institutions or individuals for the purpose of scholarly research.

I understand that my thesis may be made electronically available to the public.

An Assessment of Microclimates in Southern Ontario: The application of the Local Climate
Zone method in Toronto and the surrounding region

Master of Applied Science, 2015

E. Jerome Price-Todd

Environmental Applied Science and Management, Ryerson University

Abstract

The Golden Horseshoe is a densely populated area in southern Ontario and the population is expected to grow to 11.5 million residents by 2031. The urbanization process will likely intensify due to the current and expected population growth. The urban heat island (UHI) effect at 19 meteorological stations in southern Ontario were assessed using climate normals from 1981-2010 and the local climate zone (LCZ) method. The stations were assigned an LCZ unit based upon their calculated impervious, pervious and building surface fractions. It was found that areas representing higher urban-centric zones had higher UHI intensities (LCZ 5 with 2 K) than areas that were less urban-centric (LCZ 9 with 1.12 K and LCZ 6 with 1.37 K) revealing a continuum of “urbanicity”. The LCZ method provided greater objectivity when calculating the UHI intensity than the simpler method of an urban / rural dichotomy. With expected warming and population growth in the area the detrimental human health, environmental and economic impacts associated with the UHI effect should be given consideration for any future planning and decision making.

Acknowledgements

First I would like to acknowledge the importance of open data and data collection programs from the City of Toronto, Environment Canada and DMTI Spatial Inc. because without their sharing of data none of this research could have taken place.

I would like to thank Ryerson University and Dr. Doug Banting for their financial support which allowed me to complete my graduate work. I would like to thank the members of my committee, Dr. Claire Oswald and Dr. Andrew Millward for taking the time to be my readers and Dr. Cory Searcy for acting as chair. Their input was greatly appreciated and helped me improve on the final version of this thesis.

I would like to thank my friends and family for their continued support and patience throughout my graduate studies. I would like to especially thank my parents and siblings, Elmo, Cheryl, Will, Linda and David for their continued support and encouragement throughout my academic career. I would also like to thank Catherine and Dominic for their support and encouragement and Zoltan for helping me organize some of my data by using his impressive coding abilities. Lastly I would like to thank Amanda and Ender. Thank you for taking this journey with me. I am very lucky to have you in my life and I am thankful that you were with me every step of the way.

Finally, I would like to express my sincerest gratitude to my advisor Dr. Doug Banting. His willingness to share his knowledge and expertise is much appreciated. His many wonderful tangents put my research into a context that I could not have imagined. His reflections always provided the bigger picture while always keeping me on course. I am grateful for his mentoring about life, science, and politics.

TABLE OF CONTENTS

<i>Title Page</i>	i
<i>Author's Declaration</i>	i
<i>Abstract</i>	i
<i>Acknowledgments</i>	i
1. INTRODUCTION	1
1.1 Introduction	1
1.2 Thesis Objective	2
1.3 Thesis Outline	3
2. URBANIZATION AND URBAN CLIMATES	4
2.1 Urbanization	4
2.2 Cities and Human Modification of the Landscape	5
2.2.1 Causes of Urban Heat Island	6
2.2.2 Types of Urban Heat Islands	8
2.3 Human Health, Environmental and Economic Significance	11
2.4 History of Urban Climatology and Urban Climate Research	16
2.5 Climate Scales and Classification	17
2.6 Local Climate Zone Method	23
2.7 Climate Data and Spatial Interpolation Methods	27
2.8 Redefining the UHI	30
3. DATA COLLECTION AND METHODS	31
3.1 Study Area	31
3.2 Local Climate Zone Method	34
3.3 Statistical Analysis	42
4. RESULTS	47
4.1 Surface Cover Fractions around Meteorological Stations	47
4.2 Assigning Local Climate Zones to Meteorological Stations	50
4.3 The UHI Intensity in Southern Ontario	52
4.3.1 Seasonal Mean-Daily UHI Intensities in Southern Ontario .	62
4.4 Correlation Analysis	66
4.5 Temperature Surface of Study Area	73
5. DISCUSSION	78
5.1 The Local Climate Zone Application in Southern Ontario	78

5.2	The Urban Heat Island in Toronto and Urbanicity.	80
5.3	The Relationship Between Surface Cover and Temperature.....	82
5.4	Temperature Surface of Study Area	85
5.5	Planning and Management of Cities	86
6.	<i>CONCLUSION</i>	91
6.1	Synthesis	91
6.2	Limitations of Research	94
6.3	Future Research Initiatives	94
6.4	Additional Conclusion	96
	<i>Appendix A</i>	98
	<i>References</i>	120

LIST OF TABLES

Table 2.1: Classification of urban forms shown in approximate decreasing order of the ability to have an impact on the local climate (Oke, 2004).

Table 3.1: Three of the five surface cover properties used for classifying the 19 meteorological stations. (Stewart and Oke, 2012)

Table 4.1: The calculated impervious surface (ISF), pervious surface (PSF), building surface (BSF) and tree canopy (TCF) fractions, number of buildings, surface area of buildings for the five-hundred metre and the one-thousand metre radius thermal source zones and annual mean-daily, minimum-daily and Tmax .

Table 4.2: Local climate zone classified stations showing the potential LCZs generated by query builder and the final chosen LCZs for the five-hundred metre and the one-thousand metre radius thermal source zones. The LCZs in bold are the SQL exact matches and all others are those assigned to the nearest equivalent LCZ.

Table 4.3: The UHI intensities using Burketon McLaughlin (6151042) and Tyrone (6159048) as rural reference station, surface cover fractions.

Table 4.4: Two sample t-test results comparing the means of the two difference UHI intensities calculated using Burketon McLaughlin and Tyrone.

Table 4.5: The results from the analysis of variance used to check the difference between the grouped means of the unique LCZ classes

Table 4.6: The two sample t-test to check for differences between the seasonal mean-daily UHI intensity calculated using Burketon McLaughlin and Tyrone as the rural reference stations.

Table 4.7: The winter, spring summer and fall average UHI intensity calculated using Burketon McLaughlin and Tyrone seasonal average mean-daily UHI intensities.

Table 4.8: The analysis of variance results for the difference among seasonal mean-daily UHI intensities.

Table 4.9: The analysis of variance results for the difference among seasonal mean-daily UHI intensities.

Table 4.10: Daily mean, maximum and minimum temperature by Latitude, Elevation, Distance to Lake Ontario and Distance to Urban Core (1st Canadian Place). ** Correlation is significant at the 0.01 level (2-tail) and * is significant at the 0.05 level (2-tail).

Table 4.11: Daily mean, maximum, and minimum temperatures by surface cover fraction for thermal source zones of 500 and 1000 metre radius centred on meteorological station. ** Correlation is significant at the 0.01 level (2-tail) and * is significant at the 0.05 level (2-tail).

Table 4.12: The two-sample t-test assuming equal variances to compare the r-squared values calculated in the 500 and 1000 m scatter plots.

Table 4.13: Ordinary Kriging and ordinary co-Kriging validation measures for daily mean, daily minimum and daily maximum temperatures.

LIST OF FIGURES

Figure 2.1: The urban heat island intensity is defined as the temperature difference between the urban “peak” temperature and background rural core temperature (Oke, 1992).

Figure 2.2: The vertical structure of the atmosphere up to the planetary boundary layer (PBL) shown at the scale of a whole city and the locations of the urban boundary layer (UBL), urban canopy layer (UCL) and surface heat islands (Adapted from Oke, 1992; Roth, 2013).

Figure 2.3: A microscale look at the urban canopy layer urban heat island (Adapted by Voogt after Oke 1992).

Figure 2.4: The four scales of climate according to Yoshino (1975) and examples of each. $M_1 - M_{11}$: Microclimate, $L_1 - L_5$: Local climate, $S_1 - S_2$: Mesoclimate and A_1 : Macroclimate.

Figure 2.5: Climatic regions of the City of London. (I) Central London, (II) Inner Suburban London, (III) North London Heights and (IV) Outer Suburbs (Chandler, 1965).

Figure 2.6: General expectation of temperature response based upon local climate zones units. LCZ 1 to LCZ 10 represent built-types in descending degrees of urban zones and LCZ A to LCZ G are categorically defined land cover types representing rural zones. Two of the seventeen local climate zones are labeled. Images GoogleTM earth.

Figure 3.1: Physical geography of southern Ontario study region showing landform features and the location of the 19 meteorological stations included in the case study. (Natural Resources Canada, 2014, DMTI Spatial Inc., 2011 and Environment Canada, 2013).

Figure 3.2: Local climate zone classification workflow. The orange fill represents the LCZ method proposed by Stewart and Oke (2012).

Figure 3.3: The City of Toronto land cover map used to calculate land cover areas and land cover fractions. Image sourced from Quickbird satellite imagery acquired in 2007, with 60 cm resolution. (City of Toronto, 2009, DMTI Spatial Inc., 2011, Environment Canada, 2013)

Figure 3.4 Ontario land use polygons dataset used to capture the land cover within the 500, 1000 metre radii centred on the meteorological station location. Burlington and Bowmanville are shown as examples. (DMTI Spatial Inc., 2011).

Figure 3.5: Process for calculating surface cover fractions for fourteen of the nineteen meteorological stations used in this case study.

Figure 3.6: Flowchart of methods. The orange flowchart diagrams signify the local climate zone method (Stewart and Oke, 2012) shown previously.

Figure 4.1: The thousand metre radius around meteorological stations Toronto, Oakville Gerrard, Richmond Hill, Tyrone and Burketon McLaughlin showing their pervious, impervious and building surface covers.

Figure 4.2: The average mean-daily UHI intensity shown in ascending percentage of impervious surface fraction at the 500 metre radius thermal source zone.

Figure 4.3: The average mean-daily UHI intensity shown in ascending percentage of impervious surface at the 1000 metre radius thermal source zone.

Figure 4.4: The average mean-daily UHI intensity shown in ascending percentage of pervious surface fraction at the 500 metre radius thermal source UHI intensity graphs.

Figure 4.5: The average mean-daily UHI intensity shown in ascending percentage of pervious surface at the 1000 metre radius thermal source zone.

Figure 4.6: The average mean-daily UHI intensity shown in ascending percentage of building surface fraction at the 500 metre radius thermal source zone.

Figure 4.7: The average mean-daily UHI intensity shown in ascending percentage of building surface fraction at the 1000 metre radius thermal source zone.

Figure 4.8: The average mean-daily UHI intensity compared between unique LCZ classes. Also shown are the average minimum-daily and average maximum-daily UHI intensities.

Figure 4.9: Average spring and fall mean-daily UHI Intensities sorted by local climate zones representing low urbanicity to high urbanicity.

Figure 4.10: Winter and summer average mean-daily UHI Intensities sorted by local climate zones representing low urbanicity to high urbanicity.

Figure 4.11: The \bar{T} plotted against the impervious, pervious, building surface and tree canopy fraction calculated within the one-thousand metre radius around the meteorological stations.

Figure 4.12: The T_{min} plotted against the impervious, pervious, building surface and tree canopy fraction calculated within the one-thousand metre radius around the meteorological stations.

Figure 4.13: The T_{max} plotted against the impervious, pervious, building surface and tree canopy fraction calculated within the one-thousand metre radius around the meteorological stations.

Figure 4.14: The diurnal temperature range plotted against the impervious, pervious, building surface and tree canopy fraction calculated within the one-thousand metre radius around the meteorological stations.

Figure 4.15: The comparison of r-squared values from Table 4.11 between the 500 m and 1000 m thermal source zones.

Figure 4.16: The \bar{T} , T_{min} , T_{max} surfaces of study area in Southern Ontario using ordinary Kriging.

Figure 4.17: The \bar{T} , T_{min} , T_{max} surfaces of study area in Southern Ontario using ordinary co-Kriging.

Figure 5.1: The average mean-daily UHI intensity calculated based upon the co-Kriging interpolated \bar{T} and shown along with the locations of the classified LCZs.

Figure 6.1: Synthesis of research, expectations, findings and contributions.

1. INTRODUCTION

1.1 Introduction

The Golden Horseshoe is a densely populated area in southern Ontario (8.7 million residents) and the population is expected to grow to 11.5 million residents by 2031 (Pond, 2009, p. 415). The urbanization process will likely intensify due to the current and expected population growth under way in this region. The City of Toronto, the most populated area in the region, has long been recognized as being distinctly warmer than the less urban areas outside of the City. Interest in the nature of this “urban heat island” (UHI) intensity has been evolving to add details regarding the magnitude of these differences (*i.e.* urban core versus periphery) and how these differences respond to land cover and land use conditions. These insights can reveal the contribution that urbanization has on affecting the climate of Toronto and this information can lead to adopting urban planning approaches that minimize the impact of urbanization on climate.

The first insight into the spatial distribution of temperature over Toronto was presented by Middleton and Millar (1936) in their paper investigating the temperature profile in Toronto. Their study was the first traverse, or measuring trip investigation undertaken outside of Europe (Stewart, 2011b). They showed the extent to which the temperature can vary in short distances (~ 15 km) revealing the existence of microclimates and an UHI. They discovered “urban” temperatures 2 – 3 °C warmer than rural areas about 5 km north of Bloor Street (Middleton and Millar, 1936, p. 270). Thirty years later Munn *et al.* (1969) showed the migration of Toronto’s urban heat island (UHI) based on the prevailing wind direction caused by the lake-land boundary. They showed that during the cold season with off-lake breeze the UHI was located in the central and west end of Toronto. However, during the warm season, with off land wind, the warmest portion of the city was north of Bloor Street and the central business district. They also noted that the UHI was found to be more intense during light winds likely due to the decrease of convective heat losses delivered by increased wind speeds. The study revealed the dynamic nature of Toronto’s UHI prior to the current major re-development of the waterfront. In 1998, Oscar Koren, a climatologist with Environment Canada repeated the Middleton and Millar experiment and showed that the presence of the heat island extended to Finch Avenue, with the highest temperature found at Yonge and Dundas Streets about 2 km from the lake (Sanderson,

2004, p. 86). Weatherburn (2011, p. 54) investigated the mesoscale climate of Toronto and its surrounding region and showed the urbanization effect on temperature using built-up area as an independent variable. More recently, Tam *et al.* (2015) reported that the day to day variation in temperature in urbanized areas in North America was smaller than that of near rural areas. Overall the City of Toronto has shown an increasing trend in temperature since the 1920s (Gough and Razoanov, 2001) and Mohsin (2012, p. 105) showed that the upward trend in UHI intensity ranged from 0.03 °C per decade to 0.035 °C per decade from 1970 to 2000 and that higher UHI intensities occurred during the winter in Toronto.

With the most recent set of climate averages made available by Environment Canada (1981 – 2010) an increasing trend in the UHI intensity can now be investigated to determine if this pattern has continued, given the ongoing population growth and land surface changes in the region.

1.2 Thesis Objective

The overall objective is to assess the microclimates in Southern Ontario using three surface cover properties outlined in the recently proposed local climate zone (LCZ) application for urban temperature studies (Stewart and Oke, 2012). These properties were impervious surface fraction, pervious surface fraction and building surface fraction. A microclimate perspective would seem to be improved by looking for the relationships between these surface cover properties and average air temperatures. The specific objectives of this research are therefore:

1. To assess microclimates in Southern Ontario:
 - a. By estimating surface land cover types (fractions) and investigating their relationship with climatic averages, specifically the mean-daily, minimum-daily and maximum-daily temperatures.
 - b. By quantifying the intensity of the urban heat island in southern Ontario
 - c. By using spatial interpolation to explore the horizontal spatial distribution of air temperatures and UHI intensity in Southern Ontario.
2. To evaluate the local climate zone method and its ability to conduct and communicate urban climate research.
 - a. By evaluating the enhancement provided by this case study, to determine the ramifications of the LCZ method on management of urban spaces

This research is about urban microclimates in Southern Ontario. A deeper understanding of the effect of human modification to the landscape can help to promote informed current and future planning. The research undertaken in this study explored the microclimates in southern Ontario that have relevance to the daily lives of its residents. It was intended to give a spatial perspective of air temperature and answer the question of “where” there may be a growing problem. This is useful information for planners, engineers, municipal governments and the general public because they can make improvements to mitigate warming and the detrimental effects of heat in their local area.

1.3 Thesis Outline

The research presented here begins with an overview of urbanization, the human modification of the natural landscape and the problems associated with land cover changes (Section 2.1). The operational definition of urban heat island (UHI), its types and causes is discussed (Section 2.2) followed by the reasons for studying such a phenomenon in the context of human health, environmental and economic significance (Section 2.3). An historical perspective of urban climatology and urban climate research is then discussed (Section 2.4) with a section which highlights the significance of scale and classification in applying urban climate studies (Section 2.5). The recent problems associated with conducting UHI research are then presented as well as the method developed by Stewart and Oke (2012) which helped to minimize the problems associated with the UHI research methods (Section 2.6). A brief history of climate data collection in Canada and the use of geographic information systems (GIS) tools to analyze the collection of spatially distributed climate data are presented (Section 2.7). A new approach to UHI investigation is presented and the expected results from this research concludes section two (Section 2.8). Section 3 provides details of the specific method and data used. This section includes a brief description of the physical geography and climate of Southern Ontario (Section 3.1). The case study for Southern Ontario is used to assess the effectiveness of the LCZ method and to quantify the UHI intensity using the most recently made available Canadian climate averages and the results are presented in Section 4. Finally a discussion of the findings (Section 5) and some general conclusions, the limitations of this research and future research initiatives are suggested (Section 6).

2. URBANIZATION AND URBAN CLIMATES

2.1 Urbanization

In 2002 Vlahov and Galea (2002, p. S4) described urbanization as the change in size, density, and heterogeneity of cities. They went on to define the term “urbanicity” as the impact of living in urban areas which refers to “the presence of conditions that are particular to urban areas” (Vlahov and Galea, 2002, p. S5). Over the last two centuries the degree to which urbanization has progressed is linked closely to the growth of human population. Current estimates have half of the world’s inhabitants concentrated in cities (United Nations Environment Programme, 2012, p. 8) but this fraction is expected to increase to 70 per cent by 2050 with predicted population growth (Organization for Economic Co-operation and Development, 2014, p. 4). Consequently the rates of global environmental impacts such as global warming, deforestation, desertification, or loss in biodiversity are mainly driven by the increase in human population (Grimmond, 2007, p. 83). With urban areas only covering 2 per cent of the Earth’s surface, there is a significant concentration of demand on natural resources relative to rural areas (Golden, 2004, p. 323). One benefit of urban growth is that the process accelerates social and economic development for their respective countries and rural surroundings (Cui and Shi, 2012, p. 2). However this social and economic progress comes at a cost to the local environment in the form of air and water pollution (Mayer, 1999; Walsh *et al.*, 2005; Seilheimer *et al.*, 2007; McKinney, 2008; Cui and Shi, 2012) and likely irreversible unsustainable use of the land. Furthermore the urban area with its own special features and processes characterized by dense concentration of people, raw materials, production activities and energy consumption leads to the perturbation on the local microclimate (Oxizidis *et al.*, 2007, p. 96). For example increasing surface and air temperature due to urbanization has been shown through remote sensing methods (Owen *et al.*, 1998; Voogt and Oke, 2003; Imhoff, *et al.*, 2010; Maloley, 2010; Rinner and Hussain, 2011) and from data gathered through meteorological station networks across North American and other cities (Karl *et al.*, 1988; Kalnay and Cai, 2003; Mohsin and Gough, 2010). Given the current increasing trend in urbanization there are concerns about the strengthening local effects of warming (Souch and Grimmond, 2006; Grimmond, 2007; McCarthy *et al.*, 2010) and the lack of effort given in incorporating urban climate research in the

planning process to address this concern (Svensson and Eliasson, 2002; Coutts *et al.*, 2010; Mavrogianni *et al.*, 2011).

2.2 Cities and Human Modification of the Landscape

The process of urbanization involves modifying the landscape from mostly vegetation and bare earth into (1) unique urban structure (*e.g.* variation in building dimensions and street widths), (2) urban cover (*e.g.* pervious and impervious surfaces), (3) urban fabric (*e.g.* concrete, brick and soil) and (4) urban metabolism (*e.g.* heat from people and automobiles) (Oke, 2006, p. 184). These four physical characteristics of urban zones respond differently to the energy balance than the contrasting rural landscape, which then leads to higher air temperatures in cities when compared to their rural surroundings (Oke, 1988; Oke, 2006). This phenomenon is one of the most well-known atmospheric modifications attributable to urbanization (Roth, 2013, p. 143). The difference between the temperature reading in the urban core and the background rural temperature is defined as the urban heat island intensity or urban heat island magnitude (Equation 1) (Oke, 1992, p. 289) (Figure 2.1).

$$UHI \text{ Intensity} = \Delta T_{u-r} \text{ (Equation 1)}$$

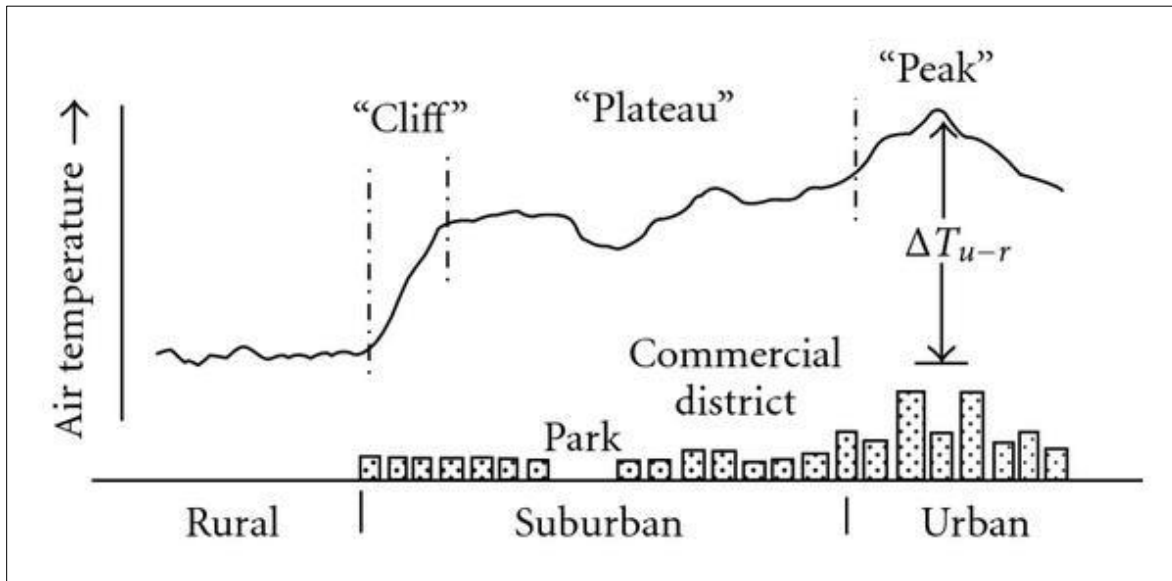


Figure 2.1: The urban heat island intensity is defined as the temperature difference between the urban “peak” temperature and background rural core temperature (Oke, 1992).

This definition (*i.e.* Equation 1) reveals the existence of the thermal phenomenon in settlements large and small (Oke, 1982, p.7). For example, Oke (1973) found a positive linear relationship between city size, measured as the logarithm of population, and the magnitude of UHI produced (Oke, 1973). Research has shown that meteorological conditions such as calm, clear days with low wind speed (*i.e.* $< 5 \text{ ms}^{-1}$) can increase the UHI intensity (Landsberg, 1970, p. 1271; Oke, 1992). The modern period of UHI research has contributed greatly to the understanding of UHI in diverse climates such as New York City, Montreal, Vancouver, Phoenix, Nagano, Colombo, Kuala Lumpur, Eilat (Israel) and Toronto (Bornstein, 1968; Sani, 1972; Oke and Maxwell, 1975; Balling and Cerverny, 1986; Sakakibara and Matsui, 2005; Emmanuel and Johansson, 2006; Sofer and Potchter, 2006; Rinner and Hussain, 2011). A large fraction of UHI studies that have been undertaken are generally located in areas near large water bodies (Stewart, 2011a). Large water bodies may have a significant lake effect which can moderate the local extremes in temperature (Munn *et al.*, 1969 and Sanderson, 2004). In a more recent study by Tam *et al.* (2015) the investigators examined the day to day temperature variability difference of five North American urban-rural pairs of climate stations in order to detect a clear urban footprint. They showed that the difference was evident in all five urban-rural pairs revealing that the minimum air temperature in urban areas is damped by the influence of the city. The research revealed that the weakest signal appeared in the pairing with the smallest urban centres. The prevalence of this effect throughout the world suggests a continued need to explore, understand and mitigate the problem it exacerbates (Section 2.3).

2.2.1 Causes of Urban Heat Island

The physical causes of the UHI effect depend on the nature of the urban environment, human activity and meteorological conditions (Grimmond, 2007, p. 83). According to Landsberg (1970) the effect of cities on climate concerns two major features: the heat and water balance, and the turbulence condition. The heat and water balance is changed by the urban cover and fabric represented by an impermeable layer to water that is better at absorbing and conducting heat (Landsberg, 1970, p. 1270) and a city environs that has redirected drainage to effectively transport water away from street surfaces (Oxizidis *et al.*, 2007, p. 97). The turbulence is changed by the increase in the surface roughness of cities due to variation in building heights

(*i.e.* urban structure) and this affects the vertical wind profile resulting in lower wind speeds near the ground (Landsberg, 1970, p. 1270) as well as gusts of wind that tumble down from the tops of buildings creating an uncomfortable environment for pedestrians (Munn *et al.*, 1999, p. 41) and reduced openness to the sky which limits the escape of longwave radiation into the atmosphere (Oke, 1992, p. 133). The reasons for the UHI phenomenon can be summarized as follows (Oxizidis *et al.*, 2007, p. 96 after Oke *et al.*, 1991, p. 356):

1. The thermal and radiative properties of materials that cover the land in urban environments differ from the materials found in rural areas. The materials in urban environments have higher heat capacity (*e.g.* higher quantity of heat added to raise temperature) and a lower albedo (*e.g.* percentage of reflectivity).
2. The lack of vegetation found in cities reduces transpiration. This means the heat loss through transpiration is reduced in urban environments. Also the higher *per cent* of impervious surface areas found in cities transports water quickly from the streets through sewer systems further reducing the latent heat loss through evaporation. So the heat that would normally go towards evaporation instead goes to heating the surfaces as sensible heat.
3. The topography in urban areas can be described as canyons which results in a more effective absorption of shortwave radiation since it allows for multiple reflections of solar radiation.
4. The canyon geometry characteristics (*e.g.* size, shape and orientation of buildings) found in urban areas decreases the efficiency with which the area can radiate longwave radiation into the atmosphere and out into space. Longwave radiation is reabsorbed because of the multiple surfaces found in the canyon thus eliminating the cooling effect through longwave radiation into the atmosphere.
5. The variation in building heights in urban areas means there is increased surface roughness. The surface winds are slowed down which decreases the sensible heat loss from the urban surface through atmospheric convection.
6. The atmosphere within urban areas carries more particulate matter and aerosols which can produce a pseudo-greenhouse effect. The particulate matter and aerosols absorb and re-radiate longwave radiation further inhibiting the radiative surface cooling.
7. The higher concentration of people found in cities means the production of more heat through the use of automobiles, construction equipment, air-conditioning use and heat loss through buildings.

Urban and rural environments respond differently to energy processes of solar radiation, terrestrial absorption, reflection, emission and conduction; mass from added precipitation and momentum governed by airflow. Taking into consideration that rural landscape, in general, is mostly covered by vegetation with very few tall structures and large vegetated areas between paved surfaces, it is expected that when comparing the temperatures of these rural regions to

urban ones, there can be a measureable difference (Equation 1). Mohsin (2009) reasoned that this temperature difference is associated with all meteorological factors including wind, cloud cover and near surface lapse rate in describing the temperature of the standard screen-height observation at each site (Mohsin, 2009, p. 55). Since the temperature is representative of the surrounding area this means that the temperature recorded in an urban setting takes into account the effects from physical attributes like imperviousness, building density and amount of vegetation. Similarly the temperature observed at a rural site is indicative of the contributions from its physical attributes. Therefore the resulting UHI intensity should not be considered just as a difference in temperature but a reflection of all the contributing factors that are unique to the area experiencing the temperature and this is the basis for Stewart and Oke's (2012) most recent research.

One particular parameter that shows divergent quantities when comparing urban and rural areas is the percentage of impervious surface cover. In 1996 Arnold and Gibbons stressed the importance of impervious surface cover as a key environmental indicator because of its association with water quality issues (Arnold, Jr. and Gibbons, 1996). However research in the last twenty years has also correlated impervious surfaces with urban heat islands and air pollution (Lee and French, 2009, p. 477) and Yuan and Bauer (2007) identified a strong linear relationship between land surface temperature and percentage of impervious surface. The influence on long term climate can also be detected. For example, in downtown Los Angeles the air temperature cooled by 2 K from 1882 until the 1930s due to an increase in irrigation and the growing presence of orchards, however since the 1930s the city has warmed by 3 K due to decreases in tree cover and an increase of asphalt (Shashua-Bar and Hoffman, 2000, p. 221). The environmental significance of impervious surface cover may be relevant to urban climatology because its abundance could be associated with elevated temperatures.

2.2.2 Types of Urban Heat Islands

According to Roth (2013) there are four types of urban heat islands and, for convenience, they are categorized based on spatial scale and the physical process involved. In order of increasing spatial scale they are the surface and subsurface heat island, the urban canopy layer (UCL) heat island and the urban boundary layer (UBL) heat island (Figure 2.2).

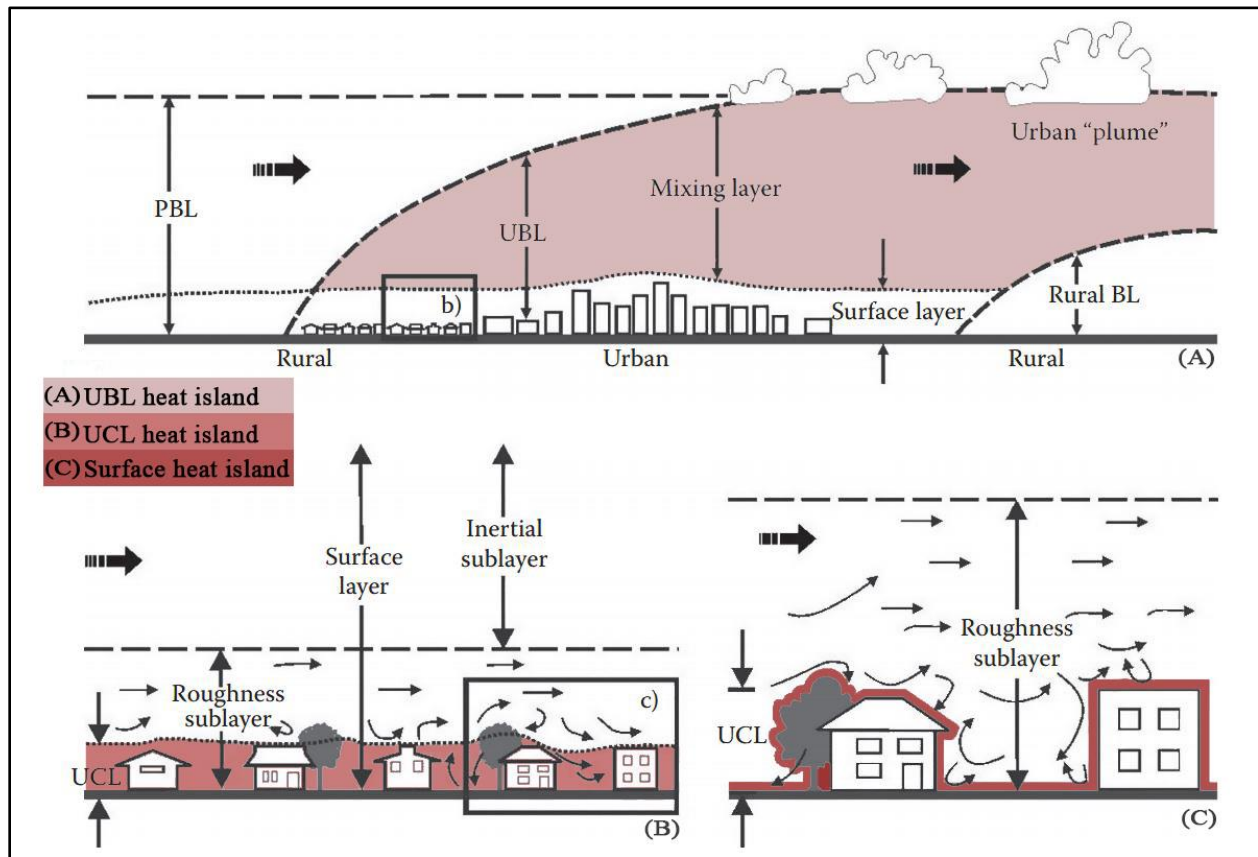


Figure 2.2: The vertical structure of the atmosphere up to the planetary boundary layer (PBL) shown at the scale of a whole city and the locations of the urban boundary layer (UBL), urban canopy layer (UCL) and surface heat islands (Adapted from Oke, 1992; Roth, 2013).

Roth (2013, p. 146) described the surface and subsurface as two types of UHI that span up to hundreds of metres in the horizontal direction and that have the strongest UHI during the daytime because of incoming solar radiation. Solar heating is recognized to create large differences in temperature between vegetated surfaces and pavement. The UHI magnitude of the subsurface phenomenon is small and the timing of its greatest intensity can be either day or night. The magnitude of the surface UHI can be very large during the day when the warmest surfaces are generally located in industrial and commercial areas with large flat-topped buildings and large open areas of paved surfaces (*e.g.* airports, shopping malls). The surface UHI is generally studied using remote sensing methods utilizing thermal infrared measurements (Imhoff *et al.*, 2010; Rinner and Hussain, 2011).

The canopy layer UHI is the atmosphere found above the ground surface but below the tops of buildings and trees. In the urban canopy layer (UCL) airflow processes and energy exchanges are controlled by microscale, site-specific characteristics such as the urban cover, urban fabric and urban structure (Arnfield, 2003; Oke, 2006, p. 184). The urban canopy layer can span up to ten kilometres in the horizontal direction and tens of metres in the vertical direction. This layer is home to all activities undertaken by humans, plants and animals (Figure 2.3). It is distinctive in that the UHI magnitudes in this layer are lower when compared to the surface UHI and the peak magnitude for a canopy layer UHI is found just after sunset (Roth, 2013, p. 146).

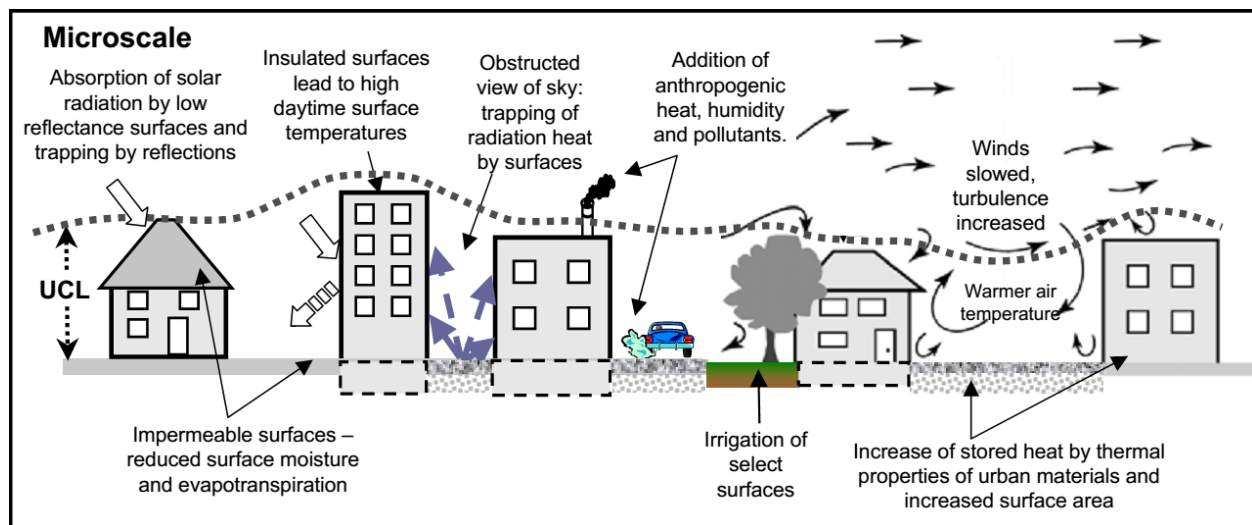


Figure 2.3: A microscale look at the urban canopy layer urban heat island (Adapted by Voogt, 2007 after Oke, 1992).

Furthermore, the urban canopy layer UHI is studied using temperature observations taken 1 to 2 metres above the ground surface. Climate stations throughout the world that adhere to the standards set forth by the World Meteorological Organization (WMO) are generally situated 1.5 metres above ground in a louvered shelter (*e.g.* Stevenson screen). The shelter eliminates direct and reflected sunshine but permits free circulation of air minimizing the bias in recorded temperature values (Brown *et al.*, 1980, p. 12). The urban canopy layer UHI is the most studied effect throughout the globe because of the availability and standardization of temperature data. The importance of monitoring the atmospheric properties in this layer is reflected in the standards set forth by WMO and the active temperature monitoring networks carried out by

many countries around the world. The urban canopy layer UHI is also increasingly studied using a temperature gauge mounted on top of a vehicle which traverses across the city and into rural areas revealing a continuous temperature along the route, but this method involves applying a time correction due to regional temperature changes during the observation time (Stewart, 2011b, p. 16).

The urban boundary layer UHI spans tens of kilometres in the horizontal and vertical directions. Due to the difficulties in obtaining data at the heights involved in UBL heat island investigation there is little attention paid to the phenomenon at this scale. Its formation is due to the urban heat spreading upward and beyond a city (Roth, 2013, p. 146).

Although the UHI is broken into these four different types, they are interrelated and do not occur in isolation from one another. For example, during a calm clear day there is strong radiation absorption by the surface leading to the surface UHI effect. Then during the evening and night the heat stored in the urban fabric (*e.g.* pavements and concrete) is released as longwave radiation. The longwave radiation (converted to heat) is trapped within the urban canyons due to the reduced sky view. The tall buildings within an urban core reduce the amount of visible sky from the surface and forces longwave radiation to remain within the canopy layer resulting in elevated temperature (*i.e.* canopy layer UHI). The UCL phenomenon is of the most relevance to people.

2.3 Human Health and Environmental and Economic Significance

Cities, due to their higher population, require a larger proportion of resources than their rural counterparts for heating and cooling, transportation of people and goods and industrial processing which leads to higher emissions (Grimmond *et al.*, 2010, p. 247). Cities are responsible for more than seventy *per cent* of the anthropogenic carbon emissions and at present wealthier cities in developed countries are the main contributors (Grimmond *et al.*, 2010, p. 247). The forthcoming warming climate will have exacerbated human health effects because of heat stress from heightened warming in cities. In 1995 the city of Chicago was struck by a heat wave resulting in 437 excess deaths (*i.e.* above normal) during a four day period in July and then again in 1999 resulting in 80 deaths (Naughton *et al.*, 2002, p. 221). Almost a decade later the 2003 heat wave in Europe reported 14,800 excess deaths in France and the city of Paris was

disproportionately affected (Cadot *et al.*, 2007, p. 467). During heat waves, the only form of relief other than from the use of air conditioning comes from the nighttime minimum temperature, but if the nighttime temperature remains high as it often does in the presence of an UHI then there is little relief from the exposure to intensified heat. With urban growth continuing and future climate warming expected, this issue is not likely to improve without some effort to minimize the local warming.

It has been reported (Mavrogianni *et al.*, 2011) that an increase in outdoor ambient temperatures can have interconnected effects. Depending on the regional climatic background the area is set in and the time of year, the unique city climates can have beneficial as well as detrimental effects. Even though a warmer city during the winter months is welcomed by the public and puts less stress on heating costs, higher temperatures during the summer in combination with lack of air movement, and heightened air moisture content compromises the capacity of humans to maintain a comfortable core temperature (*i.e.* 37 °C) (Forkes, 2010, p. 7). Humans generally feel comfortable at an environmental temperature of 20 – 25 °C (Oke, 1992, p. 218). In order to meet this comfort requirement there will be an increase in energy use during the summer but less demand during the winter months. The public health problem of summer heat waves will be a growing concern in North American cities because of increasing intensity, duration and frequency of extreme heat events, as reported by Meehl and Tebaldi (2004, p. 994). For example, in Toronto between 1961 and 1990 there was an average of 15 days per year when temperatures rose above 30 °C , however Environment Canada predicts that with climate change that number will more than quadruple to about 65 days per year by 2080 (Gower *et al.*, 2011, p. 3). Research has found that more deaths are due to heat in temperate climates than in warmer climates because people in warmer climates are acclimatized to the elevated temperatures (Harlan *et al.*, 2006, p. 2847). As a result North American cities may be susceptible to the threat of local warming.

There are numerous metrics to assess the temperature at which the comfort level of humans is affected. The ones most used for perceived outdoor comfort are apparent temperature, wind chill and humidex. Apparent temperature is a metric that combines air temperature and humidity into an index that is appropriate to perceived temperature and humidex is an index developed by Canadian meteorologists to provide a measure reflective of what is actually felt in

hot and humid weather (Kershaw and Millward, 2012, p. 7331). For example some discomfort starts at a humidex greater than 30, with great discomfort beginning at 40 and dangerous levels beyond 45 (Environment Canada, 2014). The adverse impact from heat waves will depend on their frequency, their duration and intensity. Addressing the harmful effects from extreme heat may become a priority in Southern Ontario, especially considering that the population of the Greater Golden Horseshoe (GGH) is predicted to reach 11.5 million by 2031 (Pond, 2009, p. 415).

There are indirect consequences of elevated temperatures found in city environments. For example higher air temperatures as a result of solar radiation produce the right condition for atmospheric nitrogen oxides and volatile organic compounds to transform into ozone which can then lead to photochemical smog (Forkes, 2010, p. 8). The cycle of formation and destruction of nitrogen oxide and ozone produces no additional ozone but the hydrocarbons from vehicles which are found at higher concentrations in urban areas leads to an imbalance in the cycle and a net production of ozone (Oke, 1992, p. 319). Ozone in the stratosphere helps to protect the earth from harmful ultraviolet rays however its presence near the ground leads to detrimental environmental and human health impacts. Ozone is known to cause visible plant damage reducing plant growth, (Oke, 1992, p. 319); its presence can be harmful to humans due to its association with increased asthma morbidity and mortality (Stathopoulou *et al.*, 2008, p. 227). Health Canada warns that exposure to ground-level ozone may result in acute and chronic damage to the respiratory system and it is a special concern to individuals with cardiovascular and pulmonary diseases (Forkes, 2010, p. 8).

The creation of a warmer urban climate can influence the energy use of people living in areas affected by elevated temperatures. However instead of addressing the deteriorating outdoor thermal comfort by utilizing less energy intensive means like strategically placed vegetation, ventilation and shading (McPherson *et al.*, 2005; Erell, 2008), a more energy intensive approach is normally utilized with the use of air conditioning resulting in an added energy demand in the city. Even further outdoor thermal pollution ensues due to the added source of anthropogenic heat along with the increased contributions of carbon dioxide emissions from increased energy use. These actions have not gone unnoticed as local utility companies have seen a change from a peak energy demand in the winter to a peak demand in the summer (Konopacki and Akbari,

2001, p. 4). The magnitude of the influence a city will have on future local warming may be dependent on human behaviour, mitigation and adaptation measures taken by local authorities. This issue is especially important because in 2008 Perez-Lombard *et al.* (2008, p. 394) reported that the building energy consumption of the residential and commercial sectors has exceeded that of the industrial and transportation sector in developed countries.

Loveland and Mahmood (2014) recently stressed the importance of understanding the relationship between climate and land cover changes. The growing concern was highlighted in the United States *National Climate Assessment Report* which calls for a better understanding of land use and land cover and its feedback within the climate system in order to better prepare for future climate change and variability (Loveland and Mahmood, 2014). Cities for instance, are not immune to the impacts from global warming because it will experience the local effects from urbanization in the form of an increased urban heat island effect according to McCarthy *et al.*, (2010, p. 9705). They showed a potential for a 30 *per cent* increase in urban heat island intensity in parts of the eastern the United States and Southern Ontario in response to climate model scenarios with doubled CO₂ concentrations indicating that the magnitude of the urban heat island is not static under climate change. Current evidence shows that half the observed decrease in diurnal temperature range (*i.e.* difference between maximum and minimum temperature) over the last 50 years is due to urban and land-use changes (Kalnay and Cai, 2003, p. 528). With this in mind the collective behaviour in cities (*i.e.* the public, developers, and municipal governments) is counter to the actions needed to address the local impacts of urbanization. For example, the economic opportunities made available in condo and commercial development in high value land areas in major North American cities is driving urban development. According to the report in *Emerging trends in Real Estate 2015* released by the Urban Land Institute (Kelly and Warren, 2014), urbanization is one of the key forces shaping Canadian real estate. People are “flooding” into city cores to be near work and participate in the city lifestyle (Kelly and Warren, 2014, p. 76). As a result companies and retailers are constructing new office and commercial developments in city cores. Kelly and Warren reported that as of 2014 the downtown office space in Toronto, Canada has 5 million square feet under construction with over half already preleased (Kelly and Warren, 2014, p. 91). The influx of people into urban centres and the resulting by-product of consumption have the potential to elevate the heat stress in dense urban

cores. For example, Mizuno *et al.* (1991) showed that artificial earth surfaces tend to increase the local air temperature and that the influence radius of this effect can range from fifty metres to two-hundred metres (Mizuno *et al.*, 1991, p. 165). This is consistent with early climatologist Rudolf Geiger's assertion that by erecting new buildings humans are displacing the original climate of the area by creating warm, sunny, and dry climate on the southern exposure and a shady, cold and damp northern climate on the other (Geiger, 1965, p. 480). Integrated over the city landscape there is a likelihood of unique microclimates being formed within the city limits.

Helmut Landsberg (1970, p. 1270), an influential climatologist of the twentieth century noted years ago that "By far the most pronounced and locally far-reaching effects of man's activities on microclimate have been in cities". Therefore as major environmental issues associated with global climate change are presented in 21st century mainstream media with warming scenarios that are conceptually difficult for many individuals to comprehend, the more direct impact felt by city populations is being experienced locally. The local effect associated with warming such as heat stress (Smoyer *et al.*, 2000; Harlan *et al.*, 2006; Hajat *et al.*, 2010; Kershaw and Millward, 2012; Chuang *et al.*, 2013; Thorsson *et al.*, 2014), weather modification (Changnon Jr., 1978; Lowry, 1998), air pollution (Landsberg, 1979; Mayer, 1999; Stathopoulou *et al.*, 2008) and a general overall poor microclimate are currently being experienced by people living in major cities throughout North America and Europe.

The UHI research agenda is mainly driven by researchers looking to explore the presence or absence of the phenomenon. While the research method has recently come under some scrutiny (Section 2.6) the existence of the UHI effect is without doubt. Very little research is done on exploring the frequency of the phenomenon and given the amount of research going into the UHI program throughout major cities around the globe the simple presence/absence of the effect may not provide useful information that local governments can use to put in place beneficial policies. Furthermore understanding the causes of UHI can provide insights into strategies for temperature mitigation (Grimmond, 2007, p.87). Identifying the presence of UHI in a city can then lead to mapping its spatial extent and gradients in all directions. Then vulnerable areas can be identified and green infrastructure can be implemented. This type of problem solving approach can be made easier when urban climate studies are performed.

2.4 History of Urban Climatology and Urban Climate Research

The purpose of urban climate studies is to explore and understand the climatic condition of cities and its changes and the risks associated with and adaptation to those changes. According to Oke (2007) the field of urban climatology investigates the interaction between the atmosphere and human settlement (Oke, 2006). The urban climate reflects the impact of the atmosphere on the people, infrastructure and activities, and the effects of the latter on the atmosphere (Oke, 2006). The urban climate responds to the process of growth (or decrease) in size of cities through the development or destruction of buildings or neighbourhoods (Vlahov and Galea, 2002, p. 5). Albert Kratzer (1956, p. 1) defined city climate as “the climatic characteristics which distinguish the city from its surrounding area, and what gives rise to them”. Humans have modified the local climate since urbanization became a process that helped to advance economic and social development. Historically urban climate study was rooted in examining the climatic impact of human settlement and activities but it has grown as a research paradigm to include meteorological and climatic characteristics at the individual building scale, urban air pollution dispersion, urban design and planning, biometeorology and human comfort, energy conservations and global warming research (Arnfield, 2003, p. 5).

The first urban climate study was undertaken almost 200 years ago. In 1833 Luke Howard made a significant contribution to urban climatology by publishing his book, *The Climate of London* (1833). In this book he described a phenomenon in which London’s city temperature was warmer than its suburbs (Howard, 1833, p. 11). The urban climate became a focus in the early days of meteorological observations in cities like London and Paris because of the air and water pollution associated with ongoing industrial activity. The field of urban climatology gained attention due to the idea that cities were creating an unnatural condition. His publication brought awareness to the unintended climate modification that was due to urbanization (Stewart, 2011b).

The first published observation of this thermal phenomenon outside of London came in 1862 by Emilien Renou (Stewart, 2011b). Renou showed, on average, an urban-rural temperature difference of 1.2 K higher nighttime minimum in Paris compared to the surrounding country (Stewart, 2011b, p. 32). Larger cities across Europe performed their own observations and showed evidence of a distinct city climate. For example, stationary temperature observations of

two or three sites with one positioned in the city and another in the rural countryside were performed in Munich (1860), Berlin (1890), Paris (1895), Vienna (1924) and Moscow (1928) (Stewart, 2011b, p. 32). The urban influence of elevating temperature was detected in each of these studies. The growth of industrialization and urbanization persuaded scientists to document the inadvertent climate modification due to human invention and ingenuity. Major industrialized areas around the globe took notice of industry's influence on city climate and research paradigms grew in Japan in the 1930s (Yoshino, 1991, p. 5) and North America (*e.g.* Middleton and Millar, 1936). A shift in observation saw researchers use thermometers attached to automobiles and bicycles to obtain a continuous moving temperature record across the city landscape and into its rural surroundings. The outcome of this research was the development of temperature profiles and isotherm maps showing hot and cool spots in the urban-rural landscape (Stewart, 2011b, p. 34). Even though this research was accumulating in Europe and Japan the term “urban heat island” was not used in the English language until Balchin and Pye (1947, p. 304) included the term in their micro-climatological investigation of Bath and the surrounding area. With this new term to describe the city climate phenomenon and the advancement of technology during the 1970s and 1980s, the UHI research area expanded into the use of computer-modelling and remote sensing techniques (Yoshino, 1991) which are still used today (Imhoff *et al.*, 2010; Rinner and Hussain, 2011). The field of urban climatology is important because it has brought awareness to the very real phenomenon of human induced climate modification. The area of study is relevant today because of the intensification and increasing trend of urbanization expected in the coming decades.

2.5 Climate Scales and Classification

The concept of climate is an abstract idea because it can only be grasped by means of calculating individual meteorological parameters (Geiger, 1965). The earth's climate system for example, includes the land, ocean, and ice on the surface of the planet; the envelope of atmosphere above it, and the energy input from the sun (Taylor, 2005). The interactions among them results in the climate, or the mean state or condition on and around the surface of the planet (Taylor, 2005). The most important meteorological parameter is the temperature and its global and seasonal variation (Hidore, 1966; Taylor, 2005). However, this large scale spatial

perspective of earth's climate has little meaning to the human experience of climate sensed through weather and provides little use in monitoring ecosystem changes, assessing long term regional climate trends and application of building design in the urban environments.

It is important to understand the spatial scales of climate especially when considering its application in environmental studies. The consensus among scientists is to refer to the climate of a broad region as the *macroclimate* and climate of the medium size region the *mesoclimate* and the climate of a small area the *local climate* or sometimes *microclimate* (Yoshino, 1975, p. 3). The reality is that the processes involved in each of these scales are part of a continuum which results in some differing opinions on the horizontal and vertical extents of these distinct classes (Oke, 1992, p. 3). For example in Europe there is a disagreement with the terms local climate and microclimate however there is little disagreement among scientists concerning the concept of macroclimate and microclimate (Yoshino, 1975, p. 4). In English-speaking countries microclimatology deals with the science of the geographical distribution of the horizontal and vertical structures of atmospheric layers near the surface of the Earth (Yoshino, 1975, p. 5). This means that the condition of the ground is considered to play an important role in influencing the climate. According to Yoshino (1975, p. 12) four scales are appropriate in order to be as inclusive as possible: microclimate, local climate, mesoclimate, and macroclimate. As an example, a local climate of a mountainous or hilly region would be called topoclimate, a forest region would be a forest climate and city regions would be called urban climate (Yoshino, 1975, p. 12). An example of the spaces covered by the four scales according to Yoshino is shown in in Figure 2.4.

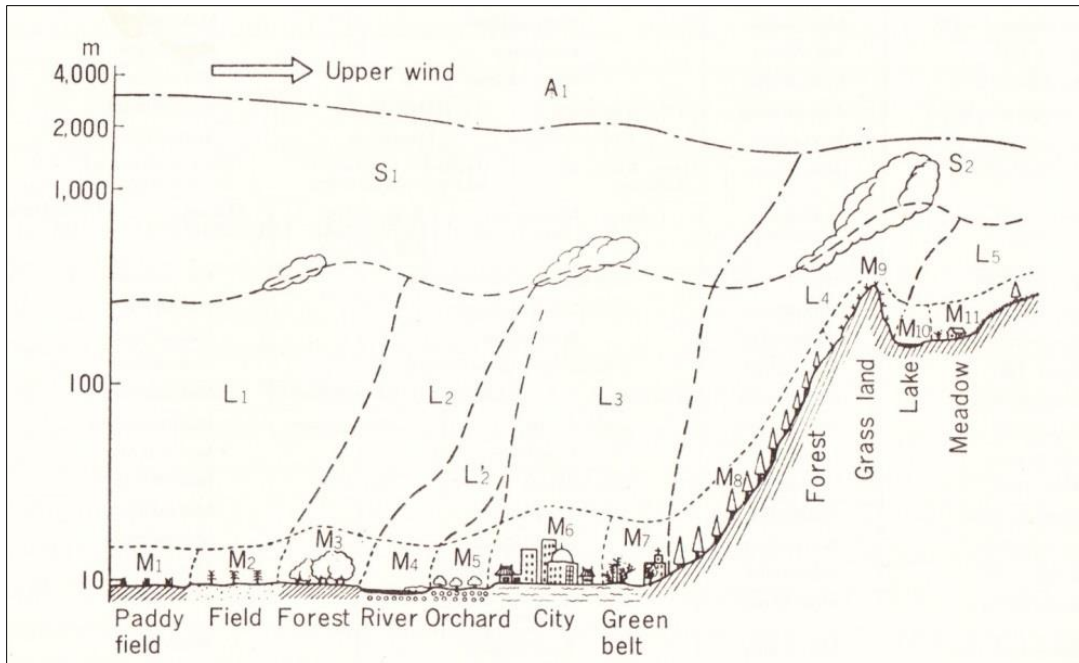


Figure 2.4: The four scales of climate according to Yoshino (1975) and examples of each. $M_1 - M_{11}$: Microclimate, L_1-L_5 : Local climate, S_1-S_2 : Mesoclimate and A_1 : Macroclimate.

According to Oke (2004, p. 2) there are three scale of interest for urban areas relating to urban climate. The urban microscale deals with the dimensions of individual elements present in the urban landscape, for example buildings, trees, roads, streets, gardens and courtyards. The local scale in urban landscapes includes the climatic effect of neighbourhoods with similar type of urban development, for example similar surface covers, and size and spacing of building and the mesoscale where the climatic influence is the entire city.

The climate of any region can therefore be delineated into zones within one of the predefined spatial scales outlined above. The zones and their transitions are variable because of the chosen climatic element and method used to classify them. Oliver (1973, p. 170) suggested that the criteria and method used can be based on the observed effects of climate or the possible causes of climate and termed them “the empiric” and “the genetic” system. Early empiric classification systems used temperature (*e.g.* Herbertson, 1905) because of the available and reliable data but soon climatologists included precipitation and the distribution of vegetation as climatic elements in order to identify climate types. The most famous is the Russian born German geographer Wladimir Koppen classification system which used maximum and minimum

values of mean monthly, seasonal and annual temperature and rainfall and the limits of vegetation types to classify world climates (Thornthwaite, 1933, p. 433). Then in the 1930s another prominent geographer, C. Warren Thornthwaite used a similar approach of vegetation limits to classify the climates. The appeal of these climate classification systems is their use in long term climate trends and the assessment of ecological and ecosystem conditions (*e.g.* Diaz and Eischeid, 2007; Chen and Chen, 2013). Classifying the climate based on causes such as air masses (*i.e.* the genetic system) did not gain the popularity as its empiric counterpart because of the greater emphasis on qualitative methods and the lack of a quantitative base (Oliver, 1973, p. 185). Furthermore its application proved to be more illustrative and used to supplement instead of replace the empiric systems (Oliver, 1973, p. 185). Despite the applicability of the empiric system the coarser resolution of the Koppen-Geiger and the Thornthwaite systems has little application in assessing local climates and microclimates associated with the built environment. A reduced spatial scale of the climate can provide a more suitable description of climatic phenomena that can be appreciated, understood and used.

The local climate defined by Oke (2004) and Yoshino (1975) can be a useful scale for assessing the climates of the city (or urban climate) and to delineate zones according to urban-centric land cover parameters that influence climatic conditions. The first attempt to create climate zones within an urban environment was by Chandler in 1965. He proposed four climatic regions for London; *(I)* Central London, *(II)* Inner Suburban London, *(III)* North London Heights and *(IV)* Outer Suburbs (Figure 2.5). He described zones based on magnitudes of attributes, including wind speeds, concentration of pollution, and number of sunshine hours, temperature, humidity and rainfall. The building patterns such as density (*e.g.* attached versus detached) and type (*e.g.* residential, industrial) influenced the climatic conditions observed by Chandler which led to a delineation of the regions he proposed. He showed a measureable impact on temperature from the influence of the urban landscapes in the city of London (Chandler, 1965, p. 241).

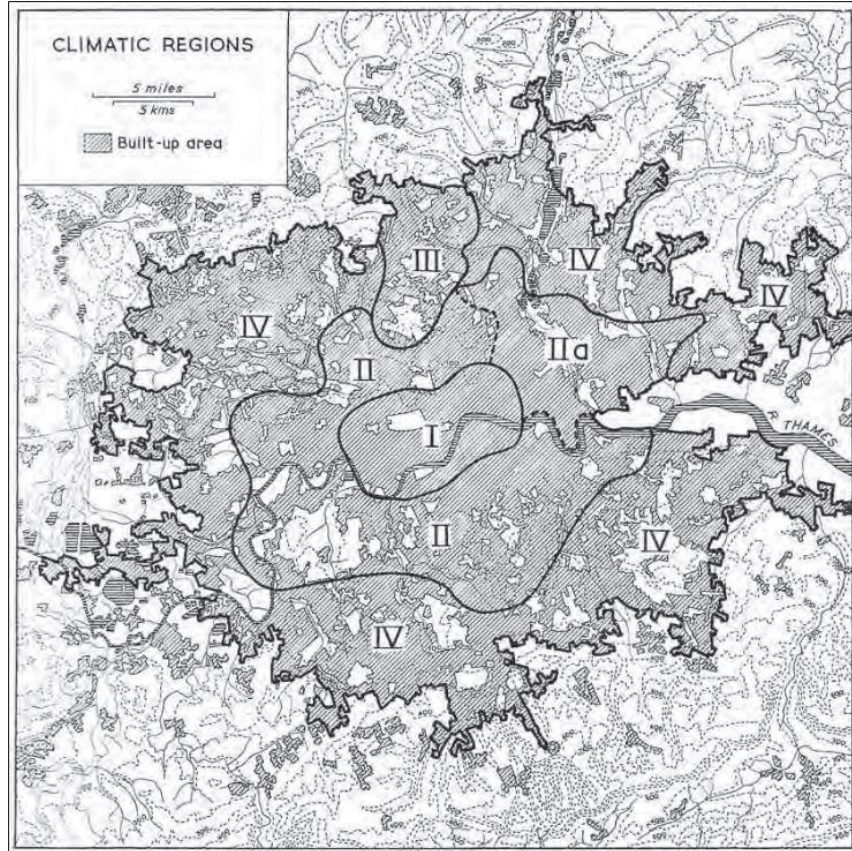


Figure 2.5: Climatic regions of the City of London. (I) Central London, (II) Inner Suburban London, (III) North London Heights and (IV) Outer Suburbs (Chandler, 1965).

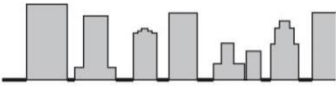






In the decades following Chandler's work environmental studies accumulated in North America suggesting the urban effects on local atmospheric behaviour and this raised concerns of the effect of urbanization on weather and climate (Lowry, 1974, p. 87). This led to a major research program called METROMEX in the United States. The group sought to identify the effects of urbanization on the frequency, intensity and duration of various aspects of the atmosphere and the physical processes responsible for the effect (Lowry, 1974). One of the outcomes of this research program was the contributions made by Auer and Dirks (1974) who used the urban area "as a natural field laboratory" to delineate the modification of the atmosphere by urban influences (Auer and Dirks, 1974, p. 106). Using LIDAR (Light Detection and Ranging) and an instrumented aircraft in the Metropolitan St. Louis area they were able to observe the urban effect on the temperature showing an increase of 0.2 – 2.0 K at about 300 m

above ground level with respect to upwind values (Auer and Dirks, 1974). Building upon the observations they made in St. Louis (*e.g.* Auer, 1976 and Auer, 1978) Auer (1978) proposed 12 meteorological significant zones based upon the percentage of vegetation and building characteristics (*e.g.* office, apartment, industrial, multi-family residential, *etc.*). While not truly climatic zones (as developed by Koppen and Thorthwaite) these areas were based on observed temperature and humidity anomalies attributed to the physical characteristics found on the urban land surface. In classifying these zones Auer (1978) had provided a physical basis for the delineated spaces which can have applications in land use planning with respect to climate. This is in contrast to a land use coding system used for administrative purposes (*e.g.* zoning bylaws) which, although it may have economic and social implications gives little consideration to the climate in the area when making planning decisions.

Similar in motivation to address inadvertent environmental impacts by human activity, Ellefsen (1991) derived a system to define 17 neighbourhood scale areas called urban terrain zones. His research was in response to the needs from scientists engaged in studies pertaining to building damage from acid rain which was gaining national attention during this time. He carried out a study that delineated zones based on physical characteristics of the urban environment. Using ten cities from the United States Ellefsen (1991) defined areas based on building construction type, ventilation characteristics, age of building, density, building surface materials and street pattern. Although Auer and Ellefsen did not intend to create climatologically defined areas, they put into motion a method to formulate climate zones in the built environment at a scale useful for planning purposes, urban temperature studies and city climate research. Building upon this research Oke (2004) designed a simple classification of city zones for the purpose of improving meteorological station siting (Stewart and Oke, 2012, p. 1883). The urban climate zones give the ability to classify areas of the built environments into districts which are “similar in their capacity to modify the local climate” (Oke, 2006, p. 10). These areas would then be the ideal locations for the placement of climate stations to capture the meteorological conditions in the area. The zones were classified according to four basic features including urban structure, urban cover, urban fabric and urban metabolism (Oke, 2006, p. 184). The measurements obtained from climate stations placed in urban environments suffer if the stations are placed in an area that does not capture the local climate near the surface; this is an ongoing difficulty that

Dr. Timothy Oke has tackled over the last decade (Oke, 2004; Oke, 2006). The simplified UCZ classification system (Table 2.1) is useful because it provides a method to create a map of similar areas in urban environments. The map can then be used to identify uniform areas where the placement of an urban climate station is appropriate. The map can be created using land cover properties derived from satellite images, detailed maps, aerial photographs or planning documents.

Table 2.1: Classification of urban forms shown in approximate decreasing order of the ability to have an impact on the local climate (Oke, 2004).

Urban Climate Zone	Image	Roughness Class	Aspect Ratio	% Built (impermeable)
1. Intensely developed urban with detached close-set high-rise buildings with cladding, <i>e.g.</i> downtown towers.		8	> 2	> 90
2. Intensely high density urban with 2–5 storey, attached or very-close set buildings often of bricks or stone, <i>e.g.</i> old city core		7	1.0 - 2.5	> 85
3. Highly developed, medium density urban with row or detached but close-set houses, stores and apartments, <i>e.g.</i> urban housing		7	0.5 - 1.5	70 - 85
4. Highly developed, low or medium density urban with large low buildings and paved parking, <i>e.g.</i> shopping malls, warehouses		5	0.05 - 0.2	70 - 95
5. Medium development, low density suburban with 1 or 2 storey houses, <i>e.g.</i> suburban houses		6	0.2 - 0.6, p to > 1 with trees	35 - 65
6. Mixed use with large buildings in open landscape, <i>e.g.</i> institutions such as hospitals, universities, airports		5	0.1 - 0.5, depends on trees	< 40
7. Semi-rural development, scattered houses in natural or agricultural areas, <i>e.g.</i> farms, estates		4	> 0.5, depends on trees	< 10

2.6 Local Climate Zone Method

A considerable amount of research and observation on urban heat islands was being undertaken during the mid-twentieth century (Chandler, 1964; Bornstein, 1968; Myrup, 1969; Munn *et al.*, 1969; Kopec, 1970; Oke, 1973; Oke and Maxwell, 1975). The contributions by these authors strengthened the knowledge and awareness of the UHI and the local effects of urbanization on climate. During this time the magnitude of the UHI effect came into question.

The general problem of empirical estimation of the magnitude of the urban effects on climate was partly addressed by Lowry (1977) in his proposed method for the estimation of urban effects. Due to the lack of pre-urban temperature records, Lowry (1977) suggested using temperature observation from nearby undeveloped land as a surrogate measure of pre-urban temperatures. Lowry (1977) provided a general framework of definitions and equations for addressing the general problem of estimating empirically the locations, timing and intensities of effects of urbanization on climate.

Recently however, a large volume of UHI literature has come under some scrutiny due to concerns with the methods, communication and definitions used in the studies (Stewart, 2011a; Oke, 2006). This is largely due to a lack of standardization in the methods used for urban temperature studies. Stewart (2011a) summarized the problems as incomplete reporting, flawed design and inconsistent procedures and found that nearly half of the urban heat islands described in the surveyed literature were scientifically indefensible. According to Stewart (2011a) this was due to weakness in the controlled measurement and openness of the method, that is, failure to communicate basic site descriptions or metadata regarding instrumentation used (*e.g.* type and placement of thermometers) and lack of control for confounding effects of site characteristics (*e.g.* slope, elevation, land cover *etc.*). For example, in a review of 190 UHI studies published from 1950 to 2007, Stewart (2011a) reported that only 23% provided full details of their instruments and only 11% provided site descriptions. Most studies (88%) used qualitative descriptors such as “green fields” and “city centre” to describe their rural and urban locations and less than 10% provided quantitative descriptors of site characteristics (Stewart, 2011a, p. 210). Therefore a simple comparison of urban and rural temperature difference (*e.g.* ΔT_{u-r}) is problematic when considering the cultural and administrative differences in the definitions of what was meant by the terms urban and rural.

The capacity to study microclimates in city environments, specifically urban heat islands, has benefited greatly by the work done by Auer, Ellefsen, and Oke (Section 2.5). They provided a foundation for the development of the local climate zone classification system introduced by Stewart and Oke in 2012. Stewart (2011b) redefined the approach to UHI investigations using his LCZ classification as a method for urban temperature studies. He defined seventeen local climate zones which have “regions of uniform surface cover, structure, material and human

activity that span hundreds of meters to several kilometres in horizontal scale” (Stewart and Oke, 2012, p. 1884). The regions are classified into types of zones based upon quantified surface cover and geometric properties. The assumption is that each LCZ has a characteristic temperature near the ground but below the roofs of buildings and tree canopy (*i.e.* urban canopy layer) and the classes are local in scale, climatic in nature and zonal in representation (Stewart and Oke, 2012, p. 1884). The spatial scale upon which the LCZ is based was suggested to be useful for microclimate studies in urban environments, weather forecasting and historical temperature analysis (Stewart and Oke, 2012, p. 1893). For example, statistical regression can use LCZ data to predict temperature patterns within city environments. The LCZ system has the potential to be the standard for climate classification for urban environments. According to Stewart and Oke (2012) the seventeen LCZ patterns should be familiar to heat island researchers in most cities and should be adaptable to most sites. They also note that the LCZ system allows zones to be easily combined into subclasses adding to the flexibility of its application around different landscapes. It can be argued that the most important potential benefit is minimizing the cultural and administrative bias associated with the terms urban and rural. This is because each site can be classified based upon their quantified surface cover and geometric properties. Another problem with urban climate studies reported by Oke (2006) was difficulties in communicating urban temperature study conclusions between cognate fields (*i.e.* engineering, architecture and planning). The LCZ method has the potential to ease this difficulty by introducing geometric and surface cover properties that can be used to describe climatic zones within the urban environs (Stewart and Oke, 2012, p. 1886).

The expectation is that a specific combination of surface cover and geometric parameters will give rise to a specific local climate zone. Once stations are classified into their respective LCZ classes they can be compared with each other or all stations can be compared to a reference rural station. The selection of a reference station is important because the UHI intensity can be over or under estimated based on the physical characteristics that influence the local climate in the rural area (Mohsin, 2009). An arbitrarily chosen rural station can inadvertently introduce a bias in the calculated UHI intensity. This is because UHI intensity is dependent on the temperature of the rural station (since ΔT_{u-r} in equation 1), so the choice of a rural station is an important step in the analysis. Most of the time the rural site is selected based on the distance

away from the urban core. Thus, selecting a reference rural site for comparison with an urban station has been troublesome due to the subjective nature of the selection process. The LCZ addresses this issue by allowing the analyst to select a site based upon quantified surface cover properties which are reflective of rural characteristics (*e.g.* few or no buildings, featureless landscape of plants). This rural site can then be used to calculate the UHI intensity (Equation 1). Furthermore any LCZ class can be compared to any other and differences can be explored.

Using the LCZ methodology, researchers can integrate urban climate knowledge with city planning because it provides a package of urban climate management units for architects, planners, ecologist, and engineers (*i.e.* geometric and surface cover properties within a specified radius). Some researchers have used the local climate zone method to delineate cities into LCZ types and develop urban climate maps (Lelovics *et al.*, 2013; Unger *et al.*, 2014), others used its principles to assess UHI intensities (Tam *et al.*, 2015) and classify measuring stations in studies to find areas susceptible to extreme heat events (Kershaw and Millward, 2012). Using vector and raster based information Lelovics *et al.* (2013) and Unger *et al.* (2014) mapped the climate zones in Szeged, Hungary. They were able to determine 7 of the 10 properties outlined by Stewart and Oke (2012) and made these calculations for a 250 metre radius centred on the measurement location. They then looked at the temperature difference between selected sites for four individual UHI events. Bechtel *et al.* (2012) attempted to differentiate the urban morphologies in Hamburg, Germany and automate the LCZ process using multispectral and multitemporal remote sensing data and then assess the UHI using five months of temperature data. Their study showed the usefulness of remote sensing data in applying the local climate zone system. Fenner *et al.* (2014) analyzed the spatial and temporal air temperature variability in Berlin, Germany and used the LCZ to classify the measuring sites. The use of the LCZ system here is to facilitate better communication of UHI studies such that comparisons can be made between cities with similar regional climates. The usefulness and application of the LCZ system is in its infancy but has shown potential to facilitate better communication of urban temperature studies as well as usefulness in applied mapping. Future research in urban climates has the potential to provide insightful and relevant climatic information for local municipalities facing climate warming in future decades.

2.7 Climate Data and Spatial Interpolation Methods

Meteorological observations in Canada began more than one hundred years before Confederation. The first observations for which there is a record were taken in Montreal in the 1740s by Dr. J. F. Gauthier and later published in the French Royal Academy of Sciences (Thomas, 1970, p. 1). The early history of meteorological data collection can be attributed to the Jesuits in the 17th and 18th century (Stupart, 1912, p. 74). Climatic phenomena such as summer, winter and droughts from the notes of Jesuits provide a general character of the climate in what is now Canada (Stupart, 1912, p. 74). Official weather observations began in the late 1830s and the Canadian Meteorological service was established shortly after Canadian Confederation at about the same time the National Services were established in the United States and parts of Europe (Thomas, 1970, p.1). The first official weather station was established on December 19, 1839 in Toronto (Thiessen, 1940, p. 331) and the first official observation of Toronto was taken on Christmas Day 1839 (Thomas, 1970, p. 3). Since Egerton Ryerson, the Superintendent of Education, established 12 weather observation stations in grammar schools in Canada West (Thomas, 1971, p. 2) the Meteorological Service experienced steady progress until it saw rapid developments during the Second World War due to the popularization of aviation (Thomas 1971, p. 9). The expansion in research and services increased over the 30 years after the war from 1947 to 1971. In 1971 the Meteorological Service of Canada became the Atmospheric Environment Service one of five departments of Environment Canada. Now Environment Canada operates over 1100 climate stations that serve to forecast daily weather conditions and warnings for the public, the travel and tourism industry and provide detailed meteorological information for agricultural and climate change analysis (Environment Canada, 2014). Climate data collection gave scientists like Dr. Oke and Dr. Munn the information needed to assess and analyze the atmospheric layer close to the ground surface in greater detail and as a result they were able to propose theories regarding the urban heat island effect and model it based on variables such as population, wind speed and urbanization (*e.g.* Munn *et al.*, “A Climatological Study of the Urban Temperature Anomaly in the Lakeshore Environment at Toronto”, 1969; Oke, “City Size and the Urban Heat Island”, 1973).

The development of Geographical Information Systems (*i.e.* computer systems that help to organize and analyze geospatial data) has made the collection, distribution and analysis of

spatially distributed climate data more manageable. The ability to collect climatic data such as temperature, at all spatial scales and at any times is now possible given the available GIS tools. For example, spatial interpolation is a procedure of estimating values of properties at unsampled sites within areas that are covered by measured point observation (Burrough, 1986, p. 147). The justification behind spatial interpolation is related to the first law of geography – that on average, points that are closer together in space are more related (or similar) than values of properties that are found farther apart (Burrough, 1986). There are varieties of spatial interpolation techniques rooted on assumptions, constraints and theoretical considerations (Tveito *et al.*, 2006). The nature of the interpolation and the fitting of surrounding values are subjects of ongoing research in geographic information science (Banting, 2014 personal communication). Some assumptions such as stationarity (*i.e.* mean and variance are independent of location and constant over space), spatial dependence (*i.e.* spatial autocorrelation), random variables and normal distribution are needed (and exploited) in order to apply a method and obtain reliable results. Thus the problem of interpolation using GIS tools is in selecting a reasonable method and model to suit the data (Tveito *et al.*, 2006).

Global techniques in interpolation create a model from all the observations of a variable of interest, whereas, local techniques allow estimating values from neighbouring points only (*i.e.* using samples in a neighbourhood or search window) (Li and Heap, 2014, p.175). Deterministic methods such as inverse distance weighting (IDW) will preserve the original data points by creating a surface that honours the measured points exactly (Longley *et al.*, 2011, p. 375). With IDW the estimated attribute at any point is based on the linear combinations of the weighted sum of the values of nearby known sites. The weights of these are proportional to the inverse of the distance between the predicted and measured point. Therefore the closer stations are weighted higher than stations farther away. Inverse distance weighting assumes that the difference between points depends on the distance between the two locations (Tveito *et al.*, 2006, p. 43-44). When using this method there is no measure of uncertainty but the analyst can use cross-validation to investigate the influence of surrounding points. The validation process involves removing one data point and estimating it using all other points; the procedure is repeated for all data points and performance measures can be calculated (Appendix A). Cross validation is simple and quick due to its integration in a GIS and the method is often used in meteorology and

climatology (Tveito *et al.*, 2006). Probabilistic methods such as regression and geostatistics (*e.g.* Kriging) involve the concept of randomness and the resulting interpolated surface can be thought of as one of many that could have been observed given the known data points (Tveito *et al.*, 2006). The benefit of the probabilistic approach is that its methods allow the analyst to calculate statistical significance of the surface and the uncertainty of the predicted values based on the underlying statistical distribution (Tveito *et al.*, 2006). There are several Kriging options that can be used to predict a value of a property at an unvisited location. The Kriging option will depend on the spatial distribution (*e.g.* random, clustered, etc.), density (*e.g.* low or high) and type (*e.g.* continuous or categorical) of the sampled data and the availability of related secondary data which can come from remotely sensed images (Meng *et al.*, 2010). In an experimental comparison of Kriging (ordinary and universal) and IDW, Zimmerman (1999, p. 375) reported that the Kriging methods performed substantially better (*i.e.* lower mean square error) than IDW across four different sampling patterns. Generally due to the greater performance and ability to provide some uncertainty estimation Kriging and its variants are generally a more popular option than IDW.

Kriging of temperature is commonly used in agricultural research (Samanta, 2012), weather forecasting/climate change research (Apaydin *et al.*, 2004) and UHI mapping (Kershaw and Millward, 2012). The purposes of each of these disciplines vary, however, they all employ similar methods to create a temperature surface of the area which does not have measured values at all locations. This is mainly due to the impractical nature of collecting data at all locations in space. The overall benefit of technological improvements and research has resulted in a multitude of available methods and GIS software for exploring and analyzing spatially distributed climate data. This is especially important when air temperature is not sampled at all locations in space but generally measured at meteorological stations in locations determined by nationally managed observing programs. Although technological improvements in GIS capabilities have made computationally demanding methods much easier, the geostatistical methods cannot be executed blindly and automatically and the procedure requires the analyst to become involved in the estimation process (Longley *et al.*, 2011, p.377). By exploring general properties of the measured values including its spatial dependence, *i.e.* how the measured

properties change over distance and direction a “better” model can be developed than one constructed blindly and automatically.

2.8 Redefining the UHI

The econometric professor, Roger Koenker, who’s named statistic, Koenker BP Stat, is often used in geostatistics to check for stationarity, has been quoted as saying that “Rather than filling gaps in the literature one of the great accomplishments of science research is to *create* gaps in the literature by debunking the nonsense of the past” (Koenker, 2015). It can be argued that Stewart (2011b) in his PhD dissertation redefined the UHI by proposing a new approach for undertaking urban temperature studies. He did this by exposing the common pitfalls and methodological flaws associated with carrying out UHI research in the past 50 years. What may be required now in urban climatology is to evaluate his process and make suggestions on what can be added to improve its application.

Given the current trend in urbanization in Southern Ontario and the expected warming climate, an assessment of the current state of the microclimate in the region can reveal pertinent information to city planners, the public and municipal governments. Using a local scale spatial perspective and the method presented by Stewart and Oke (2012) a less subjective approach to UHI studies can be made using Southern Ontario as a case study. The expectation from this research is that microclimates that have a higher degree of “urbanicity”, *i.e.* having more impervious areas and a higher number of buildings, would experience elevated air temperatures when compared to sites considered less urban. The general premise is that air temperature measured in “urban” areas (T_u) is generally greater than air temperature measured in “rural” areas (T_r) resulting in an urban heat island effect. It has been suggested that in southern Ontario the highest UHI magnitudes were found during the winter seasons (Mohsin, 2009). Therefore seasonal magnitudes of UHI intensities can also be explored to assess when the UHI effect is most pronounced. Also due to the practical limitations of collecting air temperature measurements at all locations in space, spatial interpolation by ordinary Kriging can be used to explore the general spatial pattern of air temperature in southern Ontario. The expectation from this analysis is that areas considered more urban will be warmer than less urban areas, thus it is an exploration of urbanicity (Figure 2.6).

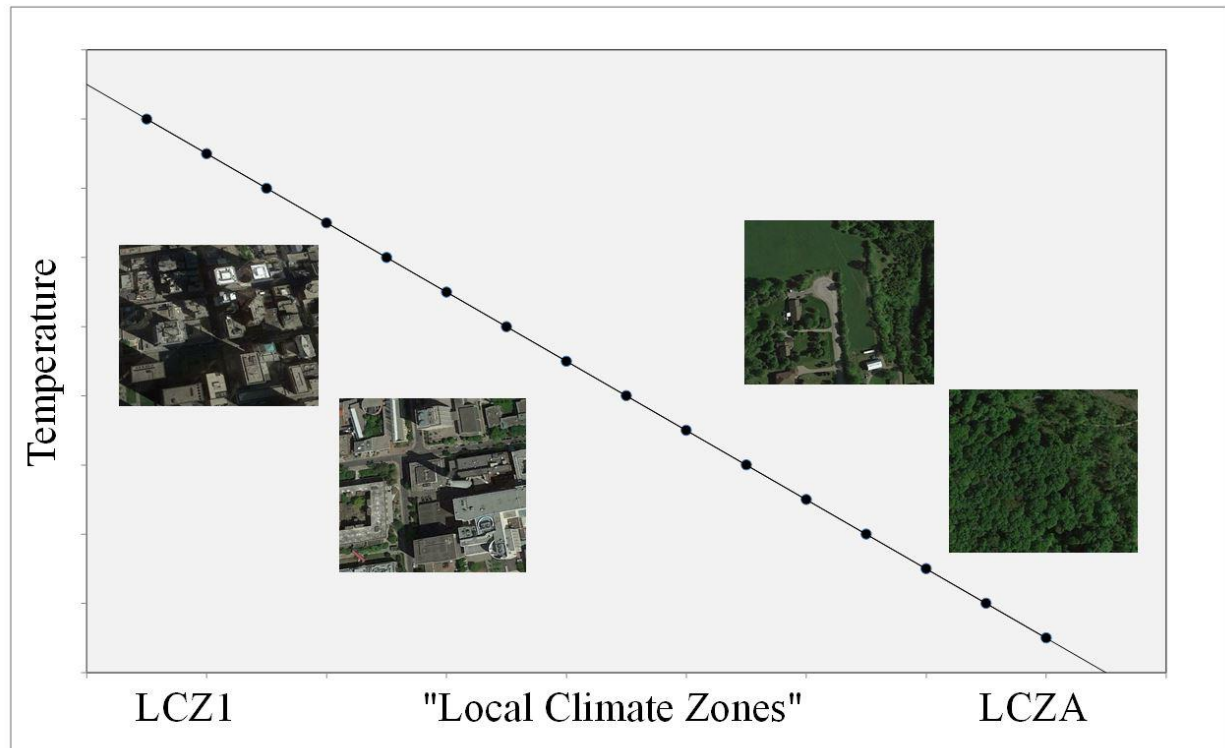


Figure 2.6: General expectation of temperature response based upon local climate zones units. LCZ 1 to LCZ 10 represent built-types in descending degrees of urban zones and LCZ A to LCZ G are categorically defined land cover types representing rural zones. Two of the seventeen local climate zones are labeled. Images Google™ earth.

3. DATA COLLECTION AND METHODS

3.1 Study Area

Southern Ontario is one of the most populated areas in Canada. The particular ecumene in this study extends from the west to east along the north shore of Lake Ontario from Burlington to Bowmanville and north to the leading edge of the Oak Ridges Moraine (Figure 3.1). The almost one-hundred and fifty kilometre stretch is home to a number of larger cities in the west and smaller cities, towns, agricultural and forested lands to the east. The mesoclimate in Southern Ontario is a result of geographical influences such as topography, latitude, elevation and distance to water bodies, whereas the local climatic controls are urbanization and surface cover characteristics.

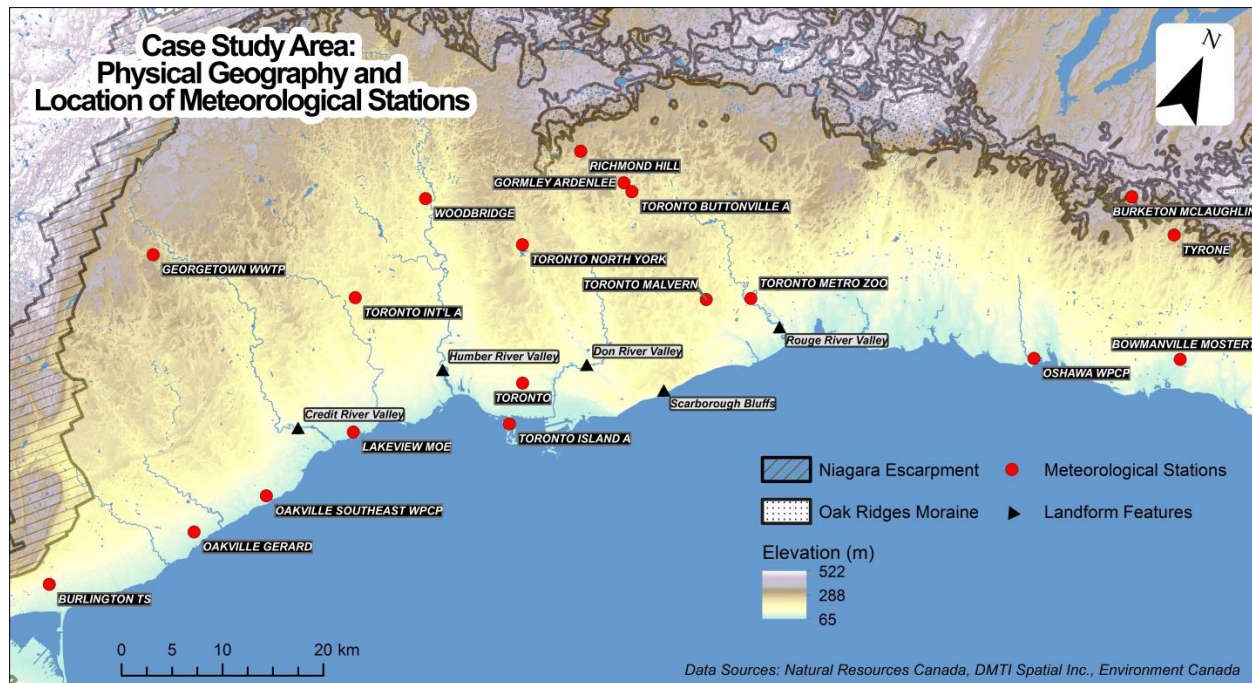


Figure 3.1: Physical geography of southern Ontario study region showing landform features and the location of the 19 meteorological stations included in the case study. (Natural Resources Canada, 2014, DMTI Spatial Inc., 2011 and Environment Canada, 2013).

The local geography of Lake Ontario's north shoreline features numerous watersheds such as the Credit, Rouge, Don and Humber river valleys. The dominant upland area is the Scarborough Bluffs. The northwest extent of the study area is the foot of the 80 to 100 metre high Niagara Escarpment and the northern extent is the Oak Ridges Moraine. This moraine represents the drainage divide and according to Munn *et al.* (1969) also functions as a significant climatological division.

At a mesoscale, southern Ontario has a modified continental climate and experiences less severe weather when compared to most other parts of Canada. The mild weather conditions experienced in this region is a major reason for industrialization and the current and expected population growth. In general southern Ontario's climate is affected by two major air sources: cold and dry polar air from the north which is dominant during the winter months and warm and moist sub-tropical air from the Atlantic Ocean and Gulf of Mexico in the summer (Baldwin *et al.*, 2000, p. 17). It is designated as a D_{bf} climate based on the Koppen classification system and Lake Ontario Shore climate by Brown *et al.* (1980, p. 8). Lake Ontario also has a profound effect on the local climate of cities and towns in close proximity. Large waterbodies show little diurnal

change in surface temperature when compared to most land surfaces (Oke, 1992, p. 167). The surface temperature differences between the land and lake produce air pressure differences above the surface resulting in a daytime lake breeze and nighttime land breeze during anti-cyclonic (*i.e.* clear skies) conditions (Oke, 1992, p. 168). These breezes happen when the air over the land is colder or warmer than that over the water with the colder air moving towards the warmer air (Brown *et al.*, 1980, p.7). As a result the lake moderates the occurrences of local temperature extremes during summers and winters (Munn *et al.*, 1999, p. 36). The temperatures at weather stations located near the shoreline (*e.g.* Lakeview MOE, Toronto, Toronto Island, and Oshawa WPCP) would be expected to experience these lake effects (Mohsin and Gough, 2010, p. 318).

The temperature data from the meteorological stations east of the Niagara Escarpment and south of the Oak Ridges Moraine were selected for this case study. These nineteen meteorological stations were chosen because they were situated in the Lake Ontario shoreline climatic region and an effort was made to minimize the moderating effects from the lake and to reduce the potential effects from major landscape features such as the escarpment and moraine. Five of the nineteen stations were located within the City of Toronto's administrative boundary limits and the remaining fourteen stations were situated to the west, north and east of the City.

The temperature data were collected from Environment Canada's (EC) climate data website (<ftp://ftp.tor.ec.gc.ca/Pub/> and <http://climate.weather.gc.ca/>). Environment Canada manages a network of climate stations that record numerous meteorological measurements such as minimum and maximum temperatures across the country. The temperature measurements are made from self-registering maximum and minimum thermometers recorded in a 24-hour period and the thermometers are housed in a louvered shelter approximately 1.5 m above the ground on a generally level and grassy surface (Environment Canada, 2013a). These observations are averaged over days, months and years for each station and from these observations climate normals are produced (also known as climate means or climate averages). The results are mean-daily temperatures that are averaged for each month and these mean-daily temperatures for the month are averaged for the year producing mean-daily, maximum-daily and minimum daily temperatures for the year and month (Environment Canada, 2013b). The World Meteorological Organization (WMO) recommends that countries produce climate normals for the official 30-year normal periods ending in 1930, 1960 and 1990 with updated climate normals made

available at the end of every decade. Every country's climate normals are calculated according to the standards set forth by the WMO (Davidson *et al.*, 1989). Although additional data were available throughout the region, they did not span the time frame or adhere to the standards set forth by the WMO and as a result the data used in this research generally represents the best available. The climate normals were available in mean-daily, maximum-daily and minimum-daily temperatures for each month and the year. The mean-daily temperature for the year is a useful variable for making comparisons within a region (Brown *et al.*, 1980, p. 14). The most recent release of climate normal, for the period 1981 to 2010, was used in this analysis. The database file from Environment Canada contained monthly (mean-daily, maximum-daily and minimum-daily) temperatures and the annual (mean-daily, maximum-daily and minimum-daily) for the period 1981 to 2010 for all 238 meteorological stations currently active in Ontario. A simple Perl script was used to extract the temperature records of the 238 stations from the database file to a workable spreadsheet file. The spreadsheet file is also appropriate for conversion to formats suitable for statistical and GIS software to operate upon (*e.g.* calculating geometric attributes including distance of each meteorological station from Lake Ontario). The temperature records for the nineteen meteorological stations identified in Figure 3.1 were extracted and used in this analysis.

3.2 Local Climate Zone Method

The local climate zone method (Stewart and Oke, 2012) was used to classify the 19 meteorological stations within the study area into one of the seventeen LCZ units. The LCZ method can be simplified into three steps (orange fill in Figure 3.2).

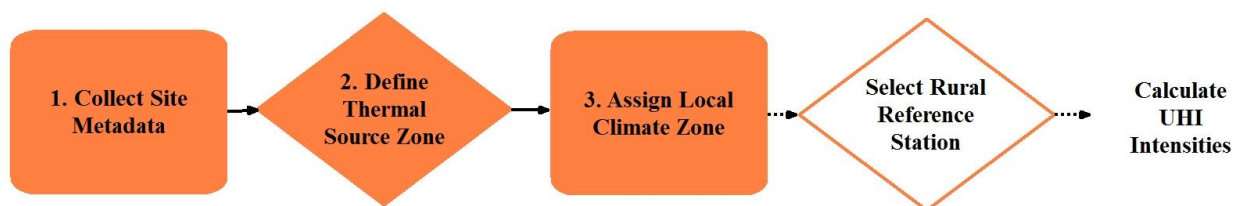


Figure 3.2: Local climate zone classification workflow. The orange fill represents the LCZ method proposed by Stewart and Oke (2012).

Site metadata includes detailed site descriptions and quantified surface cover fractions. This information was collected using satellite images, Google Earth and calculated using GIS data representing land cover (raster format) and land use (vector files). The thermal source zone is difficult to define in urban environments because of the variability in surface types (Schmid *et al.*, 1991, p. 249). Simple methods such as vectors of a wind rose representing surface wind patterns over specified time periods can be used to define an appropriate source area sensed by the climate station, but this requires complete wind data for each of the stations which are unavailable for the selected stations. In general wind patterns over a shorter time period would be shaped like an ellipse with the major axis in the upwind direction whereas over a longer time period the thermal source area would approach the shape of a circular area (Stewart, 2011b, p. 255).

Stewart and Oke (2012, p.1890) suggest that a source area for screen height temperature measurements in stable conditions would be on average a few hundred meters away and they argue that each LCZ should have a minimum radius of 200 – 500 m in order to capture conditions that influence the measured temperature. Fenner *et al.* (2014) used multiple radii (200, 350, 500, 700 and 1000 metres) to report the local landscape, however, they used only the 500 metre radius to classify the measurement sites according to the local climate zone method in their study to explore the long term and short term dynamics of air temperature variability. Therefore a circular thermal source area at multiple radii (100, 500 and 1000 metres) was assumed since the temperature observations used in this analysis were gathered over longer time periods (at least 15 years). The multiple radii were chosen in order to capture the physical characteristics of city blocks and neighbourhoods in order to explore micro to local scale climatic effects (Section 2.5).

Stewart and Oke (2012, p. 1887) identified seventeen local climate zone classes which consist of 10 built types representing urban-centric properties and 7 land cover types representing rural-centric properties. The urban zones are numbered according to a decline from more urban (1) to less urban (10), whereas rural land cover classes are categorized nominally, and coded from A to G. The code for a station is based on characteristics of its site, depending on: (1) a set of four geometric properties such as sky view factor, aspect ratio, and terrain roughness class, height of roughness elements, (2) a set of five surface cover properties such as

impervious surface fraction, pervious surface fraction, building surface fraction, surface admittance, surface albedo and (3) anthropogenic heat output (*i.e.* fuel combustion and human activity). Each of the local climate zones has a range of values for each of the parameters listed above. For this analysis the 19 stations were classified using three of the five surface cover properties designated in the local climate zone units. The surface cover properties used were impervious surface fraction (ISF) defined as the ratio of paved/rock area to total area, pervious surface fraction (PSF) defined as the ratio of bare soil, vegetation and water to total area, and building surface fraction (BSF) defined as the building plan area to total area (Table 3.1).

Table 3.1: The three surface cover properties used for classifying the 19 meteorological stations. (Stewart and Oke, 2012)

LCZ Class	Local Climate Zone Description	Building Surface Fraction (%)	Impervious Surface Fraction (%)	Pervious Surface Fraction (%)
LCZ 1	Compact high-rise	40 – 60	40 – 60	< 10
LCZ 2	Compact mid-rise	40 – 70	30 – 50	< 20
LCZ 3	Compact low-rise	40 – 70	20 – 40	< 30
LCZ 4	Open high-rise	20 – 40	30 – 40	30 - 40
LCZ 5	Open mid-rise	20 – 40	30 – 50	20 - 40
LCZ 6	Open low-rise	20 – 40	20 – 40	30 - 60
LCZ 7	Lightweight low-rise	60 – 90	< 10	< 30
LCZ 8	Large low-rise	30 – 50	40 – 50	< 20
LCZ 9	Sparsely built	10 – 20	< 20	60 - 80
LCZ 10	Heavy industry	20 – 30	20 – 40	40 - 50
LCZ A	Dense trees	< 10	< 10	> 90
LCZ B	Scattered trees	< 10	< 10	> 90
LCZ C	Bush	< 10	< 10	> 90
LCZ D	Low plants	< 10	< 10	> 90
LCZ E	Bare rock or paved	< 10	> 90	< 10
LCZ F	Bare soil or sand	< 10	< 10	> 90
LCZ G	Water	< 10	< 10	> 90

The surface cover fractions for the five meteorological stations located within the City of Toronto boundary were calculated from the digital land cover raster dataset available through the city's Open Data Catalogue (City of Toronto, 2009). The high resolution land cover raster dataset was developed as part of the Urban Tree Canopy Assessment for Toronto which was funded by the United States Department of Agriculture (USDA) Forest Service and the City of Toronto (City of Toronto, 2009). The primary image source used to create this dataset came from

Quickbird satellite imagery acquired between 2004 and 2007, with a 60 cm resolution. The land cover raster dataset was categorized into 8 land cover classes (Figure 3.3) which went through over fifty-thousand manual corrections by City of Toronto staff (City of Toronto, 2009).

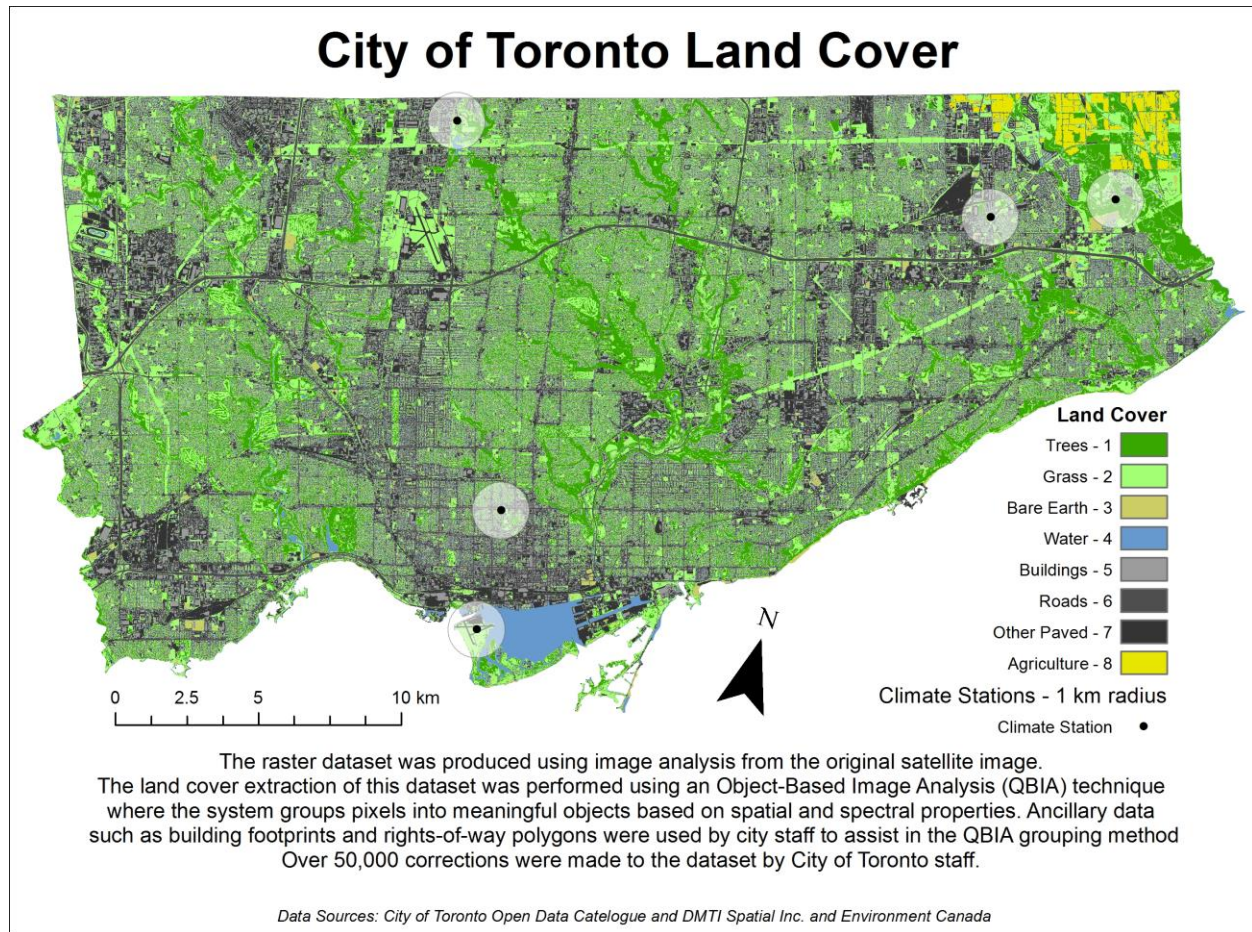


Figure 3.3: The City of Toronto land cover map used to calculate land cover areas and land cover fractions. Image sourced from Quickbird satellite imagery acquired in 2007, with 60 cm resolution. (City of Toronto, 2009, DMTI Spatial Inc., 2011, Environment Canada, 2013)

The land cover raster file was converted into a polygon (vector) layer using ArcMap v.10.2 and each of the 8 classified areas was sorted into the four surface cover categories: (i) impervious surface areas (ISA), (ii) pervious surface area (PSA), (iii) building surface area (BSA), and (iv) tree canopy area (TCA). Tree canopy area is not a surface cover parameter used in the LCZ classification system, but was included for correlation analysis to explore its relationship with temperature (Section 3.3). The tree canopy in the City of Toronto dataset is

categorized using a top down assessment which potentially overlaps with other features (*e.g.* buildings, sidewalk, grass, roots, *etc.*). The surface cover fractions (*i.e.* ISF, PSF, BSF and TCF) were then calculated using their respective surface cover areas and total thermal source zone area. The procedure was repeated for each thermal source zone (*i.e.* 100, 500, 1000 metre radius).

Additional land cover data were needed because the study area extended beyond the administrative boundary of the City of Toronto. The Ontario land use data (DMTI Spatial Inc., 2011) were used to collect surface cover areas for the 14 meteorological stations located beyond the City boundary. In general, land use (LU) mapping differs from land cover (LC) mapping in that land use specifies the designated human use of the land and land cover reflects the actual surface of the land, into classes that acknowledge the appearance which may not necessarily reflect human usage. Thus land use refers to the patterns of construction and activity that is present such as: commercial, government and institutional, open area, parks and recreational, residential, resource and industrial, or waterbody (DMTI Spatial Inc. 2011) (Figure 3.4).

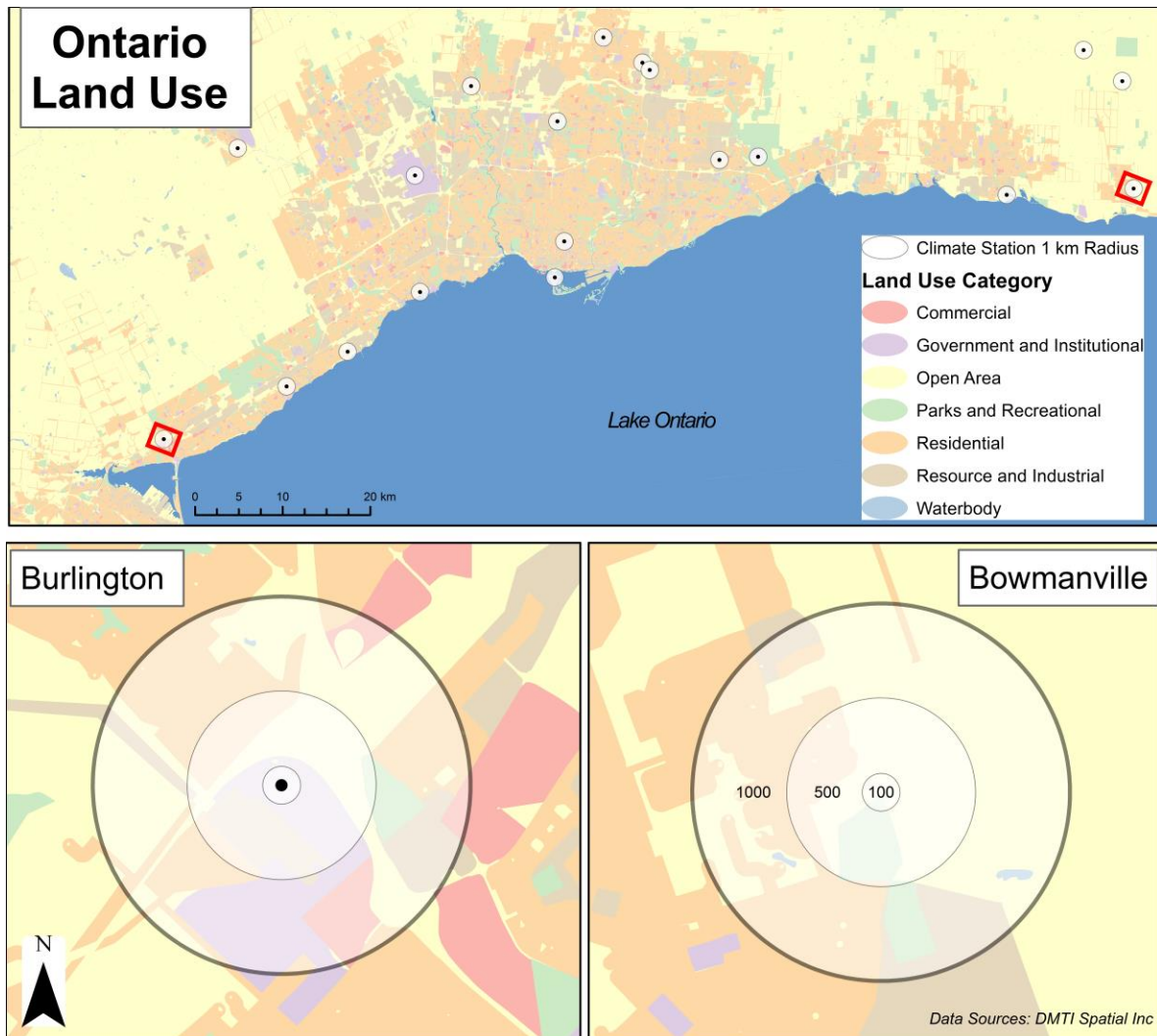


Figure 3.4 Ontario land use polygons dataset used to capture the land cover within the 500, 1000 metre radii centred on the meteorological station location. Burlington and Bowmanville are shown as examples. (DMTI Spatial Inc., 2011).

The land use vector dataset used in this analysis was initially created by DMTI Spatial Inc. using the National Topographic Database (NTDB). The NTDB was produced by the federal government and is Canada’s most detailed and accurate digital vector dataset with coast to coast coverage (DBx GEOMATICS Inc., 2012, pp.27). This dataset was realigned and reclassified by DMTI Spatial Inc. using up-to-date sourcing from their own geospatial data products such as CanMap Streetfiles and Enhanced Points of Interests (EPOI) (DMTI Spatial Inc., 2011). As a result the available LU data had more detail or “high resolution” (*i.e.* smaller polygons) when compared to LC data which had “low resolution” (very large polygons). The zones around the

stations in the LU dataset zones provided a basis for establishing the abundances of land cover needed to calculate the surface cover parameters associated with the LCZs. Therefore the decision to use LU data over LC data was made because of the greater detail in the LU dataset. Having small polygons (*i.e.* the DMTI Spatial Inc. LU dataset) made updating and editing the surface cover easier and provided a relevant spatial scale to carry out this research. Furthermore smaller polygons made it possible to break up the editing and updating process into manageable tasks.

The base-map add-on function in ArcMap v.10.2 was used as a backdrop to delineate the surface cover areas. The base-map satellite images were originally captured between 2011 and 2013 and sourced from DigitalGlobeTM and Centre National d'Etudes Spatiales (CNES) with a 50 cm resolution. The Ontario LU vector dataset was layered over the satellite images and the LU dataset was updated, using ArcMap's Edit Tool, to represent the four different surface cover areas (*i.e.* ISA, PSA, BSA, and TCA). The tree canopy was represented by forest patches generally found in large undeveloped areas. The single trees that line streets were not incorporated into the tree canopy area. The surface cover fractions were calculated using the four calculated surface cover areas that were generated by editing the vector polygons to match the surface below (Figure 3.5).

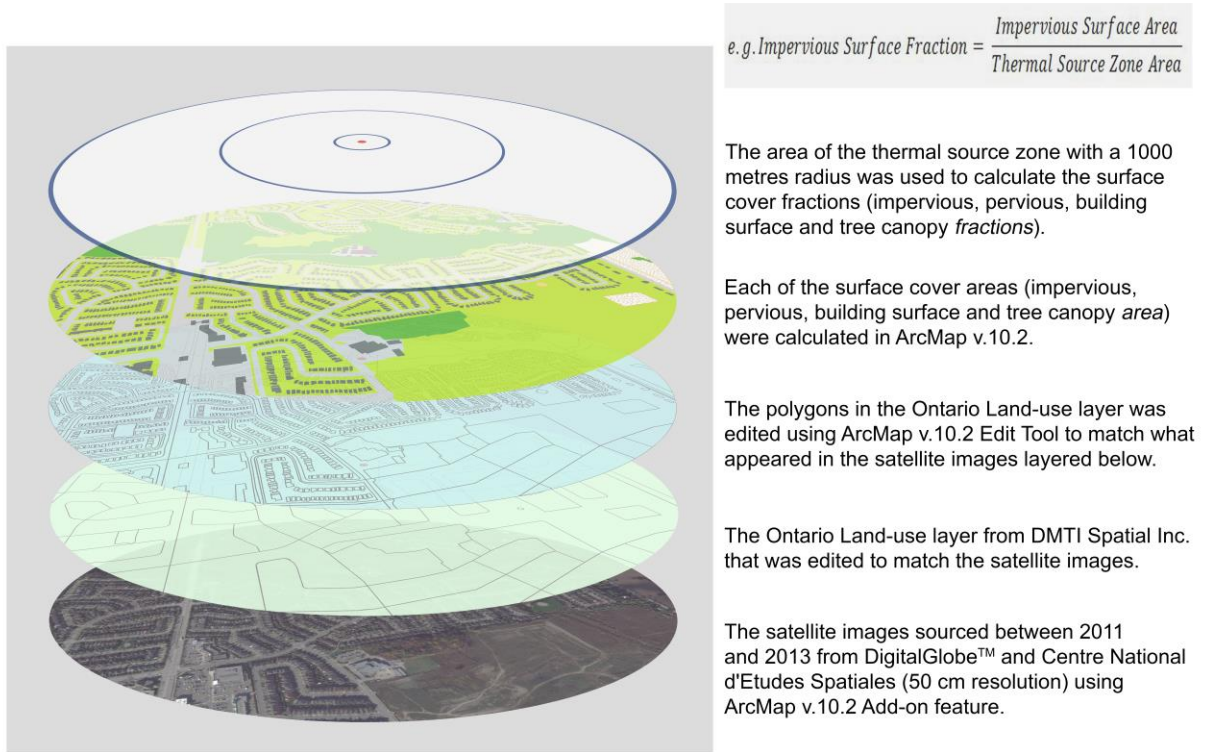


Figure 3.5: Process for calculating surface cover fractions for fourteen of the nineteen meteorological stations used in this case study.

The 19 meteorological stations were assigned a local climate zone class based upon the calculated impervious, pervious and building surface fractions. Candidate LCZs for each of the 19 meteorological stations were generated using Query Builder in ArcMap v. 10.2. Query Builder uses Structured Query Language (SQL) expressions to select a subset of table records based upon attribute values (ESRI, 2014). A series of SQL expressions for each LCZ shown in Table 3.2 were used to identify potential LCZ candidates. Stewart and Oke (2012) suggested that any stations that matched poorly with those in the LCZ were assigned to the nearest equivalent LCZ.

The UHI intensity (Equation 1), specifying the difference between the urban and rural temperature is typically calculated based on a single reference meteorological station defined as rural. Stewart *et al.*, (2013) suggest using one of the land cover types (*i.e.* LCZ A through LCZ D) as a reference station for calculating UHI intensities, however, the temperature differences can be explored between any two local scale settings (*i.e.* any two LCZs). If multiple rural

station candidates are generated then they can all be used to calculate the UHI intensity and their differences can be explored and commented on. The two sample t-test was used to check if there is any significant difference between the two UHI intensities calculated with two different sample rural stations. The mean-daily, minimum-daily and maximum-daily temperatures for the year (hereafter \bar{T} , T_{\min} , T_{\max}) were compared between the selected reference rural stations and all other stations using equation 1 (Section 2.2). Similarly the monthly mean-daily temperatures were grouped into seasons, December to February representing winter conditions, March to May representing spring conditions, June to August representing summer conditions and September to November representing fall conditions.

In light of classifying the stations according to climate zones, the terms urban and rural are no longer required to assess the difference between any two sites and therefore based upon Stewart and Oke (2012) research, the UHI was defined as

$$UHI\ Intensity = \Delta T_{LCZ\ X-LCZ\ Y} \text{ (Equation 2)}$$

where LCZ X is the station that is being compared to the reference station LCZ Y (or any other station). This equation, like equation 1 will reveal the magnitude of the UHI intensity in units K (kelvin) where a positive value signifies the presence of a “heat” island and a negative value signifies the presence of a “cool” island (Fenner *et al.*, 2014, p. 320).

3.3 Statistical Analysis

Statistical analysis was performed using IBM SPSS software, Microsoft Excel and ESRI’s ArcMap v.10.2. All descriptive statistics such as means, standard deviations, maxima, minima and their respective graphical representations, and two sample t-tests and analysis of variance (ANOVA) were calculated using Excel and SPSS. The temperature parameters (*i.e.* mean, minimum, maximum and DTR) and surface cover fractions were tested for normality using the Shapiro-Wilk’s test because of the small number of observations ($n < 50$). Ordinary least squares (OLS) regression was performed in ArcMap v.10.2 with each of the temperature variables as the dependent variable (*e.g.* daily mean, daily maximum, daily minimum and diurnal temperature range) and each of the four surface cover fractions as explanatory variables to

explore the relationships between temperature and each of the surface cover fractions at the local spatial scales (*e.g.* at a radius of 100, 500 and 1000 metres). The \bar{T} , T_{\min} , T_{\max} were regressed with latitude, elevation, distance to Lake Ontario, and distance to the urban core in order to assess the influence of these confounding factors on the local temperatures. The benefit of using the OLS option in ArcMap is that a set of diagnostics can be generated by the OLS Tool. Diagnostics checks such as the correlation coefficient (r) and coefficient of determination (r^2) were used to check for model performance. The correlation coefficient is a measure that is used to describe the relationship between the independent variable and the dependent variable and the coefficient of determination provides a measure of the proportion of the variance in the dependent variable that is explained by the independent variable (Allen, 1997 and Mendenhall *et al.*, 2011). Model bias was checked in ArcMap v.10.2 using the Jarque-Bera statistic where if the statistic is statistically significant then the model was considered biased, suggesting that the residuals are not normally distributed (Jarque and Bera, 1987).

One of the most popular methods of spatial interpolation for temperature is Kriging. Kriging assumes that the spatial variation of a variable is neither totally random nor deterministic (Chang, 2010). Alternatively the spatial variation may consist of three components, (1) a spatially correlated component, (2) a structure representing a trend, and (3) a random error term (Chang, 2010, p. 327). The interpretation of these components has led to different Kriging techniques. Regression-Kriging is one of the most used and involves one deterministic model and one stochastic residual model (Dobesch *et al.*, 2007). The deterministic model is based on the relationship between temperature and different physiographical characteristics such as topographical, land use and land cover properties. The physical characteristics (or parameters) that can be included will depend on the spatial scale (*e.g.* macro, meso, local or micro) and coinciding climate conditions of the study area as well as the available datasets describing the locations to be mapped (Dobesch *et al.*, 2007). The deterministic component most used is a multiple regression model which can include many explanatory parameters. The residuals can then be interpolated by Kriging. The constraint on using regression-Kriging is that the method requires auxiliary variables that have significant correlation with environmental predictors which are available over the entire area of interest (Meng *et al.*, 2013, p. 38 and Szymanowski *et al.*, 2013, p. 579), and the need for a large set of observations (*e.g.* at least 10 per predictor) (Hengl

et al., 2007, p. 1312). Co-Kriging is used when secondary data that correlate well with the primary variable (*i.e.* the variable being predicted) are available at additional sampling locations (Baily and Gatrell, 1995). Thus the use of co-Kriging benefits when secondary data are available in locations where the primary data are not sampled and the primary and secondary variables are correlated. Then the method of estimating and modelling this correlation involves the cross-variogram between the two variables *i.e.* the spatial association between the primary and secondary variables (Bailey and Gatrell, 1995, p. 213). Ordinary Kriging (OK) is another popular method though simpler to use (Appendix A). The method assumes the data are stationary (*i.e.* having no significant trends) over the study area, but more importantly within the search neighbourhood (Baily and Gatrell, 1995, p. 192), and the focus is on exploiting the spatially correlated component using a fitted semivariogram (*i.e.* the spatially correlated component) for the interpolation (Holdaway, 1996 and Chang, 2010). A semivariogram can also be used to check for isotropy (*i.e.* spatial correlation that changes with distance) and anisotropy (*i.e.* spatial correlation that changes with direction) in the Geostatistical Analyst Tool found in ArMap v.10.2 (*e.g.* Explore Data) (Johnston, *et al.*, 2003, p. 107). Holdaway argued that regional trends are usually not a problem because the stationarity assumption applies to the search neighbourhood used in the interpolation and at a local scale the area may be reasonably homogeneous (Holdaway, 1996, p. 216). For example, in trying to interpolate monthly temperature records Holdaway (1996) reported that moderate trends in the data (*e.g.* lake effect) did not seriously degrade the application of ordinary Kriging and argued that the small improvement gained through de-trending did not warrant the greater computational effort (Holdaway, 1996, p.224). However, if the mean values change abruptly over very short distances (*i.e.* non-stationary) then de Smith *et al.* (2015) suggest alternative models be used (*e.g.* Universal Kriging or Kriging with a trend). These geostatistical approaches require input and interpretation from the analyst and thus it is not a process that can be run automatically.

Given the small number of observations and lack of continuous environmental secondary data for the study area, regression-Kriging is not likely an ideal geostatistical approach for interpolating the air temperature for the given study space. Ordinary Kriging is generally preferred over simple Kriging because OK requires neither knowledge nor stationarity of the mean over the region of interest and it is easier to implement (Li and Heap, 2014, p. 176).

Therefore, ordinary Kriging was used to create a temperature surface of the study region in order to examine the spatial structure of the climatic averages (*i.e.* mean, minimum and maximum temperatures). The general equation to estimate a value at an unsampled point using ordinary Kriging is (Lloyd, 2001 and Chang, 2010):

$$z_0 = \sum_{i=1}^n z_s W_s \text{ (Equation 3)}$$

where z_0 is the estimated value, z_s is the known value at point s , W_s is the weights associated with point s and the weights are calculated using the semivariance (*i.e.* the spatial dependence between known points) and n is the number of sample points used for estimation.

The performance of the interpolation method was assessed using the difference measure of the mean error (ME) and the root-mean-square error (RMSE) which should be as small as possible if the resultant temperature surface is accepted as a representation of its spatial pattern. Mean error (ME) is the averaged difference between the measured and the predicted values, thus a value close to zero is desirable and the root-mean-square error indicates how closely a model predicts the measured values. Therefore the smaller the RMSE value the better the model. According to Willmott (1982, p. 1310) RMSE is one of the best overall measures because it summarizes the mean difference in the units of observed and predicted values. The mean error and RMSE for the study area are automatically calculated in the Geostatistical Analyst Tool found in ArcMap v.10.2. Also in ArcMap v. 10.2 the prediction standard error can be mapped. The prediction standard error is the square root of the prediction variance, *i.e.* the variance associated with the difference between the true and predicted values. Providing the sampled temperature averages are normally distributed, then 95 *per cent* of the time the “true” value will lie within the predicted value plus or minus two times the prediction standard error (ESRI, 2014).

The \bar{T} , T_{\min} , T_{\max} were interpolated over the study area based on the observations from the 19 meteorological stations using Ordinary Kriging (OK) and Ordinary Co-Kriging (OCK). The calculated surface cover fractions of impervious, pervious and building surface abundance were used as secondary data in the OCK model. The average distance between all pairs of points was used as the lag size in the semivariogram model since directional influences can be

accounted for when the semivariance increases more rapidly in certain directions (ESRI, 2010). Directional influences were checked with the Geostatistical Analyst Tool using the semivariance cloud to identify anisotropy. The corresponding angles were used in the Kriging method with anisotropy enabled. The number of lags was varied and the model was allowed to be optimized by ArcMap v.10.2. The model with lowest RMSE was chosen as the model used to create the temperature surface for the study area.

A full summary of all the analyses is shown in Figure 4.6. The workflow can be summarized as follows: using the dataset of land cover and land use three of the five surface cover properties were calculated for each of the 19 meteorological stations using land cover/land use found within the thermal source zones. Each station was classified based upon its surface cover fractions using SQL expressions. The least urban, or “rural” site was identified and the \bar{T} , T_{\min} , T_{\max} UHI intensities as well as the seasonal mean-daily UHI intensities were calculated. The calculated surface cover fractions were then used to perform correlation analysis with temperature. The \bar{T} , T_{\min} , T_{\max} for the study area were interpolated using ordinary Kriging and the prediction errors for the study area were mapped.

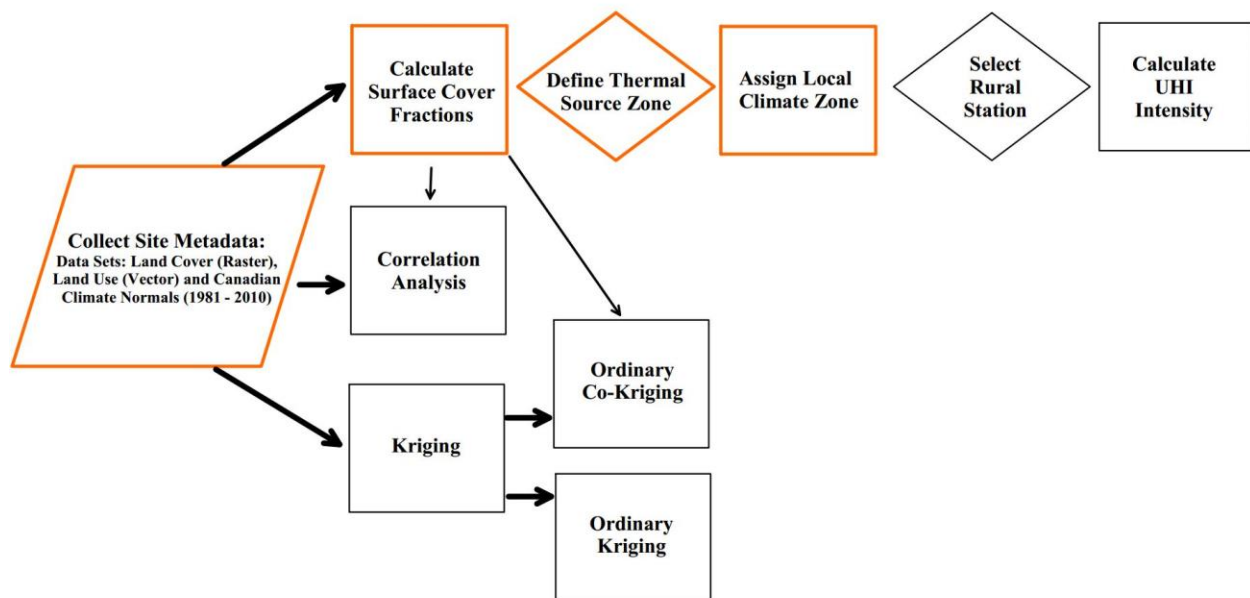


Figure 3.6: Flowchart of methods. The orange flowchart diagrams signify the local climate zone method (Stewart and Oke, 2012) shown previously.

4. RESULTS

4.1 The Surface Cover Fractions around the Meteorological Stations

The surface cover fractions for the nineteen meteorological stations were calculated in order to report appropriate landscape properties that surround the locality of each station. These properties are used to identify the most urban and most rural stations and then used to assign each of the stations an LCZ designation. The impervious surface fraction, pervious surface fraction, building surface fraction and tree canopy fraction were calculated for the area covering both the five-hundred metre and the one-thousand metre radius around each meteorological station. The surface cover fractions including the total building count for the five-hundred metre radius and one-thousand metre radius, the temperature normals and the means and standard deviations for each variable are shown in Table 4.1 in descending order of \bar{T} . All temperature variables (\bar{T} , T_{\min} , T_{\max}) and surface cover fractions were found to be normally distributed (with the exception of the tree canopy fraction), because there was insufficient evidence to reject the null using the Shapiro-Wilk's test (Table A1 and A2 in the Appendix A).

Table 4.1: The calculated impervious surface (ISF), pervious surface (PSF), building surface (BSF) and tree canopy (TCF) fractions, number of buildings, surface area of buildings for the five-hundred metre and the one-thousand metre radius thermal source zones and annual \bar{T} , T_{\min} , T_{\max} and diurnal temperature range (DTR).

Station Name (Climate ID and Location)	Surface Cover Fractions (%)								Number of Buildings		Climate Normals			
	ISF		PSF		BSF		TCF		Count		Air Temperatures (°C)			DTR (K)
	500 m	1000 m	500 m	1000 m	500 m	1000 m	500 m	1000 m	500 m	1000 m	Mean	Min	Max	
Toronto (6158350) 43.666, -79.4	31.8	30.3	39.0	39.2	29.2	30.5	19.8	22.7	554	2,822	9.4	5.9	12.9	7.05
Oakville Gerard (6155PD4) 43.428, -79.696	14.2	24.0	62.5	62.5	13.2	13.5	0.0	1.7	674	2,098	9.11	4.38	13.8	9.42
Burlington TS (6151064) 43.333, -79.833	43.9	32.5	59.8	59.8	1.8	7.7	1.4	7.1	24	537	9.07	4.44	13.69	9.25
Toronto North York (615S001) 43.78, -79.467	21.5	28.3	64.5	55.0	14.0	17.5	31.1	25.3	50	477	8.55	3.71	13.36	9.65
Toronto Island A (6158665) 43.628, -79.395	33.9	16.3	63.8	81.5	2.3	2.2	2.6	6.2	30	122	8.49	4.84	12.11	7.27
Lakeview MOE (6154310) 43.566, -79.566	23.1	24.7	64.4	64.2	12.5	11.1	0.7	0.9	476	1,548	8.44	4.2	12.65	8.45
Toronto Pearson (6158733) 43.677, -79.63	50.9	50.3	26.7	42.4	22.4	7.0	0.0	0.3	32	44	8.17	3.32	13	9.68
Oshawa WPCP (6155878) 43.866, -78.833	15.3	22.5	76.2	70.2	8.6	7.3	22.0	13.3	179	950	8.12	4.1	12.12	8.02
Toronto Malvern (6158738) 43.8, -79.233	33.7	41.1	47.0	42.1	19.3	16.8	17.4	13.9	605	1,451	8.05	3.85	12.3	8.45
Oakville WPCP (615N745) 43.483, -79.633	11.2	13.7	81.0	79.1	7.6	7.3	27.0	23.1	325	1,044	8.05	3.16	12.92	9.76
Richmond Hill (6157012) 43.877, -79.447	15.0	24.1	69.6	60.3	15.4	15.6	0.8	6.4	766	2,285	7.9	3.16	12.61	9.45
Toronto Buttonville (615HMAK) 43.862, -79.37	39.2	34.5	54.2	53.9	6.6	11.6	0.0	3.9	28	367	7.72	4.84	12.9	8.06
Toronto Metro Zoo (6158741) 43.816, -79.183	8.8	10.1	88.6	87.0	2.6	2.8	63.3	52.2	95	559	7.59	2.99	12.17	9.18
Woodbridge (6159575) 43.783, -79.6	25.9	22.9	60.1	63.3	14.0	13.7	6.7	8.2	499	1,808	7.56	2.51	12.58	10.07
Gormley Ardenlee (6152953) 43.866, -79.383	37.1	31.7	50.4	54.6	12.4	13.7	0.7	5.3	76	576	7.39	2.21	12.55	10.34
Bowmanville Mostert (6150830) 43.916, -78.667	4.5	8.4	89.7	84.2	5.8	7.4	15.5	14.6	127	676	7.14	2.53	11.74	9.21
Georgetown WWTP (6152695) 43.64, -79.879	10.7	16.7	77.9	71.4	11.3	11.9	39.8	24.1	476	2,071	7.1	1.26	12.92	11.7
Tyrone (6159048) 44.0166, -78.733	0.5	0.8	99.5	99.0	0.0	0.2	34.6	45.7	0	22	6.81	1.87	11.73	9.86
Burketon McLaughlin (6151042) 44.033, -78.8	0.4	0.4	99.0	99.3	0.5	0.2	29.5	37.4	20	40	6.76	2.29	11.21	8.92
Mean	22.2	22.8	67.0	66.8	10.5	10.4	16.5	16.4	265	1,026	7.97	3.45	12.59	9.1
Standard Deviation	15.0	12.9	19.5	17.9	7.8	7.2	17.8	15.2	264	863	0.8	1.2	0.7	1.1

The Toronto Pearson station (6158733) had the highest impervious surface fraction (50.9%) while the Toronto station (6158350) had the highest building surface fraction (30.5 %) for both thermal source zones. The Burketon McLaughlin (6151042) station had the highest pervious surface fraction (99.3%) along with the lowest impervious surface and buildings surface

fraction (0.4 % and 0.2 %). In the Toronto station's one-thousand metre radius there was a total of 2,822 buildings and in the Oakville Gerrard (6155PD4) station's five-hundred metre radius there was a total of 674 buildings. These counts represented the highest number of buildings found in any of the five-hundred and one-thousand metre radius thermal source areas. In comparison, Burketon McLaughlin and Tyrone were comprised of a mixture of open grass fields (with some agriculture) and large wooded patches. There were twenty buildings found in Burketon McLaughlin and no buildings found in Tyrone within the five-hundred metre radius and forty buildings found in Burketon McLaughlin and twenty-two buildings found in Tyrone within the one-thousand metre radius. The spatial distribution of impervious surface, pervious surface and building surface cover at six of the nineteen stations are shown in Figure 4.1.

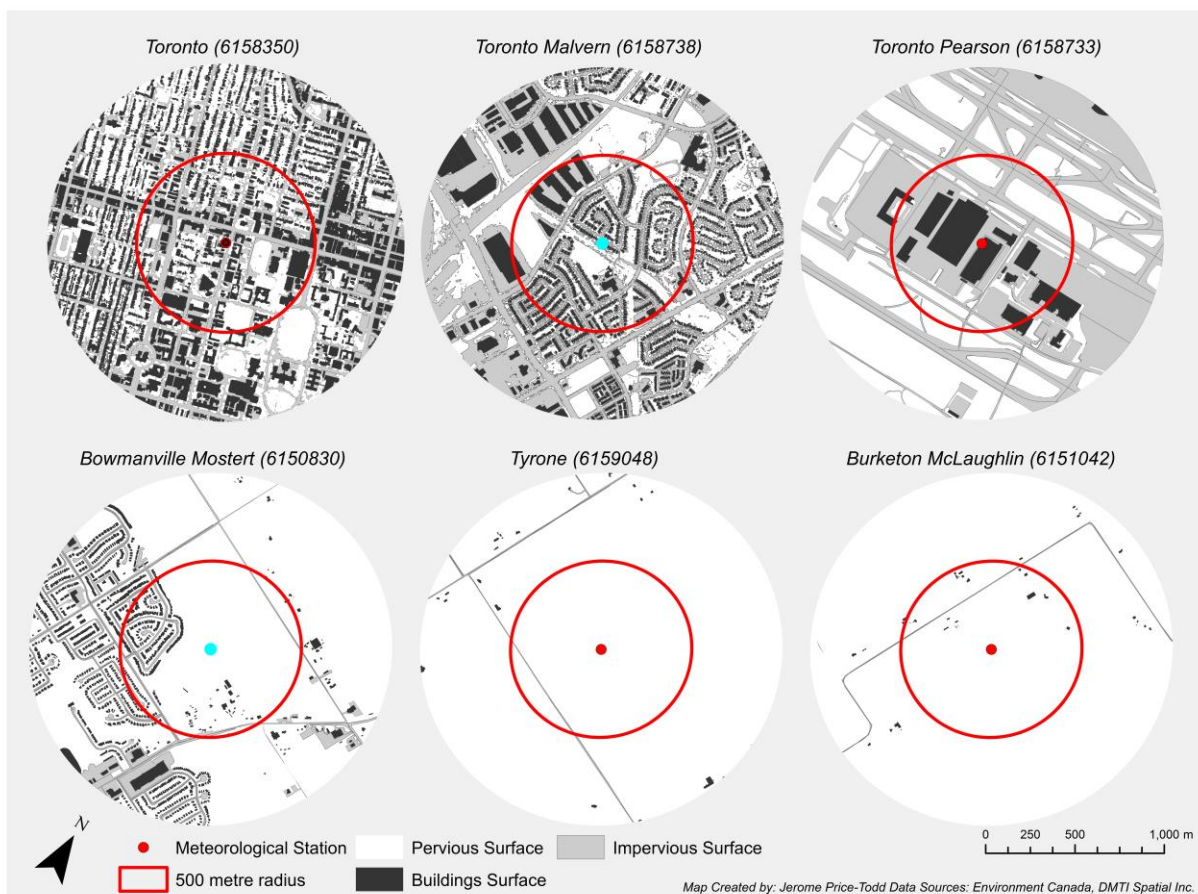


Figure 4.1: The thousand metre radius around meteorological stations Toronto, Toronto Malvern and Toronto Pearson, Bowmanville, Tyrone and Burketon McLaughlin showing their pervious, impervious and building surface covers.

The contrasting impervious and pervious surface covers are evident when comparing the Toronto, Toronto Malvern and Toronto Pearson with the Bowmanville, Burketon McLaughlin and the Tyrone stations (Figure 4.1). Similarly the temperature averages for the Toronto station (6158350) was 9.39 °C representing the highest \bar{T} while the Burketon McLaughlin (6151042) and Tyrone (6159048) stations had the two lowest \bar{T} (6.76 and 6.81 °C). The two stations with the highest \bar{T} , Toronto (6158350) and Oakville Gerrard (615PD4) have relatively higher impervious and building surface fractions and stations with the lowest impervious and building surface fractions (Tyrone and Burketon McLaughlin) had the lowest \bar{T} .

4.2 Assigning Local Climate Zones to the Meteorological Stations

In order to calculate the UHI intensity using equation 2 all stations needed to be classified into their respective local climate zones. The local climate zone identified as the most rural was used as the reference station to calculate the UHI intensity at all other stations. The calculated surface cover fractions were used to match the five-hundred meter and thousand meter thermal source zone to a local climate zone class. Structured Query Language (SQL) was used to formulate expressions for each of the LCZs outlined in Table 3.2 in order to find an LCZ that matched with the calculated impervious, pervious and building surface fractions (see Table A3 in Appendix A for SQL expressions). Each expression was run for each thermal source zone (*i.e.* 500 and 1000 metre radius) and the 19 meteorological stations were classified according to their three surface cover values and assigned an LCZ designation. The potential candidates that were output from the SQL expression and the final chosen LCZ match are shown in Table 4.2.

Table 4.2: Local climate zone classified stations showing the potential LCZs generated by query builder and the final chosen LCZs for the five-hundred metre and the one-thousand metre radius thermal source zones. The LCZs in bold are the SQL exact matches and all others are those assigned to the nearest equivalent LCZ.

Station Name (Climate ID)	Potential Candidates (Output from SQL)		Final LCZ			
			500 m		1000 m	
	500 m	1000 m	Built Type	LC Type	Built Type	LC Type
Bowmanville Mostert (6150830)	-	-		LCZ B	LCZ 9	
Burketon McLaughlin (6151042)	<i>LCZ A - D, LCZ F-G</i>	<i>LCZ A - D, LCZ F-G</i>		LCZ C		LCZ C
Georgetown WWTP (6152695)	LCZ 9	LCZ 9	LCZ 9		LCZ 9	
Gormley Ardenlee (6152953)	-	-	LCZ 6		LCZ 6	
Lakeview MOE (6154310)	LCZ 9	LCZ 9	LCZ 9		LCZ 9	
Oshawa WPCP (6155878)	-	-	LCZ 9		LCZ 6	
Oakville Gerard (6155PD4)	LCZ 9	LCZ 9	LCZ 9		LCZ 9	
Richmond Hill (6157012)	LCZ 9	LCZ 9	LCZ 9		LCZ 9	
Toronto (6158350)	<i>LCZ 4, LCZ 5, LCZ 6</i>	<i>LCZ 5, LCZ 6</i>	LCZ 5		LCZ 5	
Toronto Island A (6158665)	-	-	LCZ 9		LCZ 9 _G	
Toronto Pearson (6158733)	-	-	LCZ 3		LCZ 5	
Toronto Malvern (6158738)	LCZ 9	-	LCZ 9		LCZ 6	
Toronto Metro Zoo (6158741)	-	-		LCZ A		LCZ A
Tyrone (6159048)	<i>LCZ A - D, LCZ F-G</i>	<i>LCZ A - D, LCZ F-G</i>		LCZ C		LCZ C
Woodbridge (6159575)	LCZ 9	LCZ 9	LCZ 9		LCZ 9	
Toronto Buttonville A (615HMAK)	-	-	LCZ 6		LCZ 6	
Oakville WPCP (615N745)	-	-		LCZ A	LCZ 9	
Toronto North York (615S001)	LCZ 9	-	LCZ 9		LCZ 6	
Burlington TS (6151064)	-	-	LCZ 6		LCZ 6	
Total			14	5	16	3
Total Unique			4	3	4	2

The query builder matched all three surface cover fractions to 10 LCZs for the 500 metre radius and 8 LCZs for the 1000 metre radius (shown in bold in Table 4.2). The unclassified stations were matched using their impervious, building and pervious surface cover fraction values that were to the nearest equivalent LCZ designation. In this set of unclassified stations, many matched with impervious and pervious surface fractions and as a result building surface fraction was matched to the closest equivalent LCZ class. The five-hundred metre radius thermal source zone resulted in the classification of 14 built types including 4 unique LCZs and 5 land cover types including 3 unique LCZs. The one-thousand metre radius thermal source zone resulted in the classification of 16 built types including 4 unique LCZs and 3 land cover types with 2 unique LCZs. The Toronto, Burketon McLaughlin and Tyrone stations had multiple potential LCZ candidates generated from the SQL run expression output. The calculated surface cover fractions for the Toronto (6158350) station resulted in a match for three LCZs for the 500 metre radius (LCZ 4, LCZ 5 and LCZ 6) and two of these LCZs for the 1000 metre radius (LCZ 5 and LCZ 6). The distinguishing geometric characteristic that separates these classes is the height of the roughness element, *i.e.* the geometric average of building heights which are greater in LCZ 4 than LCZ 5 (and LCZ6) (Stewart and Oke, 2012). Although the geometric values for these stations were not available it was reasoned that since the area surrounding the Toronto station is associated with generally mid-rise structures (*e.g.* Robarts Library, Earth Science Centre, Royal Ontario Museum) then an LCZ 5 is more appropriate than an LCZ 4 which is associated with taller high rise building (*e.g.* sky scrapers). Therefore the Toronto station was assigned an LCZ 5. The three surface cover fractions for Burketon McLaughlin (6151042) and Tyrone (6159048) matched exactly with LCZ A to LCZ D, and LCZ F and G. It was decided that these stations were most appropriately classified as LCZ C which is described as “open arrangements of bush, shrubs, and short woody trees” and the zone functions as a “natural shrubland or agriculture” (Stewart and Oke, 2012, p. 1885).

4.3 The Urban Heat Island Intensity in Southern Ontario

As shown in the preceding section the Burketon McLauhglin station (6151042) and the Tyrone station (6159048) represented the least urban of all stations, therefore, they were each used as the reference rural stations to calculate the UHI intensity at each of the nineteen defined

local climate zones. As a result, two UHI intensities for each temperature variable and for each station were generated. Using equation 2 (Section 3.2), the difference in \bar{T} , T_{\min} , T_{\max} and the difference between the diurnal temperature range (DTR) between each station and each of the two reference rural stations were calculated (*i.e.* $\Delta T_{\text{LCZX} - \text{LCXC}}$). The calculated \bar{T} , T_{\min} , T_{\max} UHI intensities of each local climate zone and their physical and geometric characteristics including elevation (EL), distance to Lake Ontario (DTL) and distance to Urban Core (DTC) (defined as 1st Canadian Place - 100 King Street West) are presented in Table 4.3 in descending order of mean-daily UHI intensities. The grouping of similar LCZs are presented in gray scale representing built types and green colours representing land cover types.

Table 4.3: The UHI intensities using Burketon McLaughlin (6151042) and Tyrone (6159048) as rural reference station, surface cover fractions.
Gray scale representing built types and green colours representing land cover types

Station Name (Climate ID and Location)	LCZ		Physical and Geometric Influences			Surface Cover Fractions (%)								Number of Buildings		UHI Intensity (6151042)				UHI Intensity (6159048)			
	500 metre	1000 metre	EL(m)	DTL (km)	DTC (km)	ISF		PSF		BSF		TCF		Count		Mean	Min	Max	DTR (K)	Mean	Min	Max	DTR (K)
						500 m	1000 m	500 m	1000 m	500 m	1000 m	500 m	1000 m	500 m	1000 m								
Toronto (6158350) 43.666, -79.4	LCZ 5	LCZ 5	113	3.2	2.5	31.8	30.3	39.0	39.2	29.2	30.5	19.8	22.7	554	2,822	2.63	3.56	1.69	-1.87	2.58	3.98	1.17	-2.81
Oakville Gerard (6155PD4) 43.428, -79.696	LCZ 9	LCZ 9	92	1.1	35.3	14.2	24.0	62.5	62.5	13.2	13.5	0.0	1.7	674	2,098	2.35	2.09	2.59	0.5	2.3	2.51	2.07	-0.44
Burlington TS (6151064) 43.333, -79.833	LCZ 6	LCZ 6	99	3.1	50.6	43.9	32.5	59.8	59.8	1.8	7.7	1.4	7.1	24	537	2.31	2.15	2.48	0.33	2.26	2.57	1.96	-0.61
Toronto North York (615S001) 43.78, -79.467	LCZ 6	LCZ 9	187	9.1	16.2	21.5	28.3	64.5	55.0	14.0	17.5	31.1	25.3	50	477	1.79	1.42	2.15	0.73	1.74	1.84	1.63	-0.21
Toronto Island A (6158665) 43.628, -79.395	LCZ 9 _G	LCZ 9	77	0.3	2.5	33.9	16.3	63.8	81.5	2.3	2.2	2.6	6.2	30	122	1.73	2.55	0.9	-1.65	1.68	2.97	0.38	-2.59
Lakeview MOE (6154310) 43.566, -79.566	LCZ 9	LCZ 9	76	0.2	17.5	23.1	24.7	64.4	64.2	12.5	11.1	0.7	0.9	476	1,548	1.68	1.91	1.44	-0.47	1.63	2.33	0.92	-1.41
Toronto Pearson (6158733) 43.677, -79.63	LCZ 5	LCZ 3	173	8.2	20.3	50.9	50.3	26.7	42.4	22.4	7.0	0.0	0.3	32	44	1.41	1.03	1.79	0.76	1.36	1.45	1.27	-0.18
Oshawa WPCP (6155878) 43.866, -78.833	LCZ 6	LCZ 9	84	0.3	50.3	15.3	22.5	76.2	70.2	8.6	7.3	22.0	13.3	179	950	1.36	1.81	0.91	-0.9	1.31	2.23	0.39	-1.84
Toronto Malvern (6158738) 43.8, -79.233	LCZ 6	LCZ 9	160	6.6	20.6	33.7	41.1	47.0	42.1	19.3	16.8	17.4	13.9	605	1,451	1.29	1.56	1.09	-0.47	1.24	1.98	0.57	-1.41
Oakville WPCP (615N745) 43.483, -79.633	LCZ 9	LCZ A	87	0.7	27.4	11.2	13.7	81.0	79.1	7.6	7.3	27.0	23.1	325	1,044	1.29	0.87	1.71	0.84	1.24	1.29	1.19	-0.1
Richmond Hill (6157012) 43.877, -79.447	LCZ 9	LCZ 9	240	19.5	25.9	15.0	24.1	69.6	60.3	15.4	15.6	0.8	6.4	766	2,285	1.14	0.87	1.4	0.53	1.09	1.29	0.88	-0.41
Toronto Buttonville A (615HMAK) 43.862, -79.37	LCZ 6	LCZ 6	198	18.2	23.7	39.2	34.5	54.2	53.9	6.6	11.6	0.0	3.9	28	367	0.96	2.55	1.69	-0.86	0.91	2.97	1.17	-1.8
Toronto Metro Zoo (6158741) 43.816, -79.183	LCZ A	LCZ A	143	2.4	24.6	8.8	10.1	88.6	87.0	2.6	2.8	63.3	52.2	95	559	0.83	0.7	0.96	0.26	0.78	1.12	0.44	-0.68
Woodbridge (6159575) 43.783, -79.6	LCZ 9	LCZ 9	164	9.1	23.1	25.9	22.9	60.1	63.3	14.0	13.7	6.7	8.2	499	1,808	0.8	0.22	1.37	1.15	0.75	0.64	0.85	0.21
Gormley Ardenlee (6152953) 43.866, -79.383	LCZ 6	LCZ 6	198	19.4	24.2	37.1	31.7	50.4	54.6	12.4	13.7	0.7	5.3	76	576	0.63	-0.08	1.34	1.42	0.58	0.34	0.82	0.48
Bowmanville Mostert (6150830) 43.916, -78.667	LCZ 9	LCZ B	99	1.7	64.8	4.5	8.4	89.7	84.2	5.8	7.4	15.5	14.6	127	676	0.38	0.24	0.53	0.29	0.33	0.66	0.01	-0.65
Georgetown WWTP (6152695) 43.64, -79.879	LCZ 9	LCZ 9	221	22.8	40.1	10.7	16.7	77.9	71.4	11.3	11.9	39.8	24.1	476	2,071	0.34	-1.03	1.71	2.74	0.29	-0.61	1.19	1.8
Tyrone (6159048) 44.0166, -78.733	LCZ C	LCZ C	206	7.1	66.2	0.5	0.8	99.5	99.0	0.0	0.2	34.6	45.7	0	22	0.05	-0.42	0.52	0.94	-	-	-	-
Burketon McLaughlin (6151042) 44.033, -78.8	LCZ C	LCZ C	312	10.5	63.3	0.4	0.4	99.0	99.3	0.5	0.2	29.5	37.4	20	40	-	-	-	-	-0.05	0.42	-0.52	-0.94
Mean			154	7.6	31.5	22.2	22.8	67.0	66.8	10.5	10.4	16.5	16.4	265	1026	1.28	1.22	1.46	0.24	1.2	1.7	0.9	-0.8
Standard Deviation			66	7.4	19.4	15.0	12.9	19.5	17.9	7.8	7.2	17.8	15.2	264	863	0.7	1.2	0.6	1.1	0.7	1.1	0.6	1.1

The built types are generally found at the top of Table 4.3 and the land cover types are generally found near the bottom. This general sequence of built types to land cover types also follows the magnitude of the mean-daily UHI intensities. For example, the Toronto (LCZ 5) station had the highest \bar{T} and T_{\min} UHI intensity (2.63 and 2.58 K, and 2.58 and 3.98 K) and the station with the highest T_{\max} UHI intensity was Oakville Gerrard (LCZ 9). In contrast stations with higher pervious surface fraction (*e.g.* Toronto Metro Zoo, Bowmanville and Georgetown) have lower mean daily UHI intensities. Some exceptions are Toronto Buttonville (LCZ 6) and Gormley Ardenlee (LCZ 6) which have considerably higher impervious surface fractions (39 and 37 %) but nevertheless lower UHI intensities.

The two different \bar{T} , T_{\min} , T_{\max} UHI intensities that were generated using the two reference stations showed relatively similar UHI intensities (Table 4.3). The two sample *t*-test with equal variance was used to check if the differences between the two magnitudes of UHI intensities generated from the two different rural stations (Burketon McLaughlin and Tyrone) were significantly different. The means and standard deviations of the UHI intensities calculated using the two reference stations and the *t*-test results are shown in Table 4.4.

Table 4.4: Two sample *t*-test results comparing the means of the two difference UHI intensities calculated using Burketon McLaughlin and Tyrone.

UHI Intensity	Rural Reference Station				Two Sample <i>t</i> -test (2-tail)	
	Burketon McLaughlin		Tyrone			
	Mean	SD	Mean	SD	t-Statistic	p-value
Mean Daily UHI	1.28	0.7	1.22	0.7	0.219	0.83
Minimum Daily UHI	1.22	1.2	1.7	1.1	2.415	0.02
Maximum Daily UHI	1.46	0.6	0.9	0.6	-1.099	0.28

There was not a significant difference between the mean-daily UHI intensities calculated from the Burketon McLaughlin (LCZ C) reference station and the UHI intensities calculated from the Tyrone (LCZ C) reference station. The same can be said for the maximum-daily UHI intensity. However there was insufficient evidence to reject the null of equal means suggesting that there may be a significant difference between the minimum-daily UHI intensities calculated

from the Burketon McLaughlin station and the minimum-daily UHI intensities calculated from the Tyrone station.

In order to simplify the analysis the two mean-daily UHI intensities that were calculated at each station using the two different rural reference stations were averaged into a single mean-daily UHI intensity for each station. This was defined as the average mean-daily UHI intensity and this new value was used to examine the relationships with the impervious, pervious and building surface fractions. The average mean-daily UHI intensity (see Table A9 in the Appendix) was graphed against impervious, pervious and building surface fractions to examine the relationship at the five-hundred metre and one-thousand metre radius around the meteorological station (Figure 4.2 – 4.7).

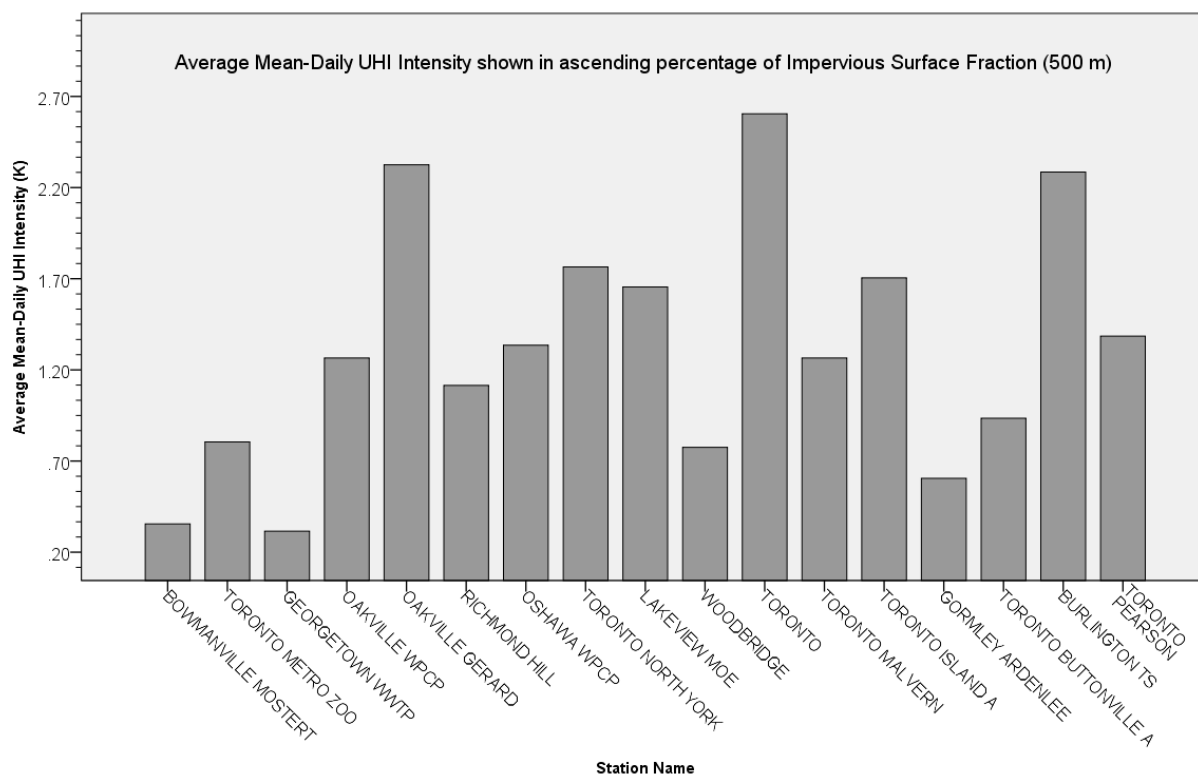


Figure 4.2: The average mean-daily UHI intensity shown in ascending percentage of impervious surface fraction at the 500 metre radius thermal source zone.

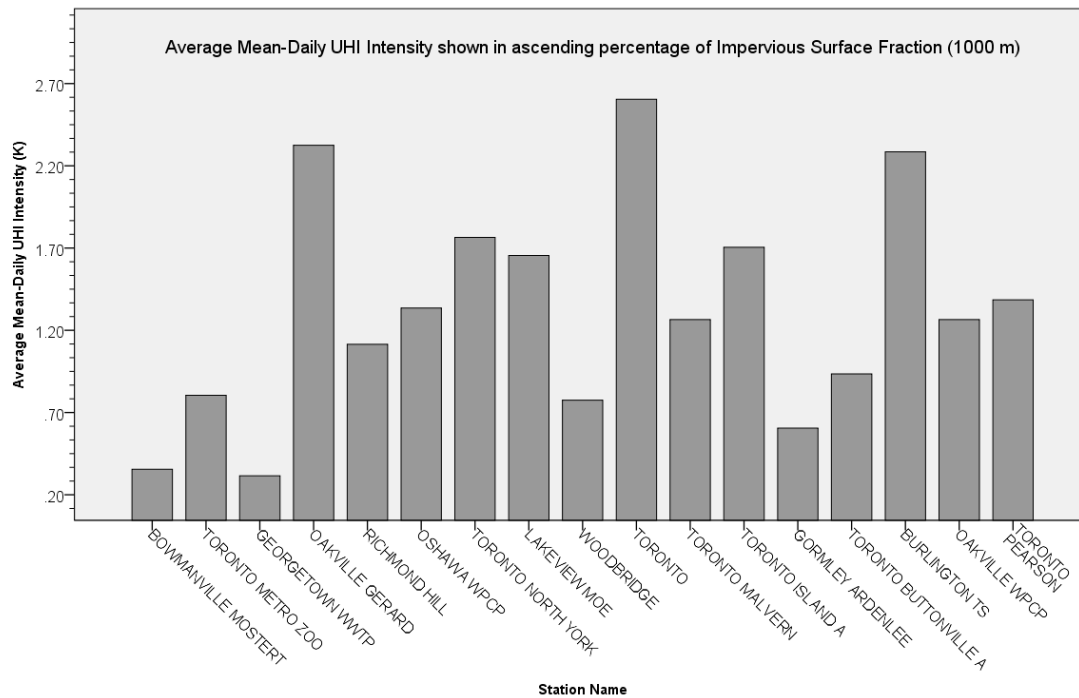


Figure 4.3: The average mean-daily UHI intensity shown in ascending percentage of impervious surface at the 1000 metre radius thermal source zone.

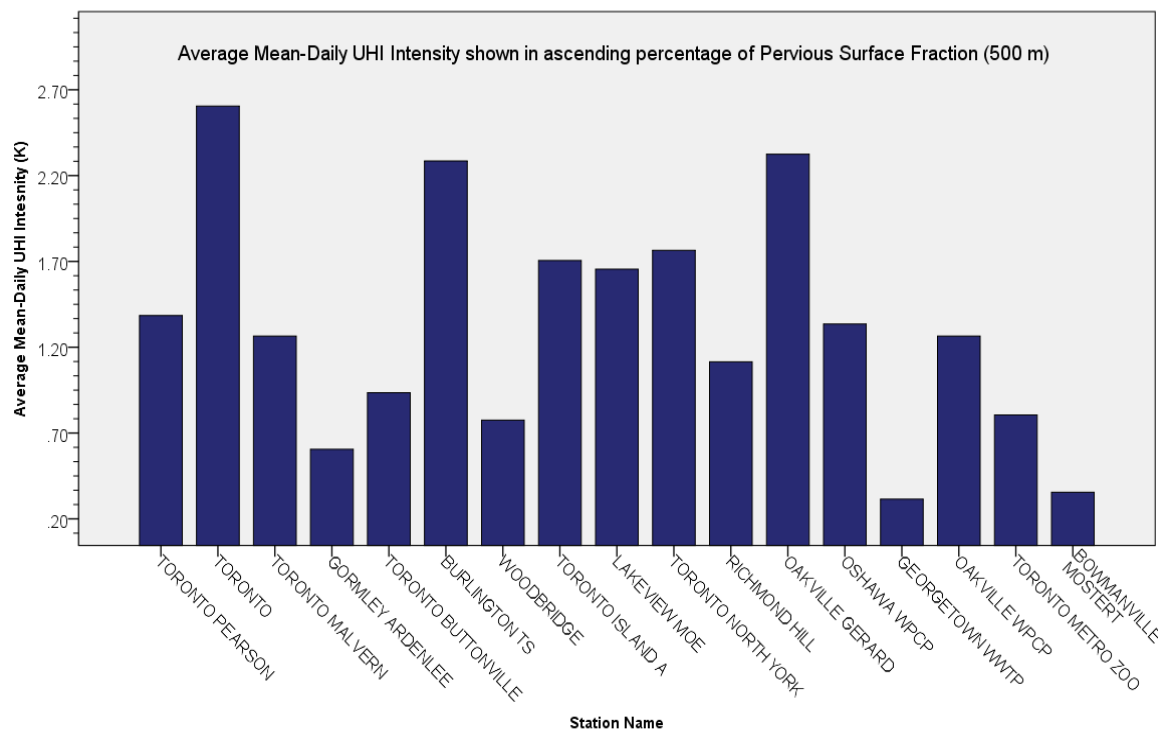


Figure 4.4: The average mean-daily UHI intensity shown in ascending percentage of pervious surface fraction at the 500 metre radius thermal source UHI intensity graphs.

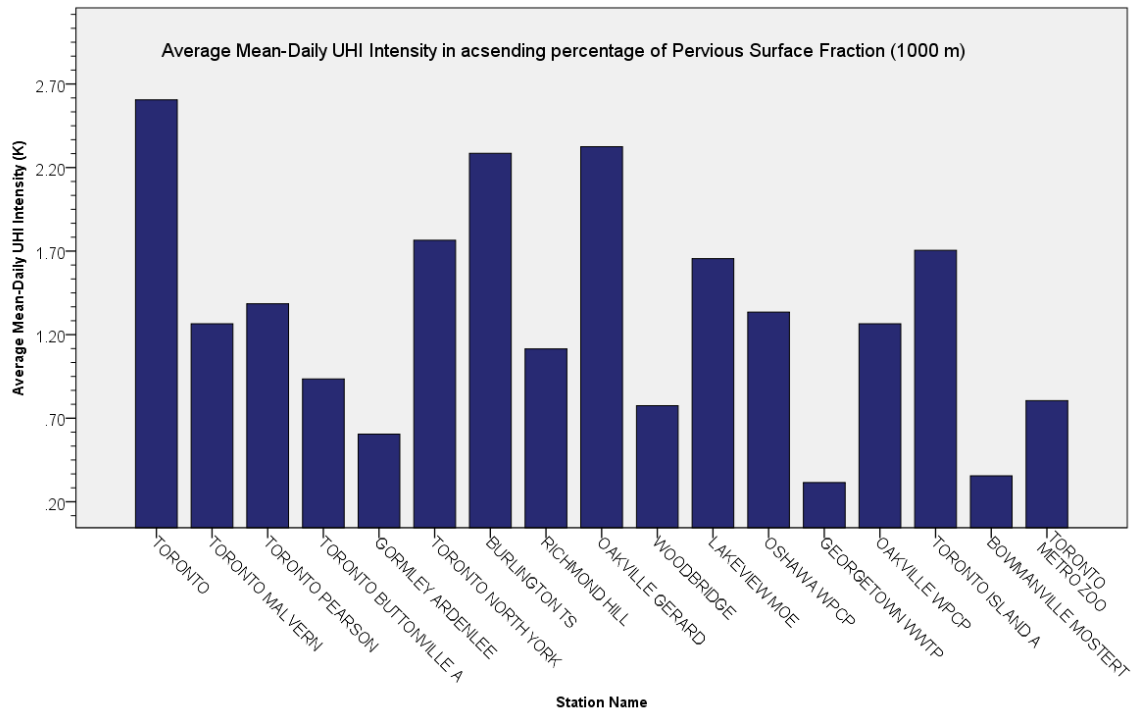


Figure 4.5: The average mean-daily UHI intensity shown in ascending percentage of pervious surface at the 1000 metre radius thermal source zone.

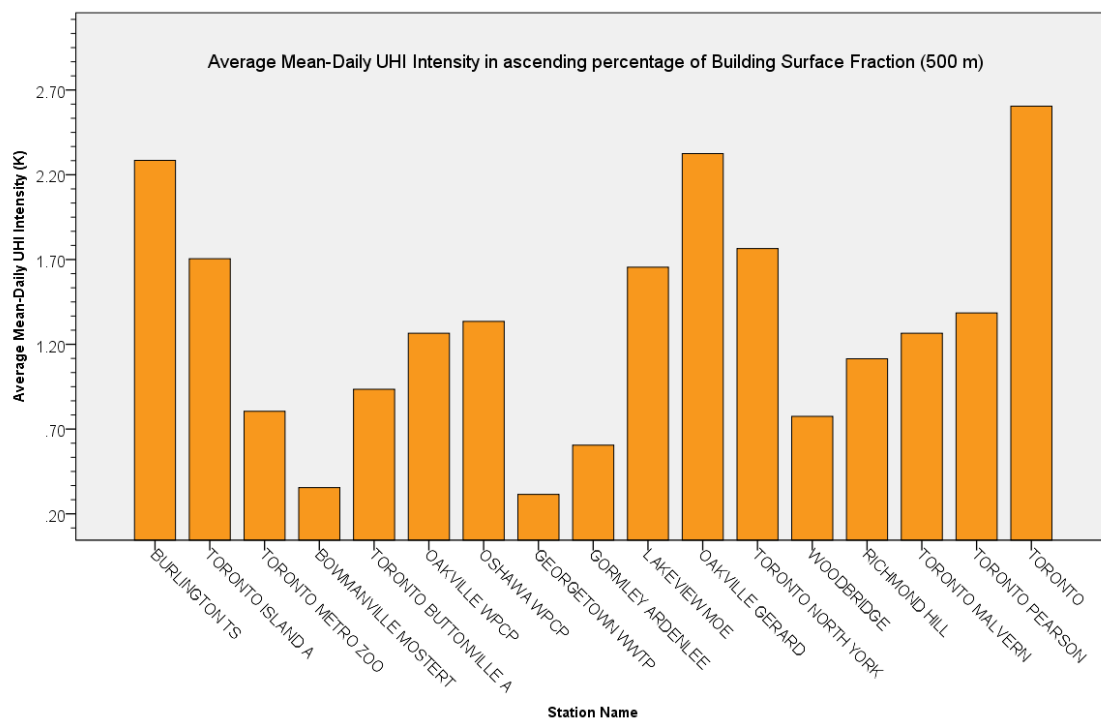


Figure 4.6: The average mean-daily UHI intensity shown in ascending percentage of building surface fraction at the 500 metre radius thermal source zone.

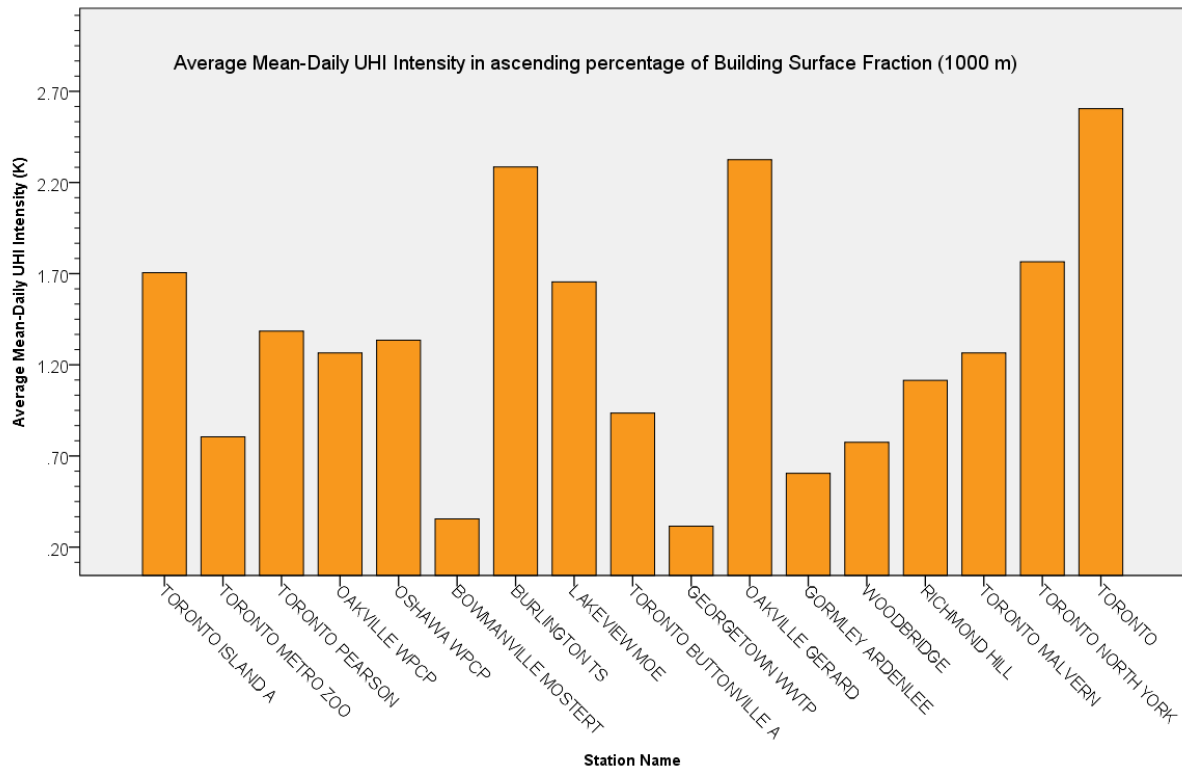


Figure 4.7: The average mean-daily UHI intensity shown in ascending percentage of building surface fraction at the 1000 metre radius thermal source zone.

There was no clear pattern or general trend of increasing average mean-daily UHI intensities with increasing impervious surface fractions (Figures 4.2-4.3). Some clustering is evident at the relatively lower values of the impervious surface fractions. The Bowmanville station which is classified as an LCZ B with the 500 metre radius but LCZ 9 with a one-thousand metre radius, the Toronto Metro Zoo station (LCZ A at both 500 and 1000 metre radius) and the Georgetown WWTP station (LCZ 9 at both 500 metre and 1000 metre radius) share lower impervious surface fraction values while also experiencing a relatively lower average mean-daily UHI intensity. Overall there is some variation of average mean-daily UHI intensities in the stations having the impervious surface fractions between 16.7% (Georgetown WWTP – LCZ 9) and 31.7% (Burlington TS LCZ 6).

The pervious surface fraction on its own does not show any clear pattern of decreasing average mean-daily UHI intensities with increasing pervious surface fraction (Figure 4.4 – 4.5). However, in general the station with the highest average mean-daily UHI intensities are found with the lowest pervious surface fraction (the Toronto station) while two of the stations with the

lower UHI intensities are found near the higher values of pervious surface fraction (Georgetown WWTP and Bowmanville). The graph reveals some variation in the average mean-daily UHI intensities at stations having the pervious surface cover fractions between 54.6% (Gormlee Ardenlee) and 71.4% (Georgetown WWTP). The stations Lakeview MOE, Oakville WPCP and Toronto Island had relatively higher average mean-daily UHI intensities however they also had higher fractions of pervious surface cover at the one-thousand metre radius thermal source zone.

There was no clear pattern in the average mean-daily UHI intensities when graphed against increasing building surface fractions (Figure 4.6 – 4.7) based upon the five-hundred metre radius. Similarly for the one-thousand metre radius thermal source zone' building surface fractions ranged between 1.8% (Burlington TS) and 13.5% (Oakville Gerrard). Overall these showed some variation in average mean-daily UHI intensities but with no discernable pattern. However, the higher building surface fraction (from 13.7 to 30.5 %) showed a trend of increasing average mean-daily UHI intensities with higher building density. Overall, the patterns were not clear or obvious between the average mean-daily UHI intensity and the three surface cover fractions.

Since no discernable trend was evident in the mean-daily UHI intensities graphed against the three surface cover fractions, the local climate zones were grouped into similar LCZ types and examined for a trend. The local climate zone classification identified six unique local climate zone classes among the nineteen meteorological stations at the one-thousand metre radius. There were two LCZ 5s, six LCZ 6s, and seven LCZ 9s, one LCZ9_G, one LCZ A and two LCZ Cs. The local climate zones 5, 6 and 9 represented the variation of built types found in the set of nineteen classified stations. The variation within these groups was examined to identify significant differences between the three built-type local climate zones. The average mean-daily UHI intensity for the groups LCZ 5, 6, 9, and A were graphed and are presented in Figure 4.8 (see Figure A1 in Appendix A for a comparison of average minimum-daily and average maximum-daily UHI intensities grouped into LCZs for 500 metre radius thermal source zones). An analysis of variance was used to test if the UHI intensities were different between LCZ classes and the results are presented in Table 4 (see Table A5-6 in Appendix for Average minimum-daily and average maximum-daily UHI intensity comparisons).

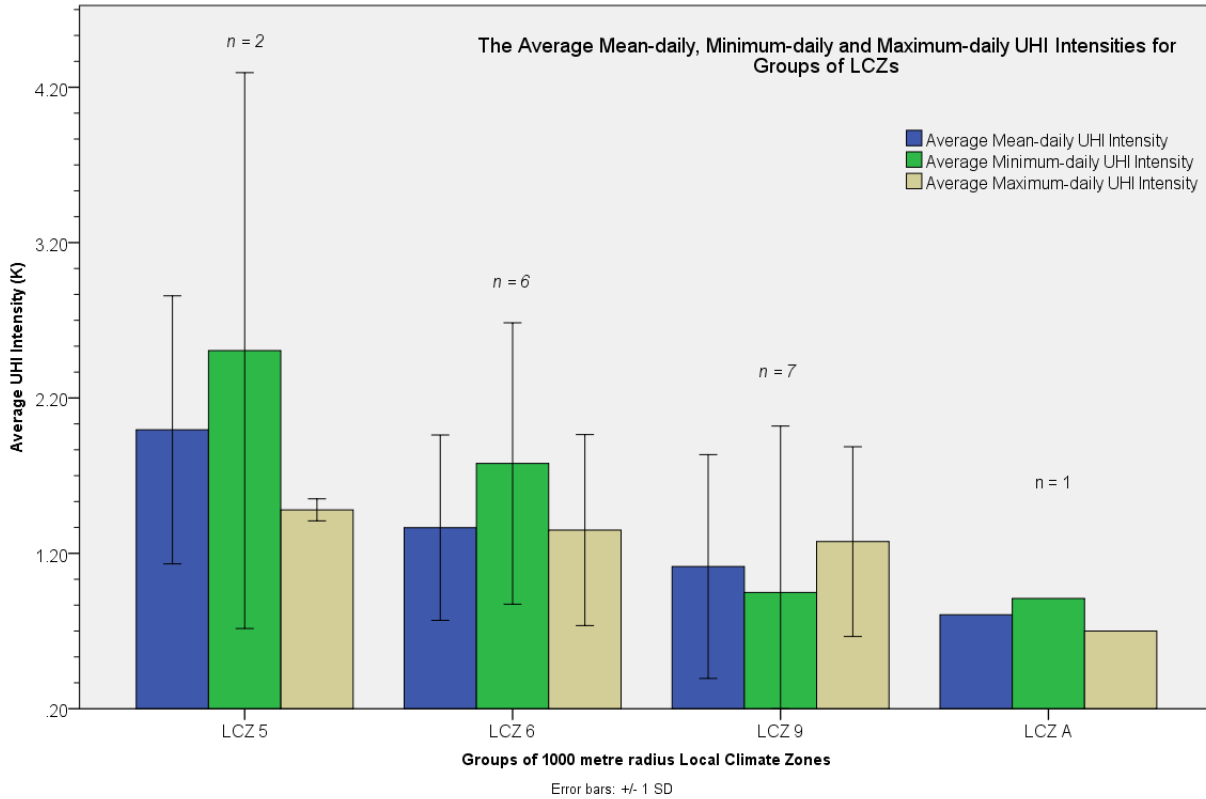


Figure 4.8: The average mean-daily UHI intensity compared between unique LCZ classes. Also shown are the average minimum-daily and average maximum-daily UHI intensities. The number of classes in each group.

Table 4.5: The results from the analysis of variance used to check the difference between the grouped means of the unique LCZ classes

LCZ Groups			Mean		Variance	
LCZ 5			2.00		0.50	
LCZ 6			1.37		0.32	
LCZ 9			1.12		0.48	
Source of Variation	SS	df	MS	F	P-value	F crit
Between Groups	2.431	2	1.215	2.906	0.072	2.511
Within Groups	11.290	27	0.418			
Total	13.720	29				

A general pattern of increasing average mean-daily UHI intensity was apparent when the stations were grouped into similar LCZs based upon their three surface cover fractions. The local climate zone 5 group (Toronto and Toronto Pearson) had a higher overall average mean-daily UHI intensity than local climate zone groups 6, 9 and A. Although the null hypothesis of no

difference cannot be rejected, the analysis of variance suggests that the difference between LCZ 5, 6 and 9 is tending towards a significant difference with a p -value between 0.05 and 0.10. The analysis of variance showed that there was a significant differences between the groups of LCZ for the average minimum-daily UHI intensity ($p < 0.05$) (see Table A5 in Appendix A).

4.3.1 Seasonal Mean-Daily UHI Intensities in Southern Ontario

The seasonal mean-daily UHI intensities were examined for significant differences between the UHI intensities calculated with the two different rural stations. The monthly mean-daily temperatures were grouped into the four seasons that are generally experienced in Southern Ontario (December to February representing winter, March to May representing spring, *etc.*) and their seasonal mean-daily temperature averages were calculated. The seasonal mean-daily temperatures (winter, spring, summer and fall) of Burketon McLaughlin and Tyrone were used to calculate the seasonal UHI intensities (winter mean-daily, spring mean-daily, summer mean-daily and fall mean-daily UHI intensities) at each of the identified local climate zones in the study area. A two sample t-test was used to check if there was any significant difference between the seasonal mean-daily UHI intensities calculated from the two rural stations (Table 4.6).

Table 4.6: The two sample t-test to check for differences between the seasonal mean-daily UHI intensity calculated using Burketon McLaughlin and Tyrone as the rural reference stations.

SeasonalUHI Intensity	Rural Reference Station				Two Sample <i>t</i> -test (2-tail)	
	Burketon McLaughlin		Tyrone			
	Mean	SD	Mean	SD	t-Statistic	p-value
Winter	1.79	1.12	1.59	1.12	0.55	0.58
Spring	0.79	0.56	0.89	0.56	-0.55	0.58
Summer	1.00	0.75	1.00	0.75	0.00	1.00
Fall	1.25	0.82	1.25	0.82	0.00	1.00

The four seasonal UHI intensities calculated with each station showed no significant difference, in fact, summer and fall had the same mean-daily UHI intensities at each LCZ (due to the same summer and fall temperatures experienced at the Burketon McLaughlin and the Tyrone stations).

The seasonal mean-daily UHI intensities were graphed against increasing urban-centric local climate zones to identify changes in UHI magnitudes and trends between the winter and

summer, and the spring and fall average mean-daily UHI intensities. The computed seasonal mean-daily UHI intensities are shown in Table 4.7.

Table 4.7: The winter, spring summer and fall average UHI intensity calculated using Burketon McLaughlin and Tyrone seasonal average mean-daily UHI intensities.

Station Name (Climate ID and Location)	LCZ 1000 m	Seasonal Average Mean-Daily UHI Intensity (K)			
		Winter (Dec. - Feb.)	Spring (Mar. - May)	Summer (Jun. - Aug.)	Fall (Sep. - Nov.)
Toronto (6158350)	LCZ 5	3.4	2.15	2.3	2.7
Oakville Gerard (6155PD4)	LCZ 9	3.3	1.45	2.1	2.5
Lakeview MOE (6154310)	LCZ 6	3	1.05	0.9	1.8
Burlington TS (6151064)	LCZ 6	2.9	1.75	2.3	2.3
Toronto Island A (6158665)	LCZ 9 _G	2.9	0.85	1	2.1
Oshawa WPCP (6155878)	LCZ 9	2.5	0.75	0.6	1.6
Oakville WPCP (615N745)	LCZ 5	2.4	0.65	0.7	1.3
Toronto North York (615S001)	LCZ 6	2.3	1.05	1.8	1.9
Toronto Pearson (6158733)	LCZ 6	1.6	1.05	1.4	1.5
Toronto Malvern (6158738)	LCZ 9	1.6	1.05	1.3	1.2
Toronto Metro Zoo (6158741)	LCZ 9	1.3	0.75	0.5	0.8
Richmond Hill (6157012)	LCZ 6	1.1	1.05	1.3	1.1
Woodbridge (6159575)	LCZ A	1	0.65	0.7	0.8
Toronto Buttonville A (615HMAK)	LCZ 9	0.9	0.75	1.2	0.9
Georgetown WWTP (6152695)	LCZ 6	0.9	0.15	0	0.3
Bowmanville Mostert (6150830)	LCZ 9	0.6	0.15	0.1	0.4
Gormley Ardenlee (6152953)	LCZ 9	0.4	0.75	0.8	0.6
<i>Mean</i>		<i>1.89</i>	<i>0.94</i>	<i>1.12</i>	<i>1.40</i>
<i>Standard Deviation</i>		<i>1.0</i>	<i>0.5</i>	<i>0.7</i>	<i>0.7</i>

The seasonal average mean-daily UHI intensities sorted by increasing urbanicity are presented graphically in Figure 4.9 and 4.10.

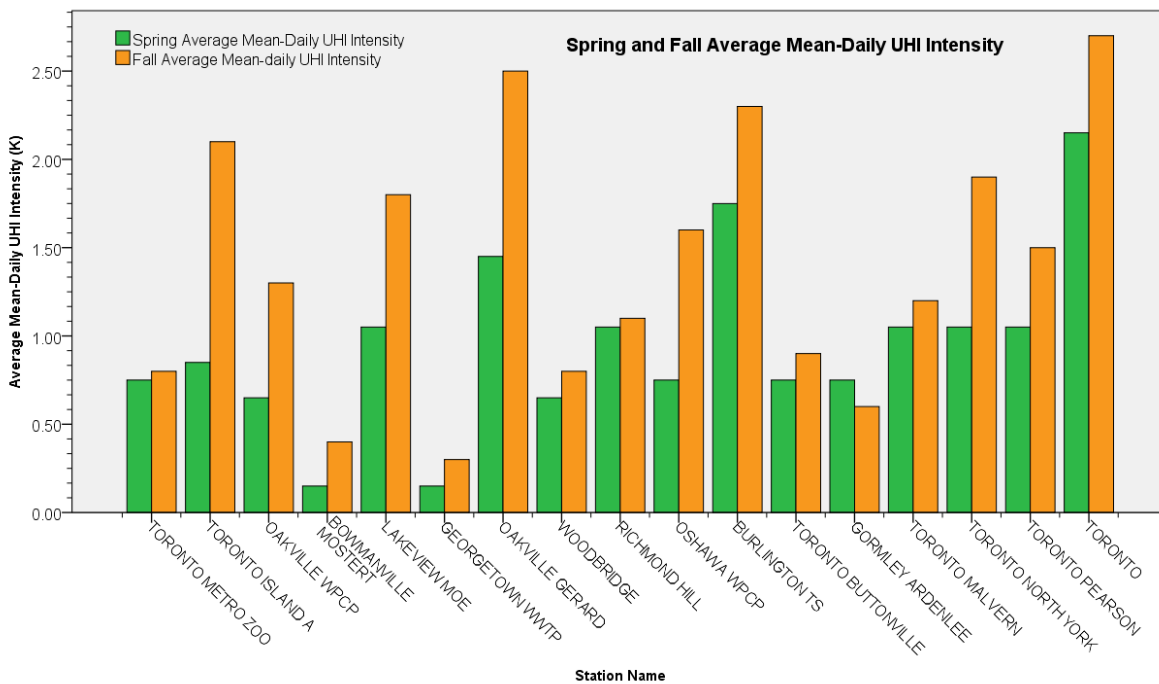


Figure 4.9: Average spring and fall mean-daily UHI Intensities sorted by local climate zones representing low urbanicity to high urbanicity.

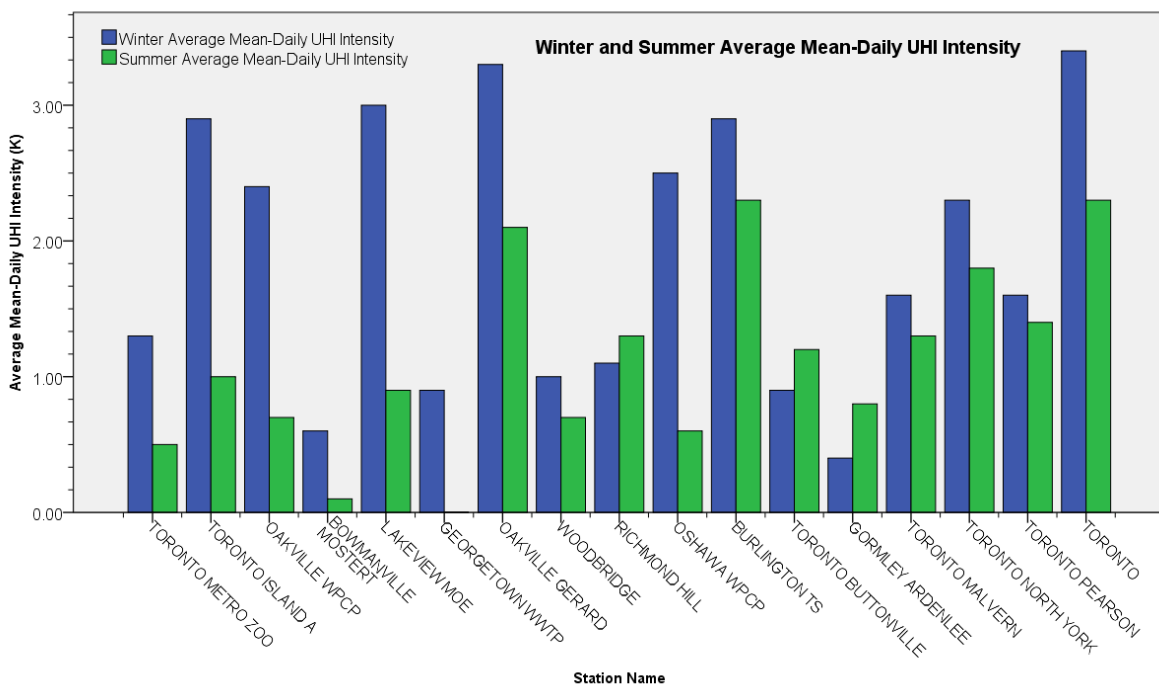


Figure 4.10: Winter and summer average mean-daily UHI Intensities sorted by local climate zones representing low urbanicity to high urbanicity.

With the exception of Gormley Ardenlee, the fall average mean-daily UHI intensity was consistently higher than the spring mean-daily UHI intensity. The Toronto station (6158350) had the highest winter, spring, summer and fall average mean-daily UHI intensities (Table 4.6) and there was consistently higher winter average mean-daily UHI intensity at most stations when compared to all other seasons. Some exceptions are Richmond Hill, Gormley Ardenlee and Toronto Buttonville which have higher magnitudes of summer mean-daily UHI intensities than winter average mean-daily UHI intensities.

Previous research has shown that in Toronto the winter UHI intensities generally have a higher magnitude than other seasonal UHI intensities (Mohsin, 2009). The seasonal average mean-daily UHI intensities shown above were assessed to identify significant differences between the UHI intensities experienced in the four different seasons of southern Ontario. An analysis of variance was used to identify if the average mean-daily UHI intensity among all four seasons were different (Table 4.8).

Table 4.8: The analysis of variance results for the difference among seasonal mean-daily UHI intensities.

<i>Source of Variation</i>	<i>SS</i>	<i>df</i>	<i>MS</i>	<i>F</i>	<i>P-value</i>	<i>F crit</i>
Between Groups	8.675	3	2.892	5.060	0.003	2.171
Within Groups	36.572	64	0.571			
Total	45.247	67				

There was a statistically significant difference between the four seasonal average mean-daily UHI intensities ($F(3,64) = 5.06, p = 0.003$). The two sample t-test assuming unequal variances was used to reveal if the average mean-daily UHI intensity among winter and summer and spring and fall seasons were significantly different (Table 4.9).

Table 4.9: The analysis of variance results for the difference among seasonal mean-daily UHI intensities.

Season	Average Mean-Daily UHI Intensity		Two Sample <i>t</i> -test (2-tail)	
	Mean	Variance	t-Statistic	<i>p</i> -value
Winter	1.89	1.01	2.60	0.01
Summer	1.12	0.49		
Spring	1.40	0.54	2.12	0.04
Fall	0.94	0.25		

There was a statistically significant difference between winter average mean-daily UHI intensity and summer average mean-daily UHI intensity ($p = 0.01$). Similar results were found

between the spring average mean-daily UHI intensity and fall average mean-daily UHI intensity ($p = 0.04$).

4.4 Correlation Analysis

The confounding factors within the study area such as latitude, elevation, distance to lake and distance to urban core were examined to identify significant correlation coefficients with \bar{T} , T_{\max} , T_{\min} and diurnal temperature range. The slope, standard error, coefficient of determination (r^2) and correlation coefficient (r) from the ordinary least squares regression are presented in Table 4.10. The r value signifies the direction of the relationship (*i.e.* positive or negative) strength of the relationships can be assessed using the r^2 value.

Table 4.10: The dependent variables (DV) \bar{T} , T_{\max} , T_{\min} by Latitude in decimal degrees, Elevation in m, Distance to Lake Ontario and Distance to Urban Core (1st Canadian Place) in metres. ** significant at the 0.01 level and * is significant at the 0.05 level (2-tail).

Mean, Maximum, Minimum, DTR by Latitude, Elevation, Distance to Urban Core and Distance to Lake Ontario					
DV	Independent Variable	Slope (β) and SE	r^2	r	p -value.
\bar{T}	Latitude	- 2.91 (± 0.65)***	0.54	-0.73	0.000
	Elevation	- 0.007 (± 0.002)**	0.39	-0.63	0.004
	Distance to Lake Ontario	- 0.00005 (± 0.00002)*	0.21	-0.46	.047
	Distance to Urban Core	- 0.00002 (± 0.000008)*	0.31	-0.56	.013
T_{\max}	Latitude	- 2.69 (± 0.53)***	0.61	-0.78	0.000
	Elevation	- 0.003 (± 0.002)	0.10	-0.32	0.187
	Distance to Lake Ontario	0.000003 (± 0.00002)	0.00	0.04	0.875
	Distance to Urban Core	- 0.00001 (± 0.000008)	0.16	-0.40	0.092
T_{\min}	Latitude	- 2.68 (± 1.34)	0.19	-0.44	0.061
	Elevation	- 0.009 (± 0.003)*	0.31	-0.56	0.013
	Distance to Lake Ontario	- 0.00007 (± 0.00003)*	0.21	-0.46	.048
	Distance to Urban Core	- 0.00003 (± 0.00001)*	0.29	-0.54	.017
DTR	Latitude	- 0.008 (± 1.38)	0.00	0.00	0.995
	Elevation	- 0.007 (± 0.004)	0.17	0.41	0.083
	Distance to Lake Ontario	0.00007 (± 0.00003)*	0.27	0.52	.023
	Distance to Urban Core	0.00002 (± 0.00001)	0.12	0.34	0.155

For \bar{T} all independent variables (latitude, elevation, distance to Lake Ontario, Distance to Core) showed significant moderate to strong correlation coefficients. However, with the exception of latitude, the slope (*i.e.* β -coefficient) was very close to zero for elevation, distance to Lake Ontario and distance to urban core which suggests that for each change of one unit in the independent variable (*e.g.* elevation, distance to Lake Ontario or distance to core) the average change in the mean of the dependent variable (*e.g.* \bar{T}) is small. The T_{\max} , T_{\min} and diurnal temperature range also had β -coefficient very close to zero which suggests that for each change of one unit in the independent variable the average change in the mean of the dependent variable is small.

The determinants of local scale factors including the impervious, pervious, building surface and tree canopy fractions were examined to identify significant correlation with \bar{T} , T_{\max} , T_{\min} and diurnal temperature range (DTR). Each of the temperature variables were regressed and plotted against each of the four surface cover fractions that were calculated within the five-hundred metre and one-thousand metre thermal source zones. The slope, standard error, coefficient of determination (r^2) and correlation coefficient (r) from the ordinary least squares regression are presented in Table 4.11.

Table 4.11: The dependent variables (DV) \bar{T} , T_{\max} , T_{\min} by surface cover fraction for thermal source zones of 500 and 1000 metre radius centred on meteorological station. ** Correlation is significant at the 0.01 level (2-tail) and * is significant at the 0.05 level (2-tail).

\bar{T}, T_{\min}, T_{\max} and Diurnal Temperature Range (DTR) by Surface Cover Fractions (500 m and 1000 m)							
DV	Independent Variable	500 metres			1000 metres		
		Slope (β) and SE	r^2	r	Slope (β) and SE	r^2	r
\bar{T}	ISF	2.64 (± 1.05)*	0.27	0.521*	3.19 (± 1.2)*	0.3	0.543*
	PSF	-2.24 (± 0.76)**	0.34	-0.581**	- 2.58 (± 0.82)	0.37	-0.606**
	BSF	4.54 (± 2.09)*	0.22	0.466*	5.61 (± 2.16)*	0.28	0.532*
	TCF	- 1.66 (± 0.96)	0.15	-0.387	- 2.23 (± 1.08)	0.2	-0.448
T_{\max}	ISF	2.22 (± 0.93)*	0.25	0.500*	3.11 (± 0.99)**	0.37	0.607**
	PSF	- 1.82 (± 0.69)*	0.29	-0.540*	- 2.36 (± 0.69)**	0.41	-0.637**
	BSF	3.43 (± 1.89)	0.16	0.404	4.58 (± 1.94)*	0.25	0.497*
	TCF	- 1.30 (± 0.85)	0.12	-0.349	- 2.06 (± 0.93)*	0.22	-0.474*
T_{\min}	ISF	4.07 (± 1.63)*	0.27	0.518*	4.21 (± 1.96)*	0.21	0.462*
	PSF	- 3.11 (± 1.24)	0.27	-0.521*	- 3.33 (± 1.38)*	0.25	-0.505*
	BSF	4.83 (± 3.47)	0.1	0.32	6.93 (± 3.59)	0.18	0.424
	TCF	- 2.67 (± 1.47)	0.16	-0.403	- 3.09 (± 1.72)	0.16	-0.4
Diurnal Temperature Range (DTR)	ISF	- 1.86 (± 1.72)	0.06	-0.254	- 1.10 (± 2.04)	0.02	-0.129
	PSF	1.29 (± 1.31)	0.05	0.233	0.96 (± 1.47)	0.02	0.157
	BSF	- 1.40 (± 3.39)	0.009	-0.1	- 2.36 (± 3.64)	0.02	-0.155
	TCF	1.37 (± 1.46)	0.05	0.222	1.03 (± 1.72)	0.02	0.143

The \bar{T} showed moderate positive correlation with the impervious and the building surface fraction ($r = 0.543$ and $r = 0.532$) and a moderate negative correlation with the tree canopy and the pervious surface fraction ($r = - 0.448$ and $r = - 0.606$). The T_{\max} and T_{\min} also showed similar relationships where a moderate positive correlation was evident in impervious and building surface fractions and a moderate negative correlation was seen in tree canopy and pervious surface fractions. The strongest relationship was found between T_{\max} and pervious surface fraction with a correlation coefficient of - 0.637. The relationship between diurnal temperature range and the surface cover fractions were weak with a correlation coefficient ranging from 0.129 to 0.157. The scatterplot of \bar{T} , T_{\max} , T_{\min} and the diurnal temperature range against the four surface cover fractions are shown in Figure 4.11 – 4.14.

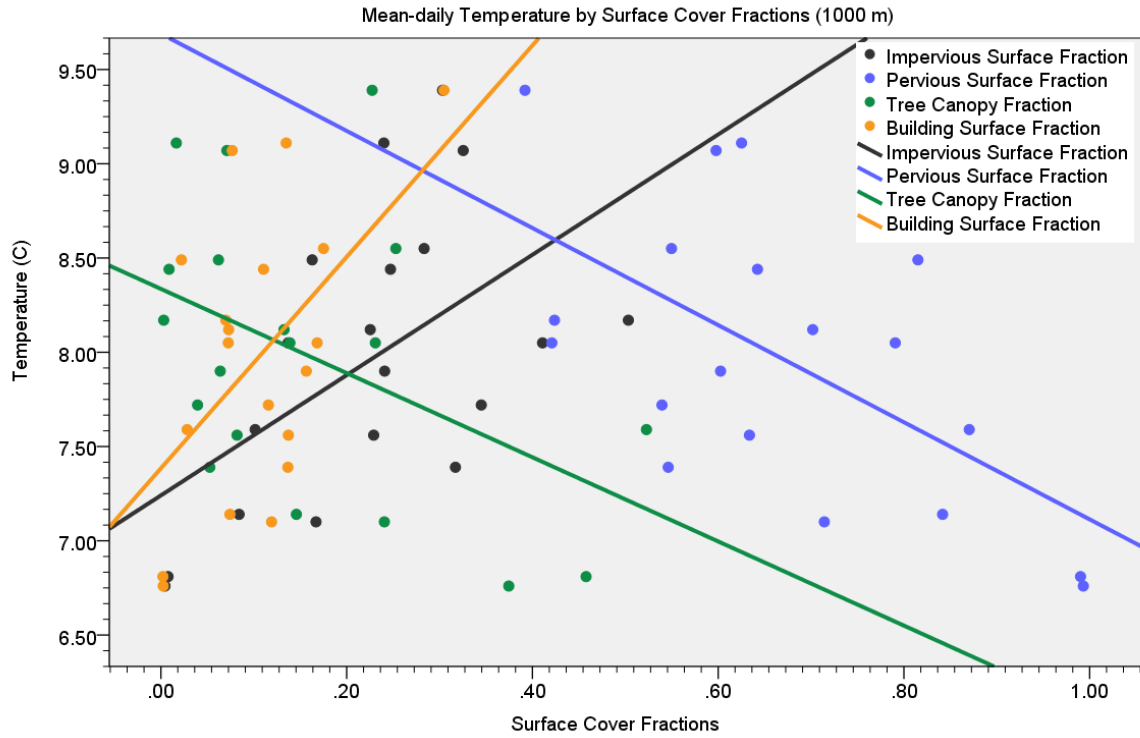


Figure 4.11: The \bar{T} plotted against the impervious, pervious, building surface and tree canopy fraction calculated within the one-thousand metre radius around the meteorological stations.

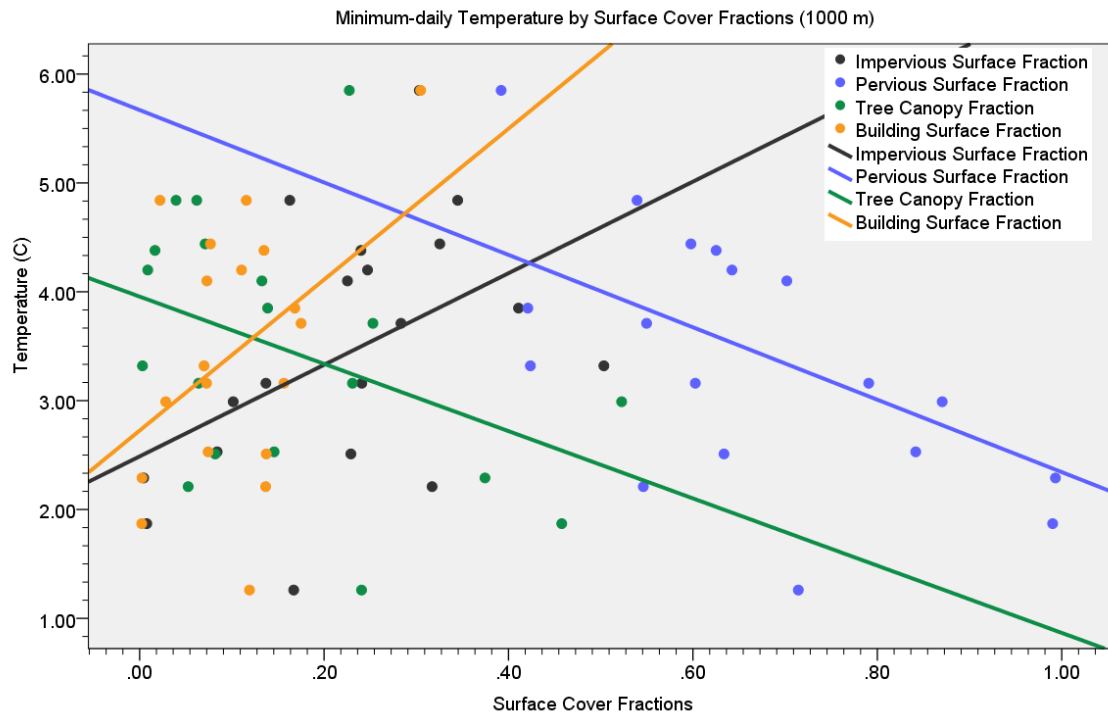


Figure 4.12: The T_{min} plotted against the impervious, pervious, building surface and tree canopy fraction calculated within the one-thousand metre radius around the meteorological stations.

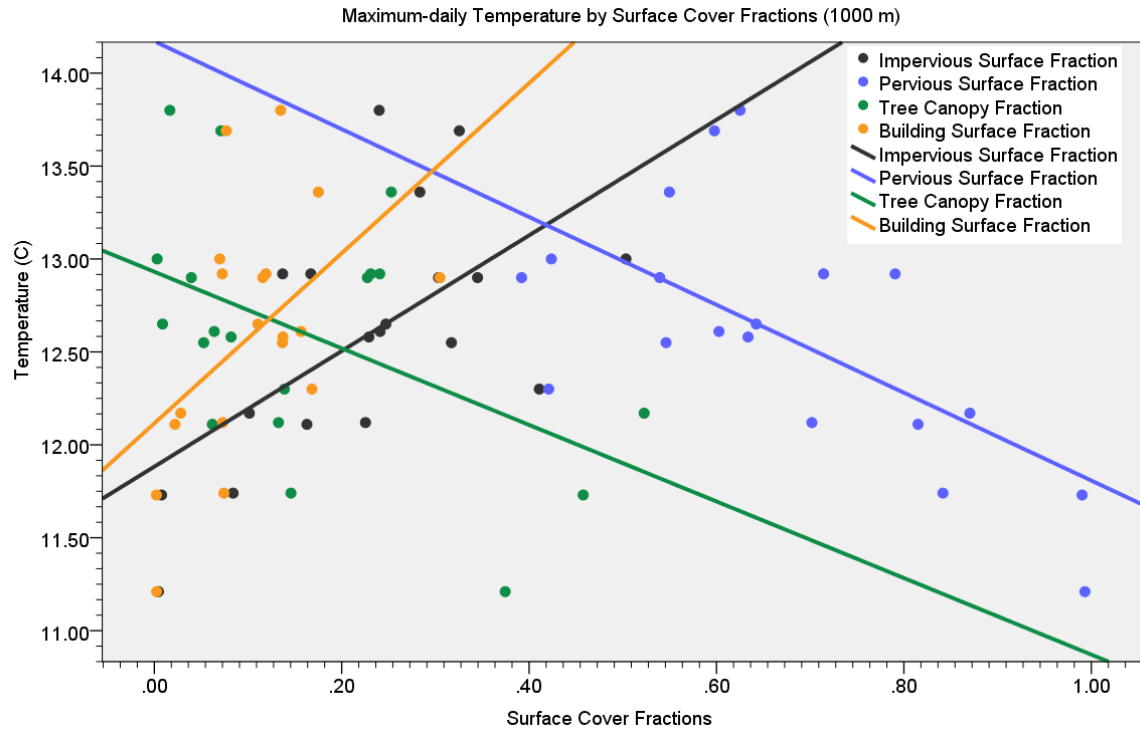


Figure 4.13: The Tmax plotted against the impervious, pervious, building surface and tree canopy fraction calculated within the one-thousand metre radius around the meteorological stations.

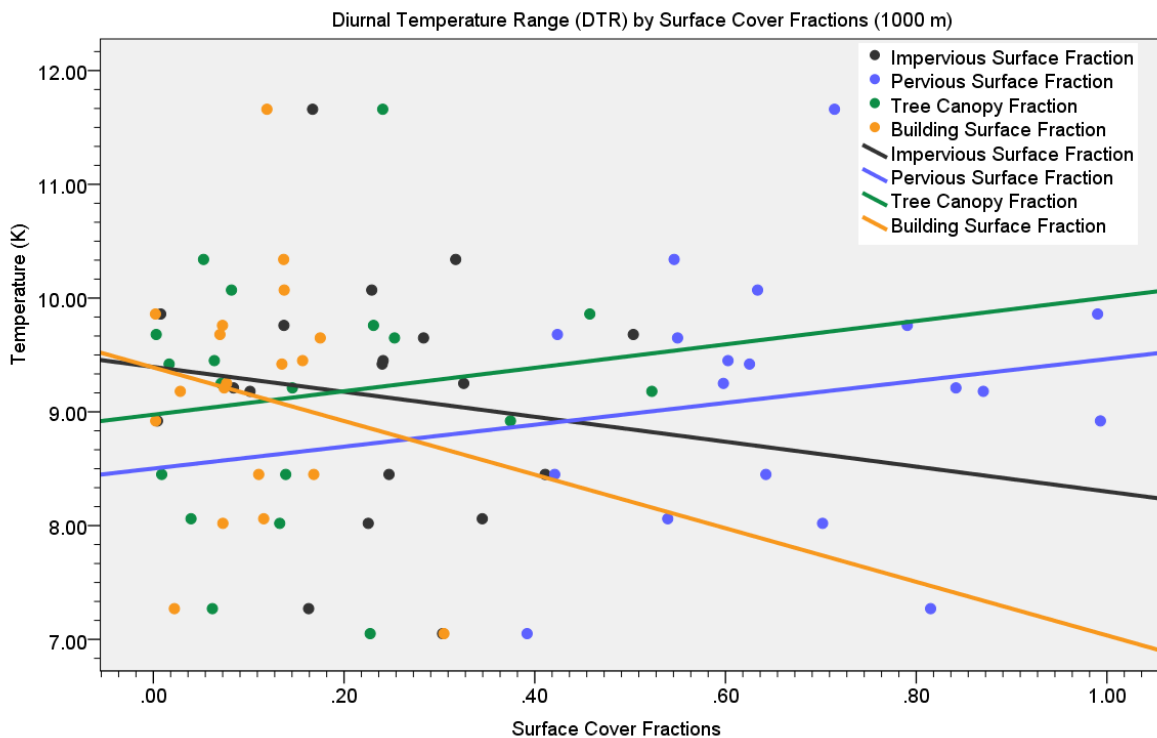


Figure 4.14: The diurnal temperature range plotted against the impervious, pervious, building surface and tree canopy fraction calculated within the one-thousand metre radius around the meteorological stations.

Correlation analysis provided evaluations of the influence of surface cover fractions on the temperature variables. There was a positive correlation between the \bar{T} and impervious ($\beta = 3.19$) and building surface fractions ($\beta = 5.61$) (Figures 4.11 – 4.14). Also, the negative correlations were found when the temperature variables were regressed and plotted against the pervious ($\beta = - 2.58$) and the tree canopy fraction ($\beta = - 2.23$). Similar relationships were evident in the linear regression of T_{\max} , T_{\min} on surface cover fraction. Furthermore the slopes of the trend lines for each relationship became more pronounced as the thermal source area increased from the five-hundred metre radius to the one-thousand metre radius thermal source zones (Table 4.11 - see Figures A9 – A16 in Appendix A for 100 metre and 500 metre radius plots). This can be better appreciated when all the coefficient of determination values (r^2) between the \bar{T} , T_{\max} , T_{\min} against the surface cover fractions were graphed according to the surface cover fractions Figure 4.15.

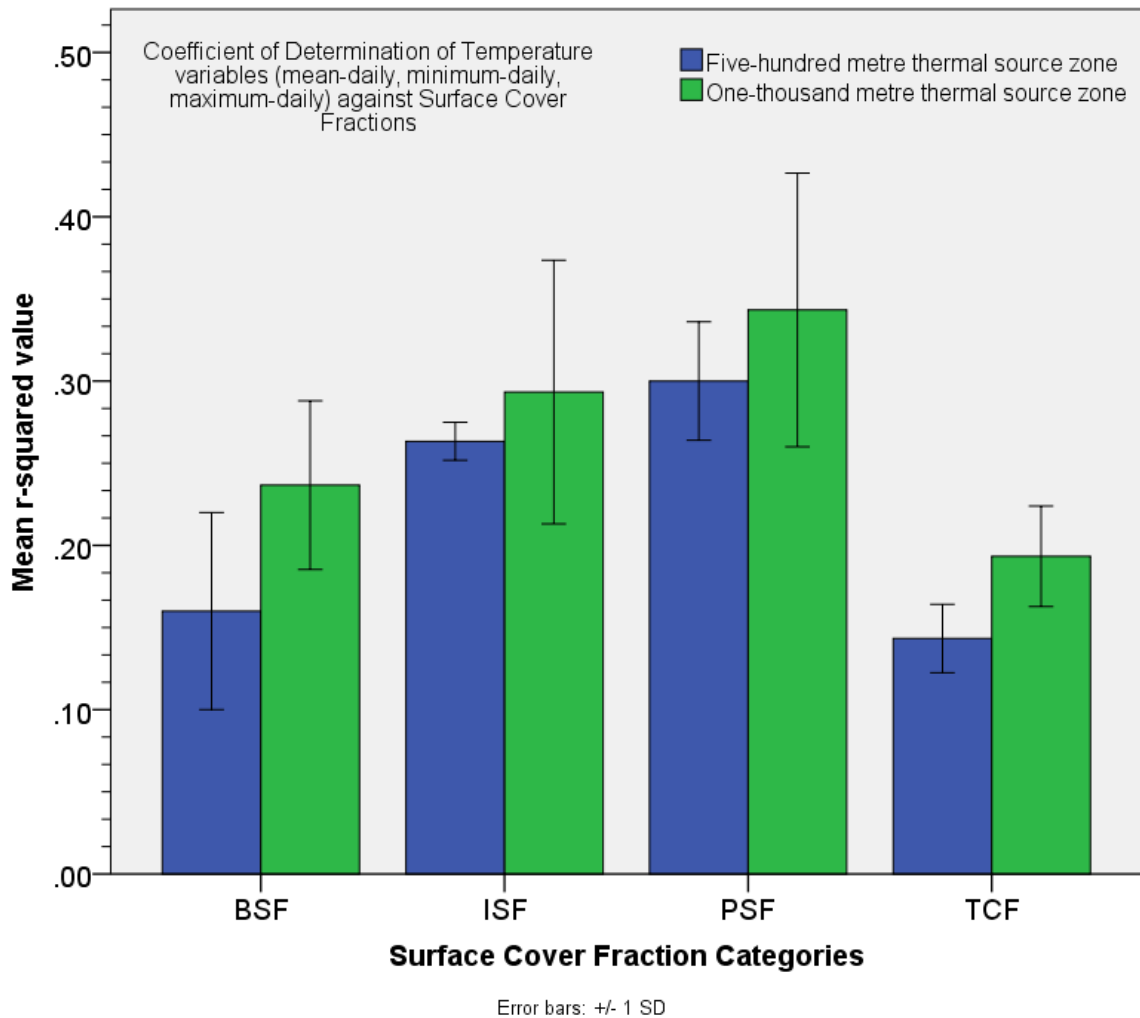


Figure 4.15: The comparison of r-squared values from Table 4.11 between the 500 m and 1000 m thermal source zones.

The general trend of increasing r^2 value as the thermal source zone increases is evident in Figure 4.10. In order to check for a statistically significant difference a two sample t-test was used to assess the difference between the means of the r-squared values in the five-hundred metre thermal source zone with the r^2 values in the one-thousand metre thermal source zones (Table 4.12).

Table 4.12: The two-sample t-test assuming equal variances to compare the r^2 values calculated in the 500 and 1000 m scatter plots.

	<i>500m</i>	<i>1000m</i>
Mean	0.173	0.205
Variance	0.010	0.017
Observations	16	16
Pooled Variance	0.014	
Hypothesized Mean Difference	0	
df	30	
t Stat	-0.770	
P(T<=t) two-tail	0.447	
t Critical two-tail	1.697	

Comparison of the average r^2 values for the five-hundred metre thermal source zone with the average r^2 values for the one-thousand metre thermal source zone showed that there is no statistically significant difference between the two average r-squared values. In other words, the two-sided p-value of 0.45 is insufficient evidence against the null.

4.5 Temperature Surface of Study Area

Ordinary Kriging and ordinary co-Kriging were used to create a temperature surface of the study region in order to examine the horizontal spatial structure of climatic averages including \bar{T} , T_{\max} , T_{\min} . Co-kriging was applied because the research conducted here had already involved collecting secondary data which can be used in co-Kriging to improve upon the ordinary Kriging method. The performance of the Kriging methods was assessed using the difference measure of mean error (ME) and root-mean-square error (RMSE). The objective was to find the mean error (ME) closest to zero and the smallest RMSE. The root mean square error is able to summarize the mean difference in the units of observed and predicted values (*i.e.* °C). The RMSE value provides a measure of how well the chosen model predicts the measured variable and the mean error (ME) is the averaged difference between the measured and the predicted values. Therefore the objective was to find the mean error (ME) closest to zero and the smallest RMSE. The model parameters and the validation of the Kriging method showing the lowest RMSE are presented in Table 4.13.

Table 4.13: Ordinary Kriging and ordinary co-Kriging validation measures for daily mean, daily minimum and daily maximum temperatures.

Temperature (N = 19)	Ordinary Kriging		Ordinary Co-Kriging	
	Validation		Validation	
	Mean Error	RMSE	Mean Error	RMSE
Mean	0.018	0.528	0.008	0.420
Minimum	0.064	1.047	0.082	0.965
Maximum	0.005	0.382	-0.012	0.324

The lowest RMSE was 0.528 °C for \bar{T} , 1.057 °C for T_{\min} , and 0.396 °C for T_{\max} with ordinary Kriging. When secondary data such as impervious, pervious and building surface fractions were used in the co-Kriging model the lowest RMSE was 0.420 °C for \bar{T} , 0.965 °C for T_{\min} and 0.324 °C for T_{\max} . These models were used to interpolate the \bar{T} , T_{\max} , T_{\min} surfaces of the study area. Also, the benefit of using Kriging in ArcMap v.10.2 is that the prediction error map can be shown, *i.e.* the uncertainty of the predicted surface can also be overlaid on the interpolated map. The prediction error provides a value for quantifying the uncertainty of a prediction. Given that the temperature variables were found to be normally distributed (Table A1 in Appendix A) then the prediction error can be used to create a 95 *per cent* confidence interval for the predicted temperatures. In other words, 95 *per cent* of the time the hypothesized true value will lie somewhere within the interval formed by the predicted value, plus or minus two times the prediction standard error given in the prediction standard error map (ESRI, 2014). The temperature surface maps for the \bar{T} , T_{\max} , T_{\min} including their prediction error using ordinary Kriging is shown in Figure 4.16.

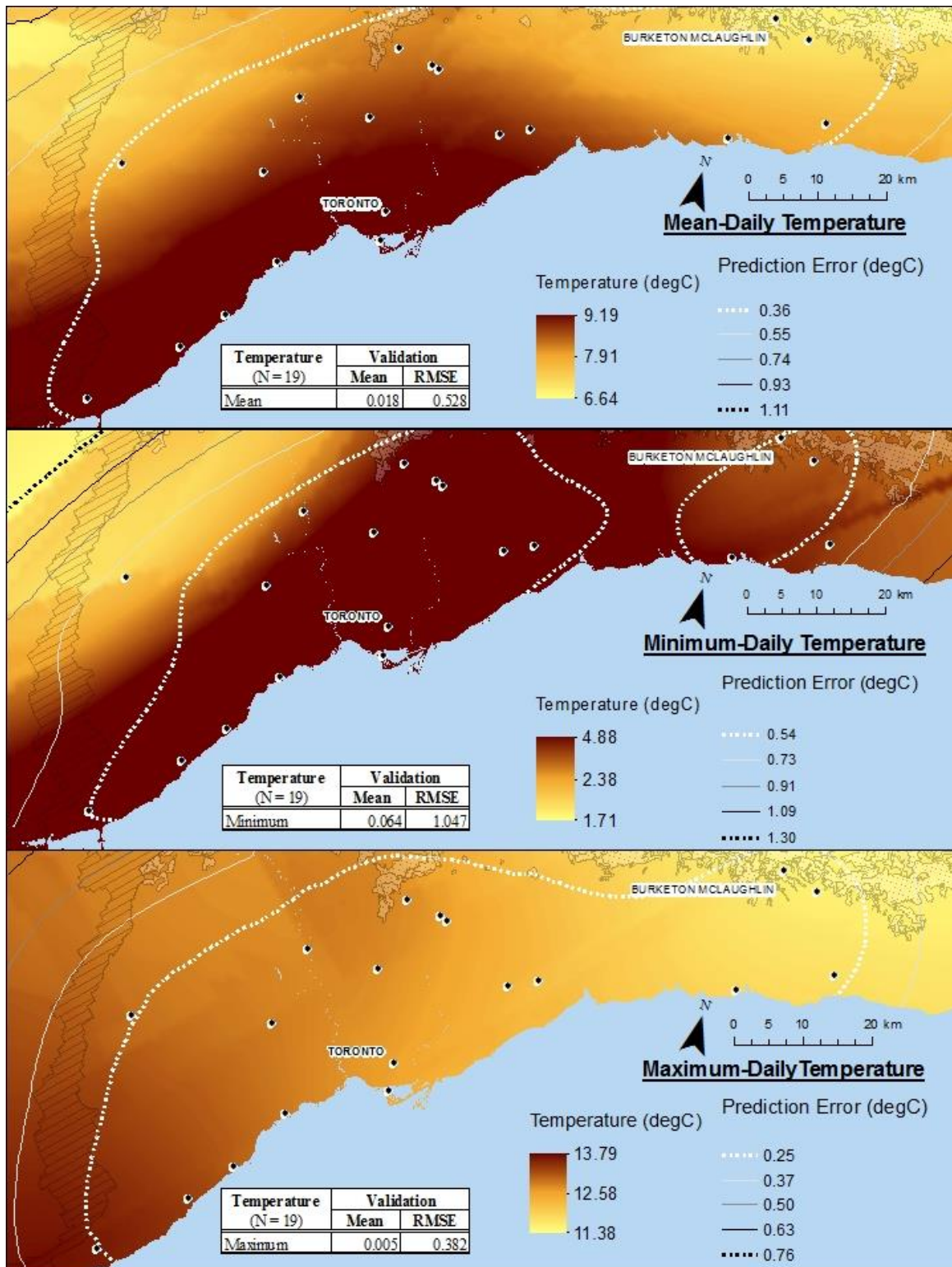


Figure 4.16: The \bar{T} , T_{\min} , T_{\max} surfaces of study area in Southern Ontario using ordinary Kriging.

The surface interpolation using OK showed there are higher \bar{T} temperatures found along the Lake Ontario shore in the west and north-west of the study area but lower \bar{T} were found in the east and north-east. The smaller prediction errors (± 0.36 °C and below) are found in the area immediately surrounding Toronto and extending westward to the Burlington TS station and east to Bowmanville for \bar{T} . The T_{\min} surface produced using OK showed a fairly constant T_{\min} throughout most of the study area with the exception of the immediate area surrounding the Burketon McLaughlin, Tyrone and Bowmanville stations. There are lower prediction errors (± 0.54 °C and below) near most of the stations with the exception of Bowmanville, Burlington TS and Georgetown WWTP (± 0.73 °C to ± 0.89 °C). The T_{\max} surface produced using OK showed higher T_{\max} in the west and generally lower temperatures in the east. The smallest prediction error (± 0.25 °C and below) is found within most of the study area with the exception of Burlington TS, Georgetown WWTP, and Burketon McLaughlin (± 0.37 °C to ± 0.50 °C). In general the predictions that have lower errors are located near the sites and within the distances separating each station and the predictions with higher errors are located at and beyond the areal extent of the study area, *i.e.* when temperatures were extrapolated. This is evident in the increasing magnitude of the prediction errors farther north, east and west away from the study area.

The \bar{T} , T_{\max} , T_{\min} were interpolated using OCK using secondary data including impervious, pervious, and building surface fractions. The interpolated surfaces are shown in Figure 4.17.

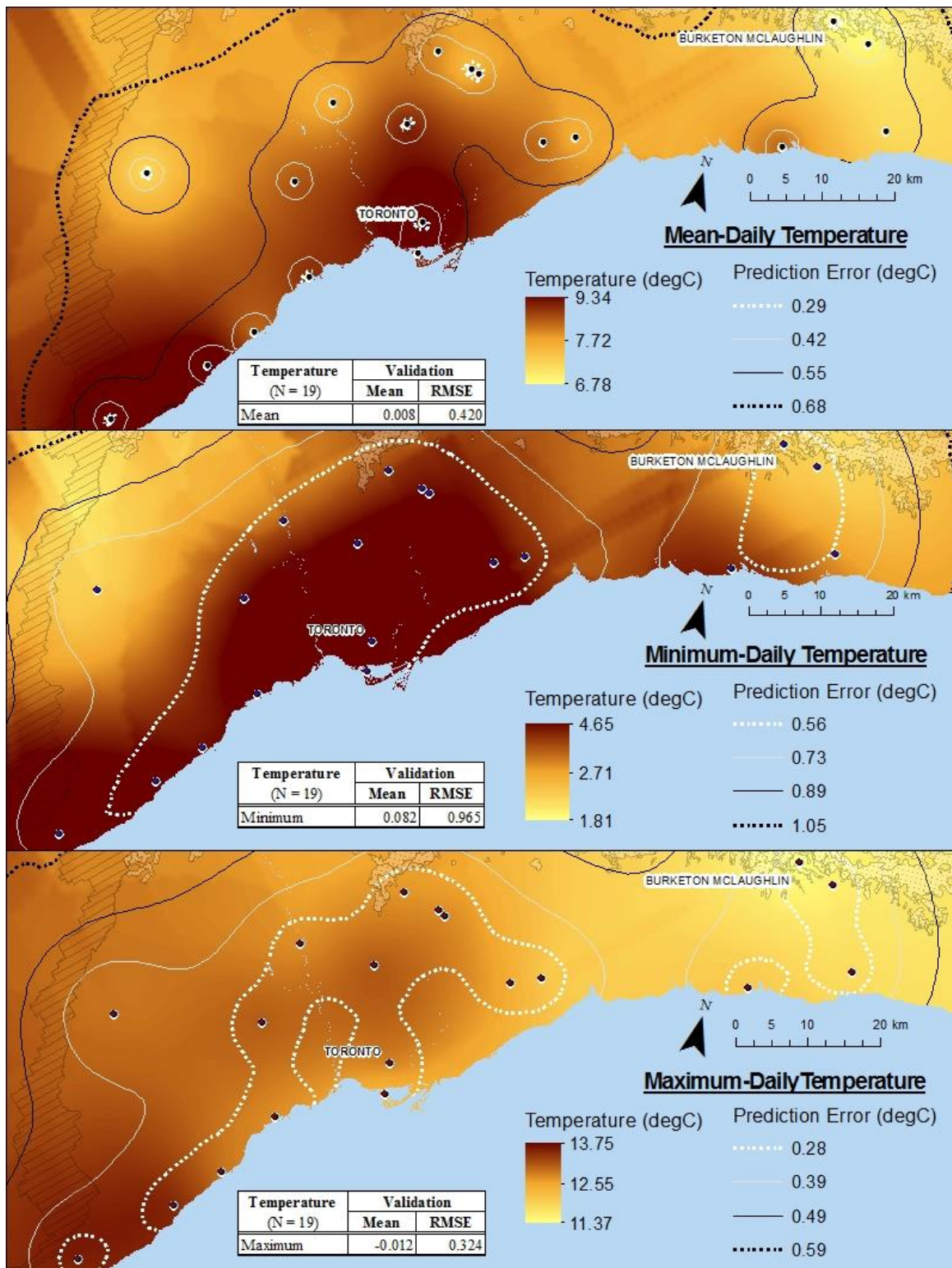


Figure 4.17: The \bar{T} , T_{\min} , T_{\max} surfaces of study area in Southern Ontario using ordinary co-Kriging.

The interpolated \bar{T} surface using OCK showed regions of higher \bar{T} in pockets around the Toronto, North York, and Oakville Gerrard and Burlington TS stations. The smaller errors (± 0.29 °C and below) are found immediately surrounding each station with larger errors (± 0.29 °C to ± 0.68 °C) within most of the study area. There were higher T_{\min} within the City of Toronto and when compared to the rest of the study area with the exception of the Oakville Gerrard and Burlington TS stations. The smaller errors (± 0.56 and below) are found within the City of Toronto and the region to the east surrounding the Burketon McLaughlin and Tyrone stations with the exceptions of the Burlington TS, Georgetown WWTP, Oshawa WWTP and Bowmanville stations having slightly larger prediction errors (± 0.56 °C to ± 0.73 °C). The T_{\max} surface identified higher temperatures around the Burlington TS, Oakville Gerrard and Toronto North York station. The lower T_{\max} were found to the east near Burketon McLaughlin, Tyrone, Bowmanville and Oshawa WWTP. The lower prediction errors (± 0.28 °C and below) were found surrounding all the sites. Larger errors (± 0.28 °C to ± 0.39 °C) were found in pockets with the City of Toronto and between the Oakville Gerrard and Burlington TS stations, overall the higher temperatures were found in regions with greater urban influence and there was more certainty with the predictions was found very near the stations.

5. DISCUSSION

5.1 Local Climate Zone Application in Southern Ontario

Research in urban climates has revealed the existence of climate modification as a result of urbanization. The urban environments in southern Ontario may experience elevated temperatures because of intensified urbanization expected in order to house the region's growing population. A current assessment of southern Ontario's microclimates, specifically the UHI effect, was made using the most recently available climate averages. In order to explore the UHI effect, the newly proposed local climate zone method was applied. The impervious, pervious and building surface fractions were calculated to describe each of the nineteen station's local surroundings. The local climate zone method provides greater objectivity because each site is classified according to its calculated surface cover properties. The surface cover fractions were calculated easily, however, the data needed to calculate the surface cover properties were not readily available. As a result, surface cover abundances were calculated from vector and raster

GIS layers representing land use and land cover. Once the surface cover properties were calculated the classification was easily implemented in a GIS using structured query language (SQL) expressions.

According to Stewart and Oke (2012, p. 1891) the surface cover properties collected should lead to the best, not necessarily exact, match of the field sites with an LCZ class. Using the three surface cover fractions 47% (9/19) of the five-hundred meter source zones were matched exactly and 42% (8/19) of the one-thousand metre thermal source zones were matched exactly. Two of the stations, Burketon McLaughlin and Tyrone, were matched to multiple LCZs (*i.e.* LCZ A to LCZ D and LCZ F and LCZ G). This is because six of the seven land cover type LCZs outlined by Stewart and Oke (2012) have the same surface cover properties and consequently the six LCZs are separated into different LCZs by geometric properties including sky view factor (*i.e.* the amount of visible sky), aspect ratio (*i.e.* mean height-to-width ratio of tree spacing) and heights of roughness elements (*i.e.* geometric average of tree heights). Since the values for these geometric surfaces were not part of the objective in this research, the final classified LCZ for the land cover types were based upon the qualitative description of the zones outlined by Stewart and Oke (2012, p. 1885). These descriptions are based on the quantitative geometric properties and therefore the descriptions of the land cover type LCZs do make it easy to identify the most appropriate LCZ for the least urban of all sites. Although the choice to match according to qualitative descriptions may seem to add some subjectivity to the classification process, it is important to note that the sites had been classified as land cover types and not built types. Thus this “limitation” may be attributed to the lack of field data and not the method itself. Regardless through the matching process some of the subjectivity was minimized because stations were assigned according to their calculated landscape properties. The rural sites identified for the calculation of UHI intensity were Burketon McLaughlin and Tyrone (both LCZ C) which are located approximately 65 km north east of Toronto. Also, there was no difference in the calculated mean-daily and maximum-daily UHI intensities between the two sites. This helps to reinforce the notion that the background rural temperatures used to calculate UHI intensities are similar. Furthermore, by averaging the UHI intensities calculated from the Burketon McLaughlin and Tyrone stations the reference rural background temperature is

confidently represented in the assessment of the UHI intensities calculated for urban areas within southern Ontario.

It is important to consider that as recently as 2001 the site chosen as “rural” to investigate the UHI effect in downtown Toronto was the Toronto Pearson airport (*e.g.* Gough and Rozanov, 2001), but the airport can no longer be considered rural and used as a reference rural station. In fact, according to the research in this study the surface cover fractions calculated for the Toronto Pearson station are considered to be one of the most urban-centric built types found within the study area (*i.e.* LCZ 5). This emphasizes the problem with what can be defined as urban and what can be defined as rural within the context of urban climate research. The main issue is that the terms urban and rural have been loosely defined and applied in previous UHI research (Stewart, 2011a) and are associated with administrative and cultural bias resulting in haphazardly chosen rural sites which may lead to different UHI intensity estimates for the same region. The research presented here shows that by taking into account the surface cover properties of the measurement location some biases can be minimized. Thus subjectivity introduced by an arbitrarily chosen rural site can be reduced by first classifying sites into their respective local climate zones then comparing the least urban site and ensuring that field evidence corroborates with absence of what is regarded as urban. The inclusion of surface cover properties in classifying stations makes the UHI estimation and its comparison a less subjective process. The result is a continuum of urbanicity that better describes the urban influence on air temperature.

5.2 The Urban Heat Island in Toronto and Urbanicity

Since the first insights into the spatial distribution of temperature in Toronto almost 80 years ago by Middleton and Millar (1936) there have been considerable changes to the size and density of the City. Mohsin (2009) reported that the annual mean temperature had started to increase after 1920 in downtown Toronto, then again after the 1960s in suburban stations. The trend had increased during the 1980s and all of these trends coincide with the pace of urbanization in southern Ontario (Mohsin, 2009). The research presented here used the recent climate averages released by Environment Canada and showed the presence of the UHI and its extension west towards Burlington and north to Richmond Hill. Based on daily mean temperature the highest UHI intensity was found in Toronto (LCZ 5) reinforcing the theory that

environments that are the most urban tend to be warmer than less urban locations. For example, the Toronto station had one of the highest impervious surface fraction and the highest building surface fraction (30.3 and 30.5 %). The Toronto Pearson station had the highest impervious surface fractions and this can be attributed to the abundance of paved area typical of large airports. There were two LCZ 6s (Toronto Buttonville and Gormley Ardenlee), which given their considerably higher impervious surface abundance still had lower UHI intensities. This is in contrast to the Oakville Gerrard station (LCZ 9) which had one of the highest UHI intensities yet it had higher pervious surface fractions (62.5%) compared to the Toronto Buttonville and Gormley Ardenlee stations (54.2 and 54.6%). The Lakeview MOE station (LCZ 9), Burlington TS station (LCZ 6) and Toronto Island station (LCZ 9_G) also had considerably higher pervious surface fractions but higher mean-daily and minimum-daily UHI intensities (the maximum-daily UHI intensities were slightly lower for these stations). The proximity to the lake should result in some cooling through convective heat loss as a result of lake breezes in summer though warmer in the winter than further inland sites would be. It is possible that the moderating effect of Lake Ontario may be masking the magnitude of the UHI intensity or that it may be ineffective in diminishing the UHI intensity in the local area surrounding these stations near the lake shore environment. That is to say the UHI intensities could possibly be even higher in the absence of the lake. Thus the ramification of intense development that is likely to continue some distance away from Lake Ontario could be problematic considering the loss of the moderating influence a large lake has on mitigating the UHI intensity.

The westward migration of the UHI effect matches with the rapid development seen in Mississauga, Oakville, Brampton and Vaughan in the last 20 years. The overall assessment showed that winter had higher UHI intensities which are consistent with theory (Oke, 1992) and recent findings (Moshin, 2009). Furthermore the UHI intensities are found to be higher west of the City of Toronto (Burlington, Oakville, Lakeview) when compared to the eastern region of the study area (Oshawa and Bowmanville) despite the east being generally downwind of Toronto's urban core. Given the trend in built up areas throughout southern Ontario, the UHI effect seems to extend further towards the north and west of the City. Other factors including anthropogenic heat input and reduced sky view may contribute to the higher UHI intensities found in the stations near the lake. In general the two extreme values of the surface cover fractions (i.e.

highest and lowest fractions) were associated with the highest and lowest temperature variables. However the range of surface cover fractions in between the two extreme values showed no discernible pattern. It is possible that the local climate zones may not be perfectly associated with pervious and impervious surface abundance and other surface cover and geometric properties may need to be included for future research.

On the other hand, the degrees of urbanicity were evident when LCZs were grouped into similar units. The general pattern of increasing mean-daily UHI intensities with increasing urban-centric built types showed that there is some value in the classification system's ability to distinguish between varying degrees of urban landscapes. The benefit is that by identifying a continuum of urbanicity, there is a shift away from the dichotomous system viewing areas as either urban or rural. The impact of urbanization on climate measured through UHI intensity can be one view of urbanicity, however other measures (*e.g.* air pollution index, water pollution, species diversity, *etc.*) can also be incorporated to define a general concept of urbanicity. Thus when stations are considered based on individual surface cover characteristics trends may be disguised, however once sites are classified based on the three surface cover fractions (and possibly more) a pattern emerges revealing the urban influence on air temperature.

5.3 The Relationship between Surface Cover Fraction and Temperature

The expected patterns between individual surface cover fractions were not easily detectable in the bar graphs presented (Figures 4.2 – 4.7) and thus systematic relationships between each surface cover fraction and \bar{T} , T_{\min} , T_{\max} were explored using linear regression. The correlation analysis revealed that pervious and impervious surface cover can have opposite effects on air temperature. Positive correlation coefficients were associated with the impervious surface fractions and the building surface fractions. This could be because the greater amounts of impervious and building surface fractions provide little heat loss through transpiration because water is quickly removed from city streets through efficiently designed sewers and paved surfaces. Once the water is lost from the surface through runoff and evaporation the cooling delivered through latent heat of evaporation is also lost and the heat goes towards heating the surface and atmosphere. This can contribute to the elevated temperature found in the zones with a greater abundance of impervious and building surface fractions. There were negative

correlation coefficients associated with pervious surface fractions which could be attributed to areas with an abundance of vegetation that is rewarded with the heat loss through transpiration. The strength of these relationships can be assessed using the r^2 value which signifies the proportion of the variance in the dependent variable (*i.e.* temperatures) that is accounted for or explained by the independent variable (*i.e.* surface cover fractions) (Allen, 1997). This research shows that 30%, 37% and 21% of the variance in \bar{T} , T_{\max} , T_{\min} is explained by the impervious surface fraction calculated for the one-thousand metre thermal source zone and 27%, 25% and 27% at the five-hundred metre thermal source zone. A greater amount of variation in the temperature variables (\bar{T} , T_{\max} , T_{\min}) was explained by impervious surface fraction when the thermal source zone was increased from the five-hundred metre radius to the one-thousand metre radius. Also 37%, 41% and 25% of the variance in \bar{T} , T_{\max} , T_{\min} is explained by the pervious surface fraction calculated for the one-thousand metre thermal source zone and 34%, 29% and 27% for the five-hundred metre thermal source zone. Here a greater amount variation in \bar{T} and T_{\max} was explained by pervious surface fraction when the thermal source area increased from the five-hundred metre radius to the one-thousand metre radius. However the strength of the relationship decreased for T_{\min} when the thermal source area increased from the five-hundred metre radius to the one-thousand metre radius. The building surface fraction was able to explain 28%, 25%, and 18% of the variance in \bar{T} , T_{\max} , T_{\min} for the one-thousand metre thermal source zone and 22%, 16% and 10% for the five-hundred metre thermal source zone. The tree canopy fraction at the one-thousand metre radius was able to explain 20%, 22% and 16% of the variation in \bar{T} , T_{\max} , T_{\min} for the one-thousand metre thermal source zone and 15%, 12% and 16% for the five-hundred metre thermal source zone, however the correlation was only significant for T_{\max} at the one-thousand metre thermal source zone. In general there was an increasing trend in the strength of the relationships when the thermal source area increased from the five-hundred metre radius to the one-thousand metre radius. The linear regression shows that the impervious, pervious and building surface fractions are good indicators of canopy level air temperatures at a local scale and the strength of the relationship increased when the thermal source area was increased from the five-hundred metre radius to the one-thousand metre radius. As the area of the thermal source zone increased the slope became more marked suggesting that there may be an ideal spatial scale at which the relationship between surface cover fraction and temperature is

expressed. This information can be used to assess the impact of proposed development on new land or re-development of existing neighbourhoods and the one-thousand metre radius may be a good starting point to assess surface cover properties in local neighbourhoods because of the greater strength in relationships evident between the air temperature variables and surface cover fractions. Furthermore the abundance of these surfaces should be of interest if the impact of urbanization on the local climate is to be minimized.

Changing the surface cover properties may lead to improving outdoor thermal environments in urban spaces. The presence of an urban tree canopy has the potential to moderate the air temperature in the adjacent locality. For example the Georgetown WWTP station (LCZ 9), Woodbridge (LCZ 9) and Bowmanville Mostert station (LCZ B) had relatively higher pervious surface fractions (with large forest patches) and they showed relatively lower UHI intensities. Pearson and Burton (2009) reported that in many urban environments in southern Ontario the presence of urban trees plays a role in cooling the urban environment as well as improving air quality, reducing stormwater runoff and enhancing biodiversity. For example Shashua-Bar (2000) showed that small green sites in the city have cooling effect that stretch out to 100 m along the streets. Therefore having small parks separated by smaller distances can provide thermal relief in the local environment. The empirical model developed by the investigators showed the cooling effect of trees with heavy traffic reached 1 K. Given the high density of streets in the City of Toronto and neighbourhoods across southern Ontario there is potential to reduce the UHI intensity and improve the thermal comfort in the outdoor city and neighbourhood environs. However growing trees along the streets of major cities require more work by city maintenance workers and urban trees have a shorter life spans than their counterparts growing in a more natural favourable setting (Buhler *et al.*, 2007). The main reason for this is due to limited soil volume and increase soil compaction found on urban streets which hinders healthy root development (Buhler *et al.*, 2007; Mullaney *et al.*, 2015). However the growth of trees can be greatly improved by implementing permeable pavements which acts as and be accounted for as pervious surface cover. Mullaney *et al.* (2015) have shown that by varying the size of the underlying drainage layer the trunk diameter of saplings increased by 55 percent when compared to traditional asphalt pavements. The addition of the permeable pavements changes the soil moisture levels by increasing the moisture levels in sandy soils and

decreasing the levels in wetter clay soils. Based on the research by Mullaney *et al.* (2015) the presence of the permeable pavements also lowered the soil temperature. The effect of moderating the soil temperature can be an added benefit of mitigating surface UHI in the local environment. Space constraints can be a problem in urban environments. This issue was investigated by Blake (2013, p. 73) who used perennial vines in Toronto's downtown and showed that growing vines on walls can be effective in mitigating rise in built surface temperatures. The problem of space in urban environments requires some innovation by architects, engineers and city planners. Millward and Sabir (2011) claimed that the trees in the City of Toronto are a significant component of the city's green infrastructure and are a public asset with benefits that have not been fully realized. As the surface cover is changed from pervious to impervious the designated LCZ of the area can be updated to reflect the environment and the resulting effects can be monitored while the LCZ method can be evaluated.

5.4 Temperature Surface of Study Area

Ordinary Kriging was used as the interpolation method to explore the horizontal spatial structure of the \bar{T} , T_{\min} , T_{\max} within the study area. Since the research conducted here involved calculating surface cover fractions, co-Kriging was also used in order to include secondary data to improve upon the ordinary Kriging method and obtain a better model. Even though the co-Kriging method showed better RSME values than the ordinary Kriging method, there were more areas which had greater uncertainty in the predictions. The benefits of obtaining a better model come at a cost of uncertainty in the predictions. The reduction of the prediction error in interpolating temperature maps could be made possible with strategically placed monitoring stations within the canopy layer. The placement of monitoring stations can be identified using the interpolated maps presented in this research (i.e. position meteorological stations in areas with higher prediction errors).

Overall the temperature surface maps created using both methods showed small RMSE values and ME values. The maps help to reveal the general pattern within the study area which can aid in the assessment of the local climates under investigation. In other words, higher temperatures were found near the lake shore and closer to urban-centric zones. These areas should consider some mitigation measures to combat their UHI intensity. In order to visualize

the UHI intensity in relation to the locations of the local climate zones, the average mean-daily UHI intensity surface was mapped using the interpolated temperatures (Figure 5.1).

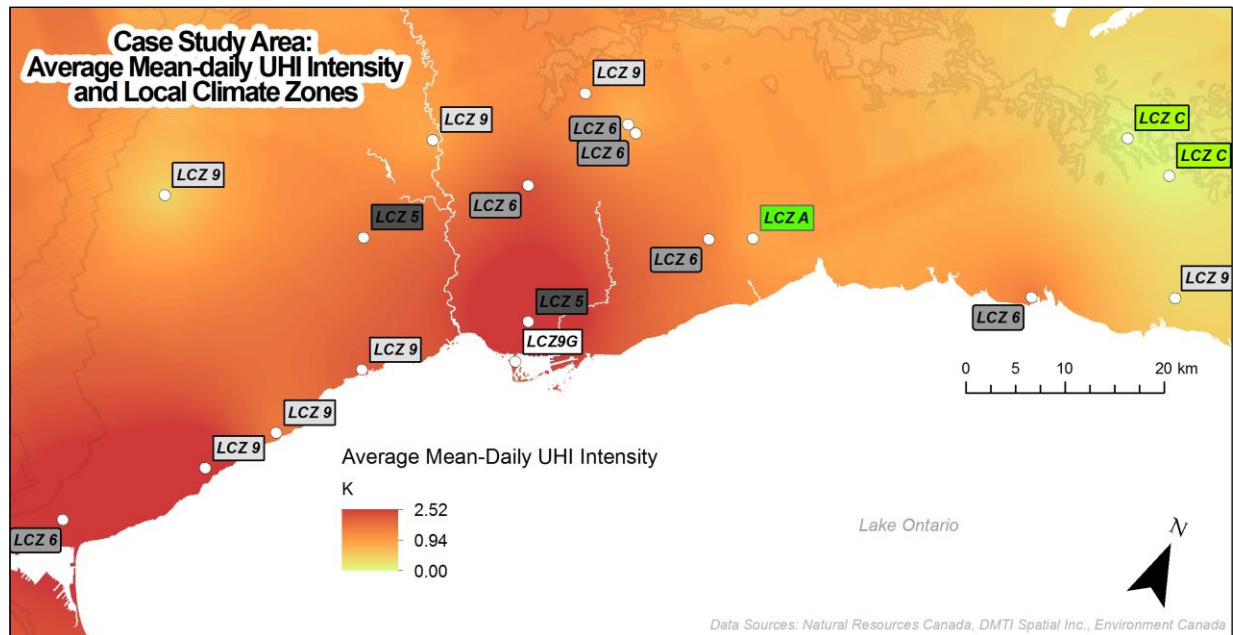


Figure 5.1: The average mean-daily UHI intensity calculated based upon the co-Kriging interpolated \bar{T} and shown along with the locations of the classified LCZs.

The distribution of higher average mean-daily UHI intensity matches well with the more urban-centric local climate zones. Similarly the distribution of lower average mean-daily UHI intensities matches fairly closely to lower degrees of urbanicity. Although the general pattern of higher urban centric zones were associated with higher UHI intensities, the microscale patterns between the defined LCZs are not evident - in other words the surface is too smooth. For example, some areas that are expected to be cooler such as High Park and the Don River Valley are shown to be associated with higher UHI intensities. This can be minimized with a dense network of monitoring stations or improving upon the co-kriging method by collecting secondary data in these areas (see future research).

5.5 Planning and Management of Cities

In the 20th century, Kratzer (1956, p. 4) suggested not accepting city climate as fact but to influence it by “composing a climatologically accurate city plan, ..., with proper distribution of industries, residential areas, green areas and street” and to “strike a blow at the haze which

plagues so many urban areas through legal measures, improved heating and electrification”. This philosophy is difficult to implement now in older cities because their footprints have already been established for some time. However there is relevance in conducting urban climate studies because of their application in design, planning and management in cities.

Recently the application and usefulness of microclimate studies for planning purposes has been suggested and there is growing interest in integrating climate knowledge in the urban planning process (Evans and De Schiller, 1996; Eliasson and Svensson, 2003). Evans and De Schiller (1996, p. 361) recommend that the knowledge obtained from urban thermal studies should be transferred to planners and architects in a way that can influence the approach to physical planning. The local climate zones identified for the given area can become the management units under focus and any surface cover or geometric properties that are changed can then be easily recalculated and assigned a new more appropriate LCZ. Then analysis can address climatic variables such as mean, maximum and minimum temperatures and evaluate the direct and indirect influence of these variables on human comfort and their relative importance to heating and cooling (De Schiller and Evans, 1996a, p. 449). Although a single value that represents the UHI intensity is an oversimplification of the phenomenon, it still has value because the value provides planners a way of measuring the impacts of urbanization and also provides a measure of success or failure which can be gauged based on any mitigation activity taken to reverse the UHI effect. Other steps including policy initiatives like providing energy related incentives for community design such as layouts (*e.g.* rezoning to minimize higher floor area ratios and open area ratios), street alignments (*e.g.* maximize north-south lots with south facing houses through east-west street orientation) and landscaping (*e.g.* community involvement by strategically planting more trees to provide some cooling in the summer and block cold wind in the winter and reducing impervious surfaces) (De Schiller and Evans, 1996a, p. 450 and Ko, 2013, p. 342) can lead to a lower degree of urbanicity or an upgrade from a more urban LCZ to a lower urban-centric LCZ. If implemented these design considerations can have potential to provide long term energy savings and possibly minimize the effect of warming or improve an already poor climate.

More recently the threat of global climate change has inspired a number of prominent urban climatology experts to promote climate information for improved planning and

management of cities (Grimmond *et al.*, 2010). The increasing trend in urbanization means that the numbers of buildings, and as a result the energy consumption rates, are going up (Oxizidis *et al.*, 2007, p. 96). Because of the altered urban microclimate, Oxizidis *et al.* (2007) suggest that the estimation of urban buildings energy behaviour needs to take into account the modified urban climatic parameters such as temperature (Oxizidis *et al.*, 2007, p. 97). An extensive climate monitoring network within the urban environment can present an improved microclimatic view of the area which could assist in modifying the performance of buildings and its resultant energy demand. However a dense monitoring network is lacking in the City of Toronto and within the study area presented in this research.

In a report by Penny (2008), the need for further research of UHI in Southern Ontario was highlighted. They suggested that the knowledge gained be incorporated into land use planning policy, that is, to identify Toronto's hotspots, what causes them and creating planning strategies such as green infrastructure to reduce them or ways to "cool" the city (Penney, 2008, p. 21). Because peak energy demand has shifted from winter to summer, mitigation efforts can address some of the concerns highlighted in the Environmental Commissioners Office's (ECO) Annual Energy Conservation Progress Report stressing conservation as the first resource considered in meeting power needs (Environmental Commissioner of Ontario, 2015, p. 2). Low impact development like green roofs, cool roofs, or permeable pavements can improve the outdoor local climate and reduce the need for indoor cooling. This will make it easier to conserve because the effects of outdoor thermal environments are mitigated. Some researchers claim that a 1 °C increase of temperature can increase the cooling energy consumption by 4 percent in the US (Lee and French, 2009, p. 479). So conservation can be a real goal. This research revealed that the local climate near the lake shore requires some attention because this area experiences some of the highest UHI intensities.

In the City of Toronto the application of climate knowledge in planning was considered in the 1960s and 1970s. In the early 1960s scientist Bruce Findlay and colleagues from the Meteorological Service of Canada were tasked with investigating the mesoclimatic variation across a 6 km area near the Rouge River valley for siting the Toronto Zoo (Munn *et al.*, 1999, p. 40). Over a two year study period they showed the daytime valley temperatures were warmer in winter and cooler in summer with little variation across the valley when compared to the

surrounding area. At night, on average, the valley was considerably colder by 5 °C. This information was used to design habitats for non-indigenous animals sensitive to temperature variation (Munn *et al.*, 1999, p.40). In 1976, the Central Waterfront Planning Committee produced a series of documents for planning purposes. They introduced climatic zones along the waterfront and provided building designs to accommodate the special waterfront climates (Smith, 1976). For example, the two main principles of design introduced were exposure to sunlight in winter but not summer and shelter from strong winter winds but exposure to cooling summer breezes. These objectives were implemented by considering orientation, placement of deciduous trees, 50 to 60 degree sloped roofs for solar collectors, and fences to act as wind shelters to the southwest and northwest. These initiatives could help to reduce the impact that urbanization has on air temperatures. These and other mitigation measures may disrupt the current LCZ classification system by revealing that some urban microclimates have lower temperatures in zones which are expected to have higher temperatures (*i.e.* LCZ 1 to LCZ 4). In essence these areas would be associated with a lower degree of urbanicity because its temperatures reveal that the impact from urbanization is minimized.

Toronto's waterfront is now growing with high rise condominium development which may act as a barrier to penetrating lake breezes. The behaviour of Toronto's lake breezes was studied by Munn *et al.* (1969) well prior to the intense condominium development in the area. The cooling effect of Lake Ontario extended further north early in the 20th century (*e.g.* Middleton and Millar (1936)) but in 1997 the effect was less because high rise buildings likely blocked cool air from penetrating further north (Mohsin and Gough, 2010, p. 318). This can be a contributing factor to higher UHI intensities near the Lake. The current behaviour of lake breezes and the consequences of the physical barriers to wind penetration into the city core at the canopy level should be revisited in order to obtain a greater understanding of air ventilation in the city's core.

The City of Toronto has included in its official city plan the importance of addressing the urban heat island in the city (City of Toronto, 2009, p. 17) and some policy initiatives have been implemented to combat the UHI effect. The Toronto Green Standard was approved by Toronto City Council in December 2008 and began implementation in September 2009. The three tier program for any new developments – the purpose of the program - is to address issues such as

energy efficiency and mitigating urban heat island impacts in the city. The City of Toronto also approved a Green Roof Bylaw in 2009 based on the research done by Banting *et al.* (2005). The by-law requires any new developments over 2,000 square metres to implement a green roof. This is the first of its kind to be implemented in North America. Although these programs are only for new developments it shows the City's initiative to address the issue of urban warming both at the urban boundary scale as well as the urban canopy scale. The results from this program may encourage municipal governments to address the issue associated with older buildings in the city and redevelopments of neighbourhoods. A climate analysis might also be useful when any new design plans are considered. The city lacks a dense network of monitoring stations in the urban canopy layer (4 stations in the recently released climate normals) which poses some difficulty in monitoring and carrying out urban climate studies. Another point that should be considered is if cities are expected to adapt to forthcoming climate change then the collection of climate data is important. On top of monitoring the environment, climate analysis can also assist in using design principles that incorporate climate information into the decision making process. Middleton and Millar (1936) showed the extent to which the climate can change within only a few kilometres of the lake, and then 60 years later the extent to which the urban influence extends has grown beyond the city core (Sanderson, 2004, p. 86). This trend is likely to continue into the future with expected population growth and intensified urbanization.

Natural elements like trees and water bodies can mitigate heat in an urban setting while the human-made elements such as buildings and paved surfaces can add to the UHI effect. Managing the natural elements with the human made ones in cities is a difficult task for any municipal planning department. This is because the general goal of cities is to provide and improve their services while minimizing or reducing the cost to provide services, so the benefits of the natural elements and their implementation are not generally considered by the governing bodies. This is a good reason to reveal the magnitude of the UHI in major cities like Toronto such that monitoring can be conducted and after mitigation activities are implemented the benefits of it can be quantified.

Microclimate studies have important implications for human health and wellbeing, as well as for energy efficient behaviours in planning and management of cities. The atmospheric layer in which microclimates are associated with is home to all humans, plants and animals;

therefore having a better climatological perspective in this layer is beneficial for any informed city planning, mitigation and adaptation measures and overall decision making. The need for continuous monitoring and research in urban climate in southern Ontario is needed because of the UHI phenomenon and its associated effects. This is especially important when one considers the expected future warming and population growth in the area.

6. CONCLUSIONS

6.1 Synthesis

The UHI effect was evident in Toronto and the surrounding region. Its spatial extent had extended north and west of the City and this thermal phenomenon has the potential, given the expected future warming and expected population growth in southern Ontario, to extend farther north and/or intensify. It has been demonstrated that the relationship between surface cover properties and air temperature became apparent as the thermal source area increased from the five-hundred metre radius to the one-thousand metre radius so there may be a prospect that it continues to reflect even more distance landscape properties. Surface cover is an important determinant of urban microclimates and a more comfortable outdoor thermal environment in urban environs can be achieved when the spatial distributions and optimal mixture and ratio of these properties are managed by planners. The overall UHI research method has progressed and it is possible that a new paradigm for conducting urban temperature studies may be under way, bringing with it a more objective continuum of urbanicity that better describes the urban influence on air temperature. The expectation of higher urban-centric zones may have higher temperatures was revealed through the application of the local climate method (Figure 6.1).

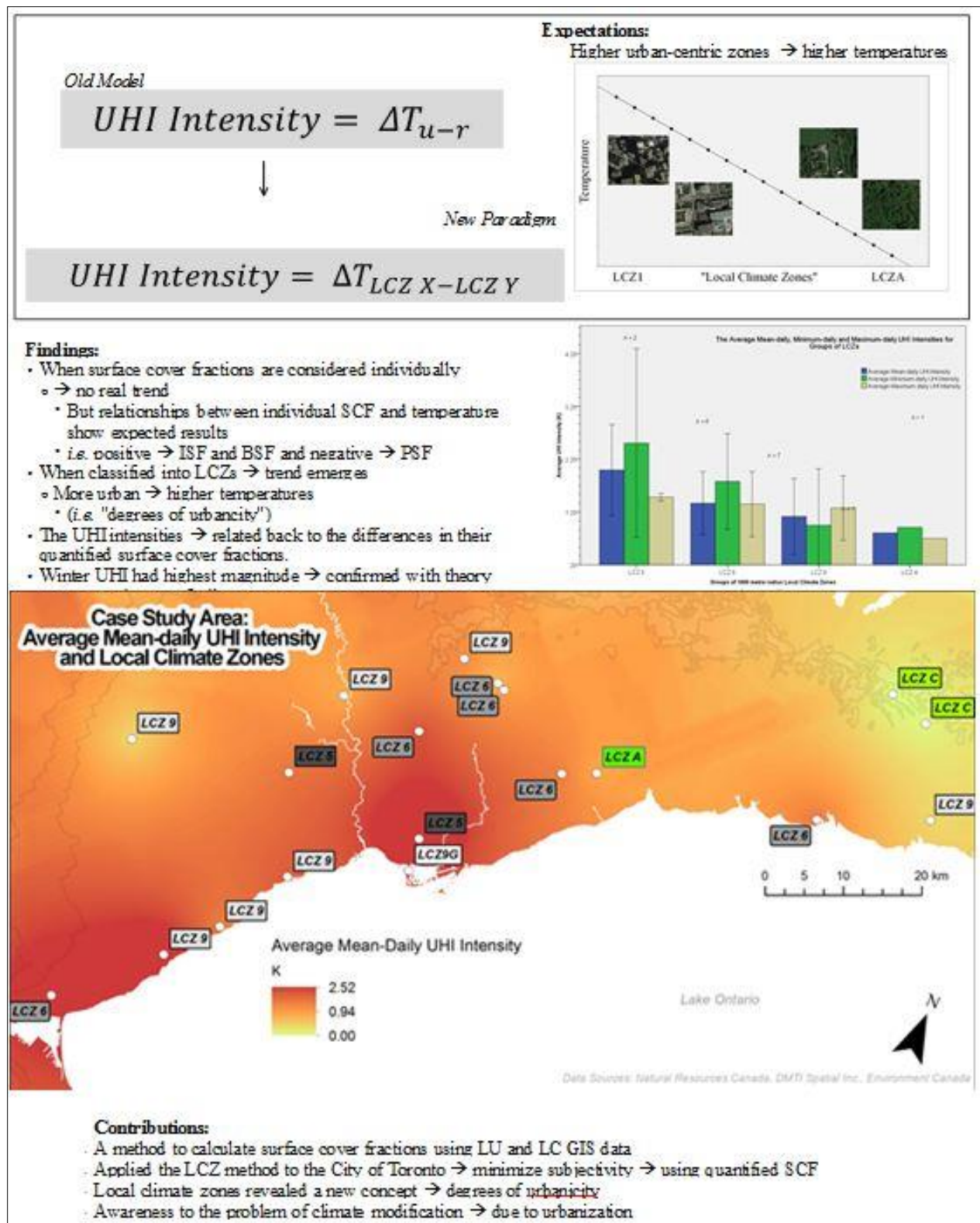


Figure 6.1: Synthesis of research, expectations, findings and contributions.

This research showed that the LCZ method can be important in communicating site descriptions (*e.g.* surface cover properties), and as a result better facilitate communication of urban temperature studies (Figure 6.1). This is because quantifying surface cover properties gives an approximate measure of microclimatological influencing factors which can be used by professionals to assess the surface condition of an area. The three surface cover properties impervious, pervious and building surface fractions are relatively easy to obtain at local scales. The collection of geometric properties like sky view and aspect ratio can improve the quantitative assessment of microclimates, however, some of this data can be difficult to obtain unless collected in primary field research. In terms of classifying the station into an LCZ unit, the analyst is restricted to classify the potential thermal source zone that has already been determined by the placement of the observing station, the placement of which is determined by nationally managed meteorological observation programs which may or may not place the observing station in a “regions of uniform surface cover”. This poses some difficulty to the analyst in classifying it according to an LCZ unit. However when urban climate research is being undertaken through placement of new stationary data collection, the analyst should focus on proper placement of the measuring device and the LCZ method should be a recommended first step to quantify and classify the surrounding environment. Research could reposition stations to more closely accommodate the abundance of LCZ types across a city at present and as the structure of the city evolves. Planned manipulations of urban environments to provide the zones that would be most suitable for human health and comfort under future climate change and variability situations could also be addressed by research. Finally, the method is quite useful in assisting meteorologists, technicians and researchers to identify the optimal position for the placement of meteorological stations in order to capture a reliable measure of the local variation in air temperature. If national, or municipal monitoring programs are considering additional monitoring stations then an assessment of potential sites should consider the LCZ method since the inclusion of surface cover properties in classifying stations gives the analyst greater objectivity. The importance of objective classification of meteorological stations using the LCZ approach is valuable, especially as it relates to planning and categorizing future and additional temperature stations to create a denser spatial network of meteorological observations.

6.2 Limitation of Research

Limitations in this study are uncertainty in the calculated surface cover fractions due to the process of visually distinguishing of different surface covers. The top down assessment, in particular, the reliance on remote sensing of the surface is sometimes difficult because the actual ground surface is impeded by large trees and shadows which may lead to underestimates of impervious spaces. Furthermore some pervious ground surfaces may behave like impervious surfaces due to compaction or the presence of roots. In fact, impervious surface fraction was likely underestimated because household driveways were not included as part of the impervious surface area. Furthermore, the surface cover fractions were calculated using static satellite imagery from 2004 to 2009. It is important to note that the climatic averages are obtained through long term observations beginning in 1981. Thus during the early part of the observation period the surface cover may not be the same as the satellite images used to derive the surface cover fractions, assuming land cover changes have occurred over the last 30 years. This may not be all that important for many of the meteorological stations located within the City of Toronto boundary, but could be more relevant in smaller centres such as Georgetown, Bowmanville, Richmond Hill, Woodbridge, Oakville, Mississauga, and Burlington where there has been recent development. This could be addressed by a long-term study which can link historical field data such as old aerial photographs, old planning documents and parcel-based attributes on the age of buildings to the historical temperature observations. The changes in LCZ and its observed temperatures can be seen through a long-term study and provide further evidence of urbancity and its impact on climate. Additionally to minimize the problem associated with using multiyear temperature averages with static satellite images the temperature observations can be linked to the time frame the satellite images were taken (*i.e.*, 2004 to 2009).

6.3 Future Research Initiative

The collection of additional data such as geometric properties of the area surrounding the 19 meteorological stations would be useful to improve upon the regression model started out in this research. Additional stations would also improve the correlation analysis as well as the temperature surface created using ordinary Kriging. Supplementary data sources could be explored, such as Weather Underground (see Kershaw and Millward, 2012) as well as new

technological improvements such as aspiration of measurements devices and sensor technologies to minimize bias associated with stagnant conditions within a louvered shelter (see Nakamura and Mahrt, 2005). A measure of anthropogenic heat output or a means to estimate it at a local scale can also improve upon the regression models, especially considering the influence anthropogenic heat output is reported to have in creating distinct microclimates in urban environments. One possible surrogate for anthropogenic heat output could be road density to measure the vehicular component. The heat output from homes can also be estimated using building science research. Furthermore the role that water plays within the urban environment and its ability to mitigate UHI intensities should also be explored.

A local climate zone map using Kriging and its variants of the City of Toronto would help urban climatologists carry out temperature studies and help planners and developers isolate areas of concern. However analysis and decisions should be based on more sites and a focus on the extremes such as minimum and maximum temperatures. The three surface cover fractions were estimated for the entire City of Toronto at 100, 500 and 1000 metre square raster cells but they were not included in this research. Further evaluation of the data was needed and the limited number of observing stations was a barrier. Through further data collection a regression model can be developed to perform regression-Kriging in order to estimate the temperature in areas currently without meteorological stations. The prediction surface can then be improved using the surface cover fractions that have been calculated for the City. An additional initiative would be to assign local climate zones to areas where there are no monitoring stations and then use co-Kriging to improve the prediction of temperature in locations lacking meteorological stations. The use of spatial interpolation, especially Kriging and its variants (*e.g.* co-kriging, regression-kriging) should be explored in future research initiatives to resolve the contentiousness of application when the sample size is small.

It is difficult to study the microclimate without a dense network of meteorological stations in the area of study. This may prove to be a limitation in conducting microclimate study with only 19 meteorological stations sparsely spread throughout the study area, and the introduction of atmospheric complexity that would arise if more distant stations were used to increase the sample size. The opportunity to collect temperature readings in all space through all time is real given the available technology including information technology, geotechnology and

atmospheric measurement instruments now available; however there are practical limitations to implementing such a research program. Of course a denser network than the current one in the city would be desirable and the drive to overcome this should focus on the valuable information that a monitoring program can provide for building with climate in mind. A microclimate model for the city can also be made with a denser network of climate data collection. For example, when checking the weather as a daily routine for planning, deciding on attire or taking part in physical activities, the air temperature measurement is usually taken at a nearby airports or city centre which in general is not a true representation of the actual temperature in every local community. The areal extent to which the temperature is too variable for distant stations to have much meaning to most people's daily lives. A microclimate model can help to predict the temperature on a local basis to help individuals plan for their daily activities. They will have access to better representation of the actual weather outside. In addition, during extreme heat incidents, localized rainfall, snowfall and windstorm events, denser sets of meteorological observations would be beneficial for frontline disaster-relief workers. Inclement weather is predicted increase with climate change so better data may well become more critical in urban areas, such as Toronto.

6.4 Final Conclusion

The words urban and rural may have lost their recognizable and specific meanings over time. Rural/urban fringes are now more diffuse than at the time when the UHI concept began; the contrast has become less dichotomous and in fact its implied descriptions have become vague because cities can be viewed as dynamic heterogeneous entities which are products of people's modification of the landscape over long periods of time. Cities are also unique to the geographic and climatic location in which they evolve, so this binary view of urban and rural may not convey the information that it originally intended because the transition from urban to rural cannot be shown in an absolute sense. The formative view that this research has begun to touch upon is the concept of a continuum of urbanization or "degrees of urbanicity". The term may have some potential to be used as a qualitative identifier for describing landscapes, with a higher degree implying greater human influence and lower degree implying lesser human influence. The term also has the potential to quantitatively, through measured observations like

temperature, to describe a continuum of urban to rural without the use of words rooted in administrative and cultural biases.

APPENDIX A

Normality Test

Table A1: Normality test for all temperature parameters.

	Kolmogorov-Smirnov ^a			Shapiro-Wilk		
	Statistic	df	Sig.	Statistic	df	Sig.
AnnMean	.084	19	.200 [*]	.971	19	.796
WinMean	.129	19	.200 [*]	.941	19	.276
SprMean	.201	19	.041	.934	19	.203
SumMean	.096	19	.200 [*]	.935	19	.211
FallMean	.087	19	.200 [*]	.969	19	.750
AnnMeanMin	.098	19	.200 [*]	.986	19	.990
WinMin	.110	19	.200 [*]	.952	19	.427
SprMin	.134	19	.200 [*]	.960	19	.564
SumMin	.106	19	.200 [*]	.977	19	.901
FallMin	.103	19	.200 [*]	.978	19	.917
AnnMax	.112	19	.200 [*]	.977	19	.897
WinMax	.147	19	.200 [*]	.960	19	.567
SprMax	.171	19	.145	.927	19	.151
SumMax	.129	19	.200 [*]	.951	19	.404
FallMax	.067	19	.200 [*]	.994	19	1.000
AnnDTR	.144	19	.200 [*]	.966	19	.694
WinDTR	.153	19	.200 [*]	.948	19	.367
SprDTR	.159	19	.200 [*]	.961	19	.599
SumDTR	.164	19	.195	.954	19	.465
FallDTR	.124	19	.200 [*]	.971	19	.797

Table A2: Normality test for surface cover fractions

	Kolmogorov-Smirnov ^a			Shapiro-Wilk		
	Statistic	df	Sig.	Statistic	df	Sig.
ISF100	.168	19	.165	.882	19	.023
ISF500	.152	19	.200 [*]	.959	19	.553
ISF1000	.123	19	.200 [*]	.979	19	.929
PSF100	.148	19	.200 [*]	.895	19	.040
PSF500	.083	19	.200 [*]	.982	19	.965
PSF1000	.136	19	.200 [*]	.956	19	.493
TCF100	.238	19	.006	.745	19	.000
TCF500	.203	19	.038	.858	19	.009
TCF1000	.180	19	.107	.872	19	.016
BSF100	.215	19	.021	.799	19	.001
BSF500	.116	19	.200 [*]	.947	19	.355
BSF1000	.122	19	.200 [*]	.923	19	.128

*. This is a lower bound of the true significance.

a. Lilliefors Significance Correction

Table A3: The structured query language (SQL) expressions used to identify potential LCZ candidates for the nineteen meteorological stations.

Local Climate Zone	Strcutured Query Language (SQL) Expressions used in query builder.
	The variables in quotations are shown for the 1000 m radius and the expression is the same for the 500 metre radius with the change from 1000 to 500 in the expression.
LCZ 1	"ISF1000" >=0.4 AND "ISF1000" <=0.6 AND "PSF1000" <=0.1 AND "BSF1000" >=0.4 AND "BSF1000" <=0.6
LCZ 2	("ISF1000" >=0.3 AND "ISF1000" <=0.5) AND "PSF1000" <=0.2 AND ("BSF1000" >=0.4 AND "BSF1000" <=0.7)
LCZ 3	("ISF1000" >=0.2 AND "ISF1000" <=0.5) AND "PSF1000" <=0.3 AND ("BSF1000" >=0.4 AND "BSF1000" <=0.7)
LCZ 4	("ISF1000" >=0.3 AND "ISF1000" <=0.4) AND ("PSF1000" >=0.3 AND "PSF1000" <=0.4) AND ("BSF1000" >=0.2 AND "BSF1000" <=0.4)
LCZ 5	("ISF1000" >=0.3 AND "ISF1000" <=0.5) AND ("PSF1000" >=0.2 AND "PSF1000" <=0.4) AND ("BSF1000" >=0.2 AND "BSF1000" <=0.4)
LCZ 6	("ISF1000" >=0.2 AND "ISF1000" <=0.5) AND ("PSF1000" >=0.3 AND "PSF1000" <=0.6) AND ("BSF1000" >=0.2 AND "BSF1000" <=0.4)
LCZ 7	"ISF1000" <=0.2 AND "PSF1000" <=0.3 AND ("BSF1000" >=0.6 AND "BSF1000" <=0.9)
LCZ 8	("ISF1000" >=0.4 AND "ISF1000" <=0.5) AND "PSF1000" <=0.2 AND ("BSF1000" >=0.3 AND "BSF1000" <=0.5)
LCZ 9	"ISF1000" <= 2 AND ("PSF1000" >=0.6 AND "PSF1000" <=0.8) AND ("BSF1000" >=0.1 AND "BSF1000" <=0.2)
LCZ 10	("ISF1000" >=0.2 AND "ISF1000" <=0.4) AND ("PSF1000" >=0.4 AND "PSF1000" <=0.5) AND ("BSF1000" >=0.2 AND "BSF1000" <=0.3)
LCZ A	"ISF1000" <=0.1 AND "PSF1000" >=0.9 AND "BSF1000" <=0.1
LCZ B	"ISF1000" <=0.1 AND "PSF1000" >=0.9 AND "BSF1000" <=0.1
LCZ C	"ISF1000" <=0.1 AND "PSF1000" >=0.9 AND "BSF1000" <=0.1
LCZ D	"ISF1000" <=0.1 AND "PSF1000" >=0.9 AND "BSF1000" <=0.1
LCZ E	"ISF1000" >=0.9 AND "PSF1000" <=0.1 AND "BSF1000" <=0.1
LCZ F	"ISF1000" <=0.1 AND "PSF1000" >=0.9 AND "BSF1000" <=0.1
LCZ G	"ISF1000" <=0.1 AND "PSF1000" >=0.9 AND "BSF1000" <=0.1

Table A4: Local climate zone classified stations showing the LCZs generated by query builder (in Bold) and those assigned to the nearest equivalent. Final LCZ is based on 1000 metre radius.

Station Name (Climate ID)	Potential Candidates (Output from SQL)		
	100 m	500 m	1000 m
Bowmanville Mostert (6150830)	<i>LCZA, LCZB, LCZC, LCZD, LCZF, LCZG</i>	-	-
Burketon McLaughlin (6151042)	<i>LCZA, LCZB, LCZC, LCZD, LCZF, LCZG</i>	<i>LCZA</i>	<i>LCZA, LCZB, LCZC, LCZD, LCZF, LCZG</i>
Georgetown WWTP (6152695)	-	<i>LCZ9</i>	<i>LCZ9</i>
Gormley Ardenlee (6152953)	<i>LCZ8</i>	-	-
Lakeview MOE (6154310)	<i>LCZ9</i>	<i>LCZ9</i>	<i>LCZ9</i>
Oshawa WPCP (6155878)	<i>LCZA, LCZB, LCZC, LCZD, LCZF, LCZG</i>	-	-
Oakville Gerard (6155PD4)	<i>LCZ9</i>	<i>LCZ9</i>	<i>LCZ9</i>
Richmond Hill (6157012)	<i>LCZ9</i>	<i>LCZ9</i>	<i>LCZ9</i>
Toronto (6158350)	-	<i>LCZ4, LCZ5, LCZ6</i>	<i>LCZ5, LCZ6</i>
Toronto Island A (6158665)	-	-	-
Toronto Pearson (6158733)	<i>LCZ2, LCZ3</i>	-	-
Toronto Malvern (6158738)	-	<i>LCZ9</i>	-
Toronto Metro Zoo (6158741)	-	-	-
Tyrone (6159048)	<i>LCZA, LCZB, LCZC, LCZD, LCZF, LCZG</i>	<i>LCZA, LCZB, LCZC, LCZD, LCZF, LCZG</i>	<i>LCZA, LCZB, LCZC, LCZD, LCZF, LCZG</i>
Woodbridge (6159575)	<i>LCZ5</i>	<i>LCZ9</i>	<i>LCZ9</i>
Toronto Buttonville A (615HMAK)	-	-	-
Oakville Southeast WPCP (615N745)	<i>LCZA, LCZB, LCZC, LCZD, LCZF, LCZG</i>	-	-
Toronto North York (615S001)	-	<i>LCZ9</i>	-
Burlington TS (6151064)	-	-	-

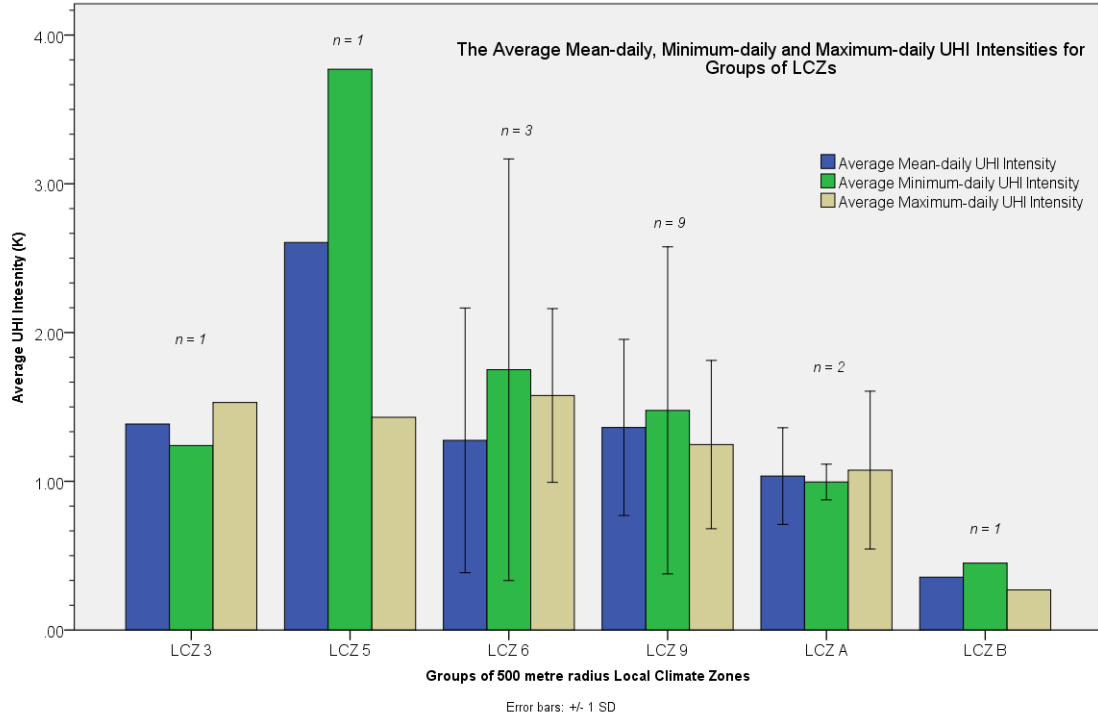


Figure A1: The average mean-daily, minimum-daily and maximum-daily UHI Intensities for groups of 500 metre radius defined LCZs.

Table A5: The results from the analysis of variance used to check the difference between the grouped means of the unique LCZ classes (minimum-daily UHI intensity)

SUMMARY						
<i>Groups</i>	<i>Count</i>	<i>Sum</i>	<i>Average</i>	<i>Variance</i>		
LCZ 5	4	10.02	2.505	2.192433		
LCZ 6	12	21.34	1.778333	0.79347		
LCZ 9	14	13.28	0.948571	1.105721		
ANOVA						
<i>Source of Variation</i>	<i>SS</i>	<i>df</i>	<i>MS</i>	<i>F</i>	<i>P-value</i>	<i>F crit</i>
Between Groups	9.222442	2	4.611221	4.194867	0.025916	2.510609
Within Groups	29.67984	27	1.099253			
Total	38.90228	29				

Table A6: The results from the analysis of variance used to check the difference between the grouped means of the unique LCZ classes (maximum-daily UHI intensity)

SUMMARY						
<i>Groups</i>	<i>Count</i>	<i>Sum</i>	<i>Average</i>	<i>Variance</i>		
LCZ 5	4	5.92	1.48	0.093467		
LCZ 6	12	16.2	1.35	0.417055		
LCZ 9	14	17.86	1.275714	0.417226		
ANOVA						
<i>Source of Variation</i>	<i>SS</i>	<i>df</i>	<i>MS</i>	<i>F</i>	<i>P-value</i>	<i>F crit</i>
Between Groups	0.135844	2	0.067922	0.178187	0.837762	2.510609
Within Groups	10.29194	27	0.381183			
Total	10.42779	29				

Model Performance Measures

Mean Error (ME) is the averaged difference between the measured and the predicted values.

$$\frac{\sum_{i=1}^n [z_o(s_i) - z(s_i)]}{n}$$

Root Mean Square Error (RMSE) indicates how closely your model predicts the measured values. The smaller this error, the better.

$$\sqrt{\frac{\sum_{i=1}^n [z_o(s_i) - z(s_i)]^2}{n}}$$

Ordinary Kriging (Bailey and Gatrell, 1995; Chang, 2010)

Ordinary Kriging uses a fitted semivariogram for interpolation. The semivariogram is used to measure the spatially correlated component and it is defined as:

$$\gamma(h) = \frac{1}{2} [z(s_i) - z(s_j)]^2$$

where $\gamma(h)$ is the semivariance between points s_i and s_j separated by a distance h and z is the attribute value. If there is spatial dependence then points closer to each other will have a lower semivariance than points farther apart which should have larger semivariances. The resulting semivariance cloud can be difficult to manage so the average semivariance is calculated using:

$$\gamma(h) = \frac{1}{2n} \sum_{i=1}^n [z(s_i) - z(s_i + h)]^2$$

where $\gamma(h)$ is the average semivariance between points separated by lag h , n is the number of points sorted by direction in the bins and z is the attribute value. If there is structure (*i.e.* presence of a sill, range and nugget) in the semivariogram then a model can be fitted (*e.g.* spherical, exponential, or Gaussian) to the variogram. The fitted model can then be used to solve for the weights required to estimate the value at the unsampled points.

The general equation to estimate a value at an unsampled point is:

$$z_0 = \sum_{i=1}^n z_s W_s$$

where z_0 is the estimated value, z_s is the known value at point s , W_s is the weights associated with point s and n is the number of sample points used for estimation.

The benefit of using Kriging is that the method can produce a variance measure for the estimated point which can provide some reliability measure of the prediction value. The variance estimation can be calculated using:

$$\sigma^2 = \sum_{i=1}^n W_i \gamma(h_{i0}) + \lambda$$

where σ^2 is the variance estimate for the predicted value, W_i is the weights for point i , $\gamma(h_{i0})$ is the semivariance of the known value and the unsampled value separated by their distance and λ Lagrange multiplier. Once the estimated value and its variance in known then a 95% confidence interval can be calculated using $1.96 \times \pm \sqrt{\sigma^2}$ giving $z_0 \pm 1.96 \times \sqrt{\sigma^2}$.

Descriptive Statistics

A7: Descriptive statistics for all temperature parameters

	N	Minimum	Maximum	Mean	Std. Deviation	Variance	Skewness		Kurtosis	
	Statistic	Statistic	Statistic	Statistic	Statistic	Statistic	Statistic	Std. Error	Statistic	Std. Error
AnnMean	19	6.760	9.390	7.96895	.760145	.578	.179	.524	-.638	1.014
WinMean	19	-5.800	-2.300	-4.01053	1.118478	1.251	.059	.524	-1.326	1.014
SprMean	19	5.600	7.800	6.49474	.558245	.312	.472	.524	.603	1.014
SumMean	19	18.800	21.100	19.80000	.747589	.559	.354	.524	-.743	1.014
FallMean	19	8.300	11.000	9.55263	.820818	.674	.146	.524	-.946	1.014
AnnMeanMin	19	1.260	5.850	3.44789	1.178137	1.388	.085	.524	-.437	1.014
WinMin	19	-9.800	-5.100	-7.84211	1.413159	1.997	.295	.524	-1.027	1.014
SprMin	19	-.400	4.000	1.60526	.954215	.911	.432	.524	1.472	1.014
SumMin	19	11.800	16.800	14.40000	1.120516	1.256	-.158	.524	.814	1.014
FallMin	19	2.900	7.700	5.13158	1.213834	1.473	.295	.524	-.200	1.014
AnnMax	19	11.210	13.800	12.59263	.663700	.440	-.105	.524	-.025	1.014
WinMax	19	-1.900	1.300	-.15263	.922779	.852	-.015	.524	-.921	1.014
SprMax	19	10.300	12.400	11.37895	.632086	.400	-.366	.524	-1.020	1.014
SumMax	19	23.900	26.600	25.16842	.834035	.696	-.010	.524	-1.208	1.014
FallMax	19	12.500	15.400	13.95789	.725194	.526	.017	.524	-.113	1.014
AnnDTR	19	7.050	11.660	9.14474	1.095163	1.199	.009	.524	.658	1.014
Valid N (listwise)	19									

Table A8: Descriptive statistics for surface cover fractions

	N	Minimum	Maximum	Mean	Std. Deviation	Variance	Skewness		Kurtosis	
	Statistic	Statistic	Statistic	Statistic	Statistic	Statistic	Statistic	Std. Error	Statistic	Std. Error
ISF100	19	.000	.507	.19068	.178555	.032	.595	.524	-.988	1.014
ISF500	19	.004	.509	.22192	.149792	.022	.253	.524	-.953	1.014
ISF1000	19	.004	.503	.22816	.129388	.017	.073	.524	-.004	1.014
PSF100	19	.000	1.000	.67251	.313761	.098	-.747	.524	-.566	1.014
PSF500	19	.268	.995	.67289	.196897	.039	-.132	.524	-.340	1.014
PSF1000	19	.392	.993	.66792	.178835	.032	.321	.524	-.609	1.014
TCF100	19	.000	1.000	.18843	.264025	.070	1.788	.524	3.763	1.014
TCF500	19	.000	.633	.16468	.177646	.032	1.065	.524	.955	1.014
TCF1000	19	.003	.523	.16438	.152556	.023	1.122	.524	.503	1.014
BSF100	19	.000	.613	.13681	.173688	.030	1.411	.524	1.649	1.014
BSF500	19	.000	.292	.10518	.077984	.006	.657	.524	.307	1.014
BSF1000	19	.002	.305	.10420	.072118	.005	.939	.524	2.073	1.014
Valid N (listwise)	19									

Table A9: Average UHI Intensities based upon the UHI intensities calculated using the Burketon McLaughlin and Tyrone stations

Station Name	LCZ1000	\bar{T} (K)	Tmin (K)	Tmax (K)	DTR (K)
TORONTO ISLAND A	LCZ9 _G	1.71	2.76	0.64	-2.12
TORONTO METRO ZOO	LCZ A	0.81	0.91	0.70	-0.21
TORONTO PEARSON	LCZ 5	1.39	1.24	1.53	0.29
OAKVILLE WPCP	LC 9	1.27	1.08	1.45	0.37
OSHAWA WPCP	LCZ 6	1.34	2.02	0.65	-1.37
BOWMANVILLE MOSTERT	LCZ 9	0.36	0.45	0.27	-0.18
BURLINGTON TS	LCZ 6	2.29	2.36	2.22	-0.14
LAKEVIEW MOE	LCZ 9	1.66	2.12	1.18	-0.94
TORONTO BUTTONVILLE A	LCZ 6	0.94	2.76	1.43	-1.33
GEORGETOWN WWTP	LCZ 9	0.32	-0.82	1.45	2.27
OAKVILLE GERARD	LCZ 9	2.33	2.30	2.33	0.03
GORMLEY ARDENLEE	LCZ 6	0.61	0.13	1.08	0.95
WOODBIDGE	LCZ 9	0.78	0.43	1.11	0.68
RICHMOND HILL	LCZ 9	1.12	1.08	1.14	0.06
TORONTO MALVERN	LCZ 6	1.27	1.77	0.83	-0.94
TORONTO NORTH YORK	LCZ 6	1.77	1.63	1.89	0.26
TORONTO	LCZ 5	2.61	3.77	1.43	-2.34

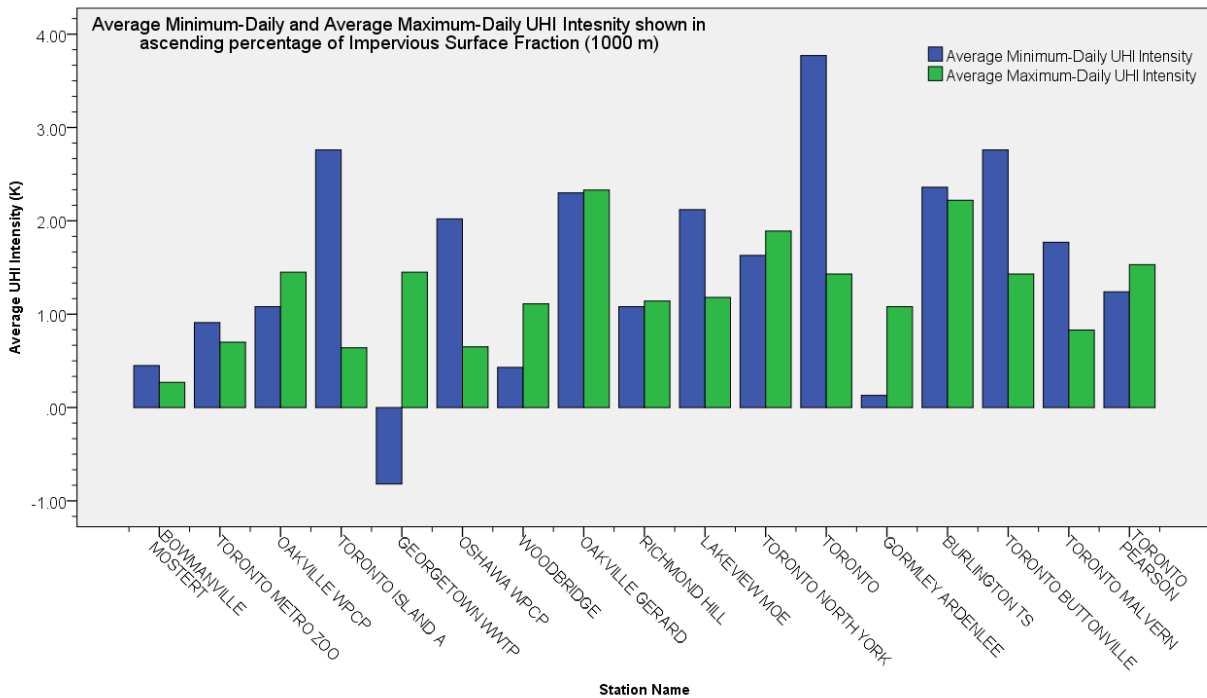
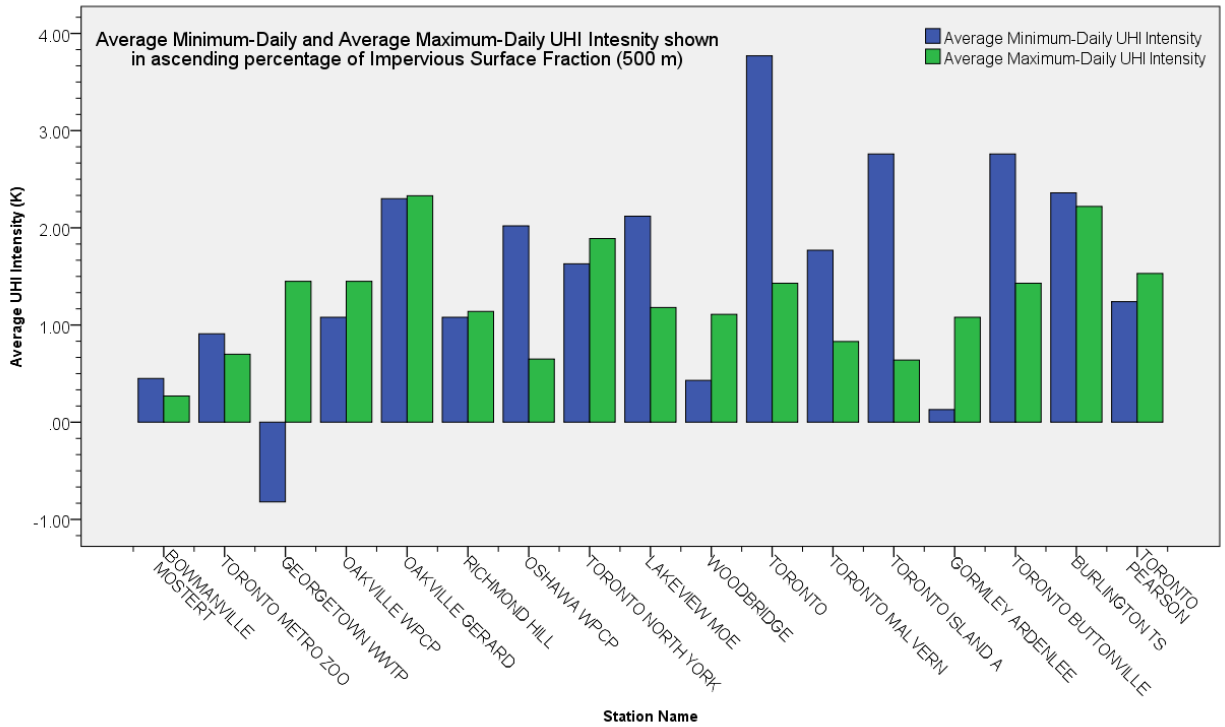


Figure A6: The average minimum-daily and maximum-daily UHI intensity shown in ascending percentage of impervious surface fraction at 500 m radius (top) and 1000 metre radius (bottom).

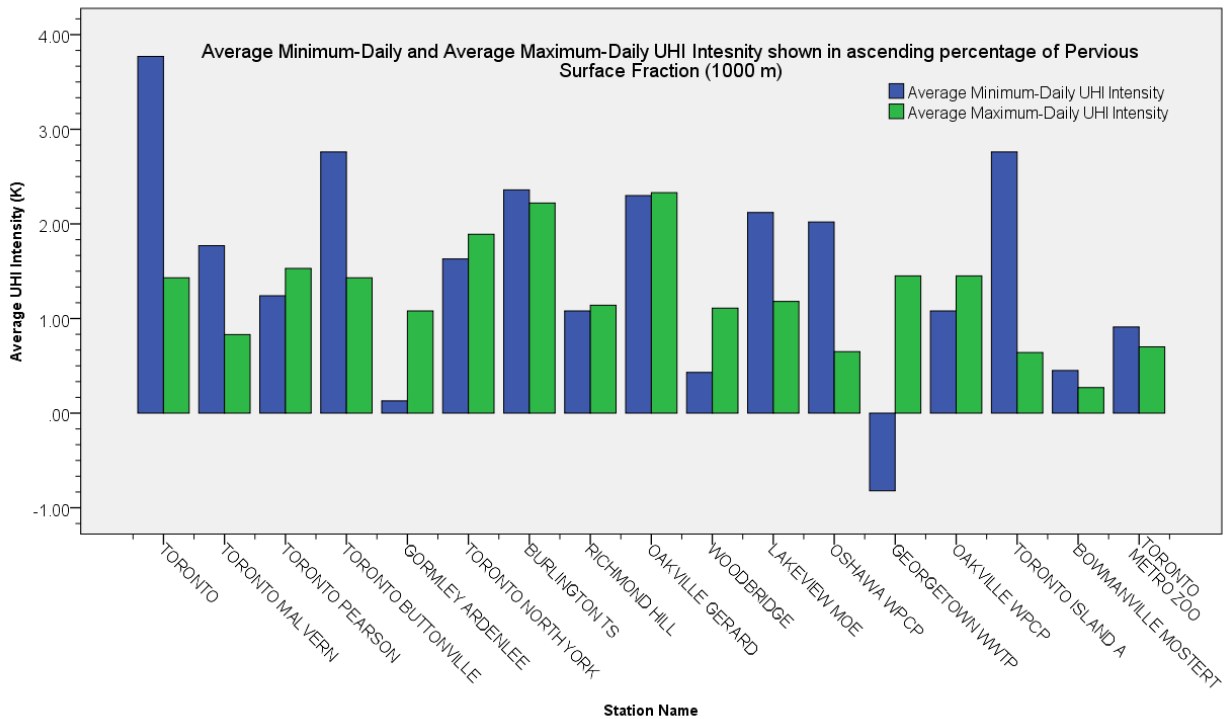
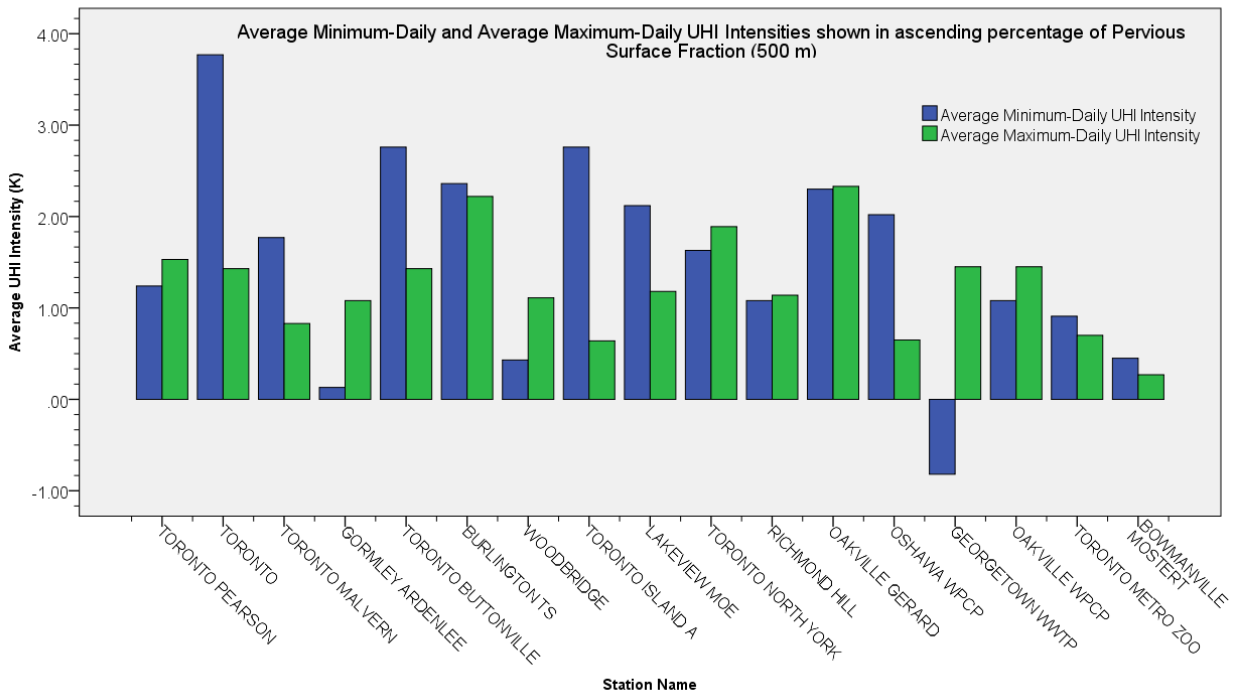


Figure A7: The average minimum-daily and maximum-daily UHI intensity shown in ascending percentage of pervious surface fraction at 500 metre radius (top) and 1000 metre radius (bottom).

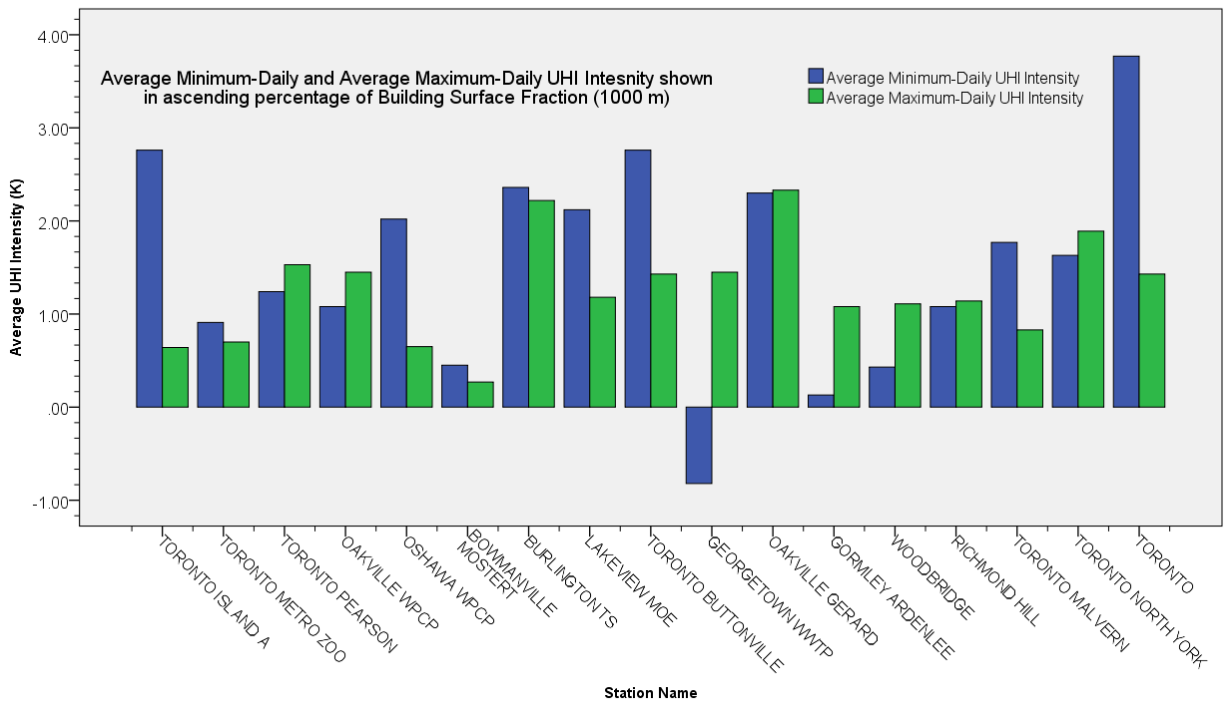
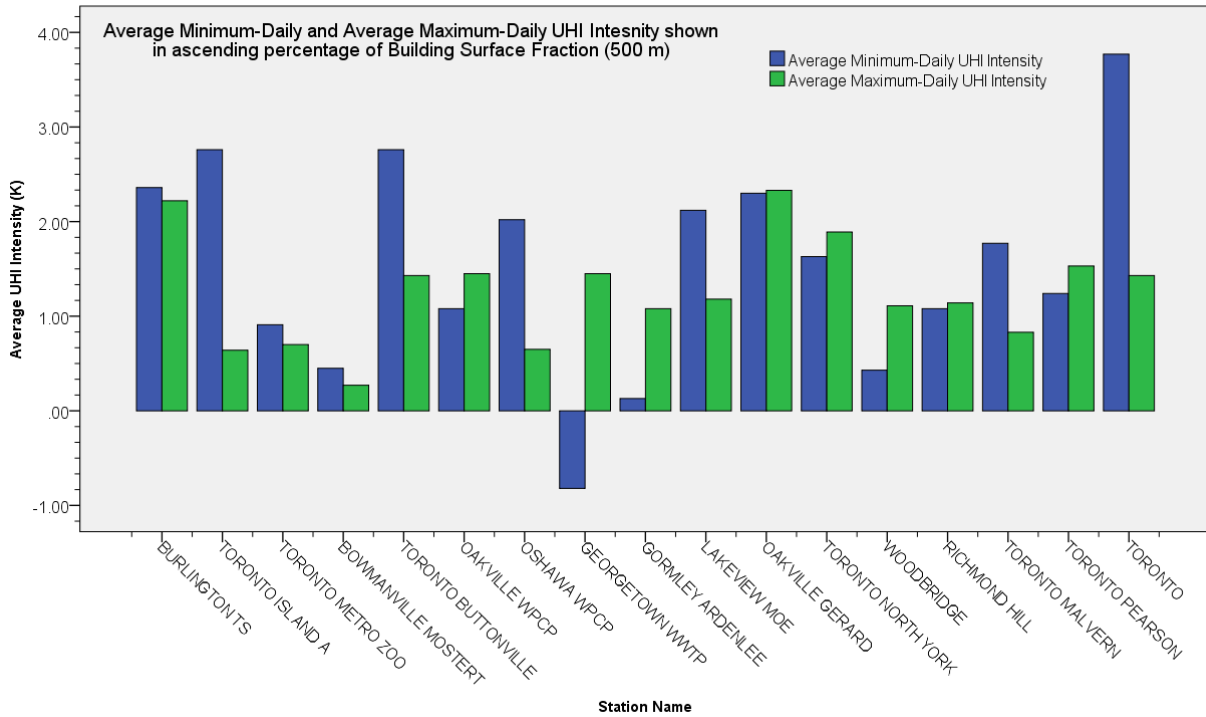


Figure A8: The average minimum-daily and maximum-daily UHI intensity shown in ascending percentage of building surface fraction at 500 metre radius (top) and 1000 metre radius (bottom).

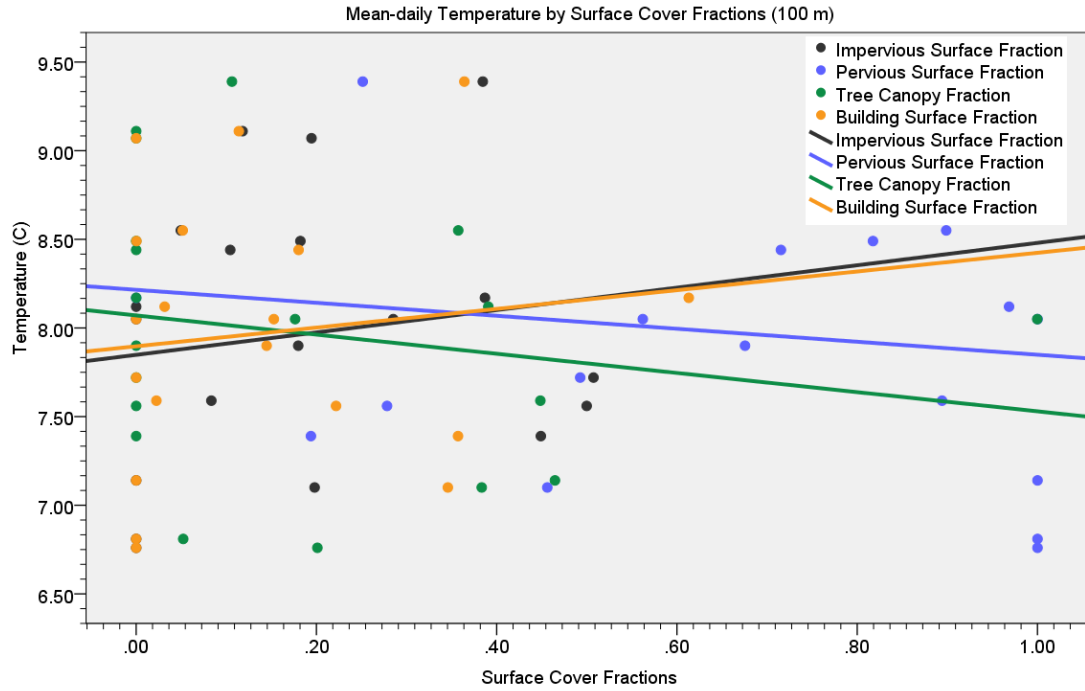


Figure A9: Scatterplot of \bar{T} against impervious, pervious, building surface and tree canopy fraction at the one-hundred metre radius thermal source zone.

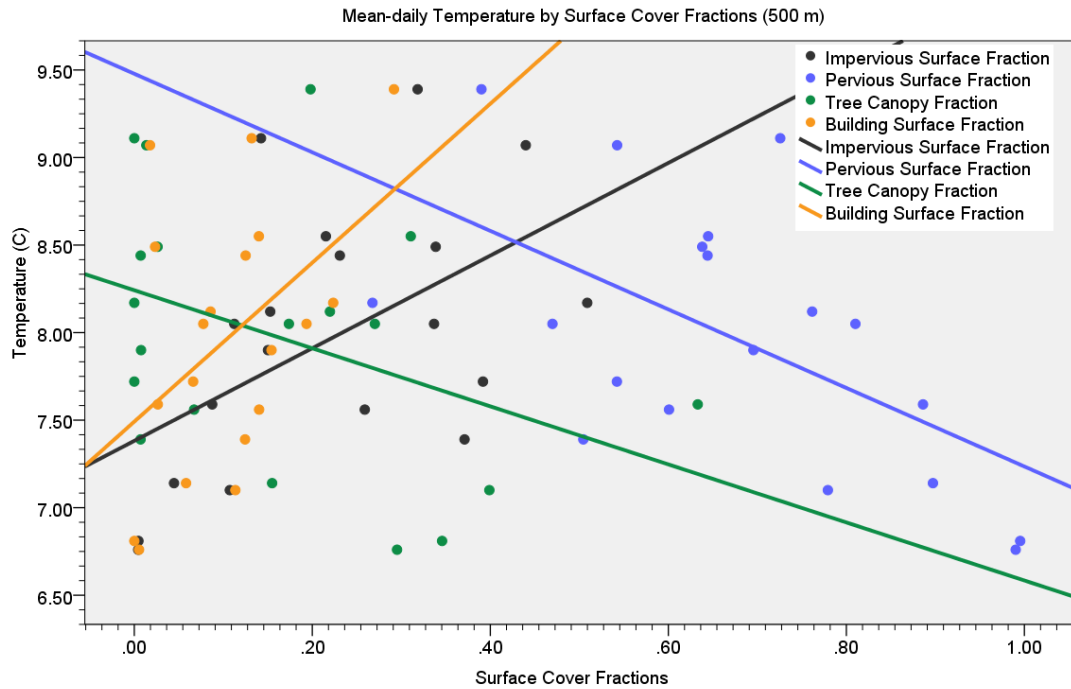


Figure A10: Scatterplot of \bar{T} against impervious, pervious, building surface and tree canopy fraction at the five-hundred metre radius thermal source zone.

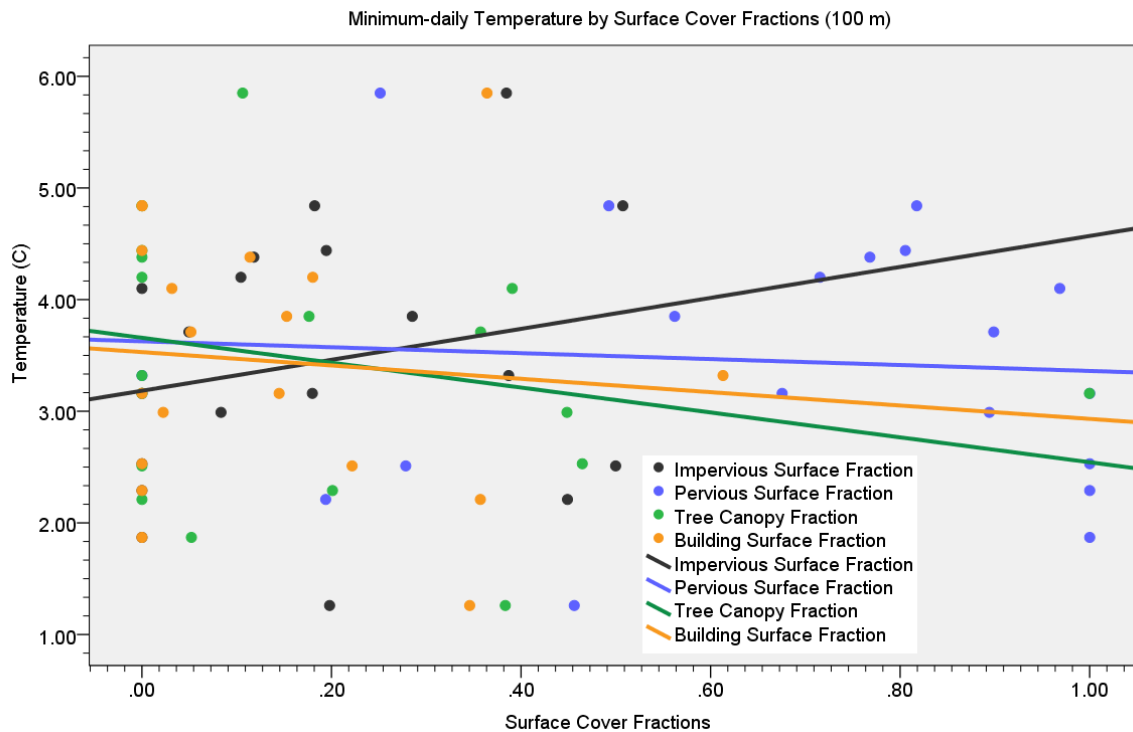


Figure A11: Scatterplot of Tmin against impervious, pervious, building surface and tree canopy fraction at the one-hundred metre radius thermal source zone.

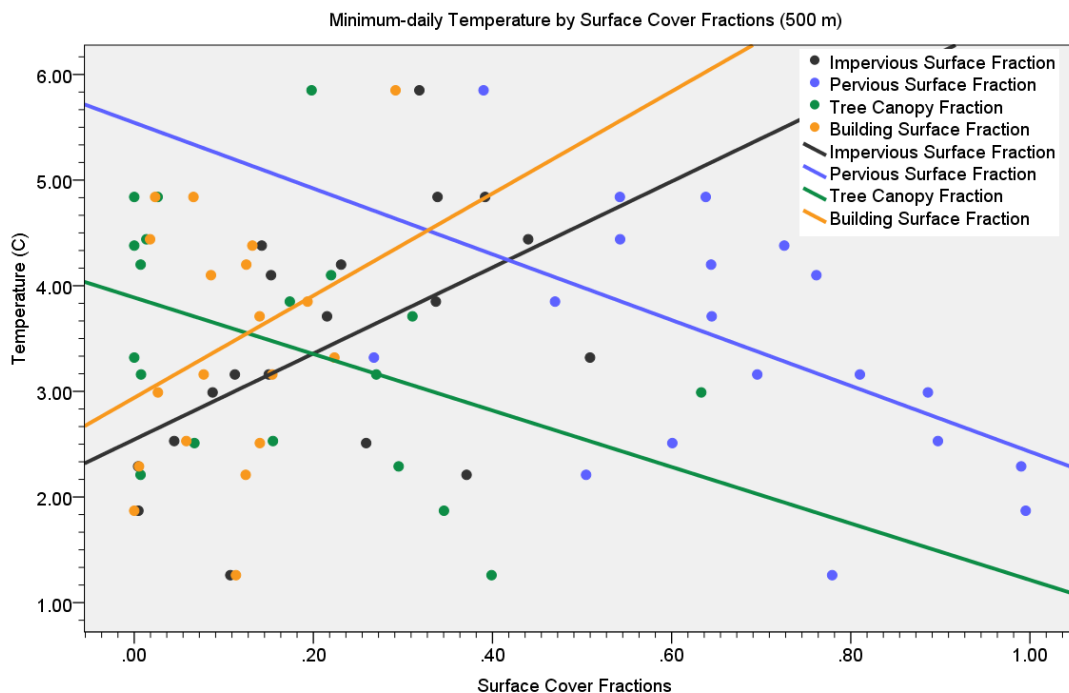


Figure A12: Scatterplot of Tmin against impervious, pervious, building surface and tree canopy fraction at the five-hundred metre radius thermal source zone.

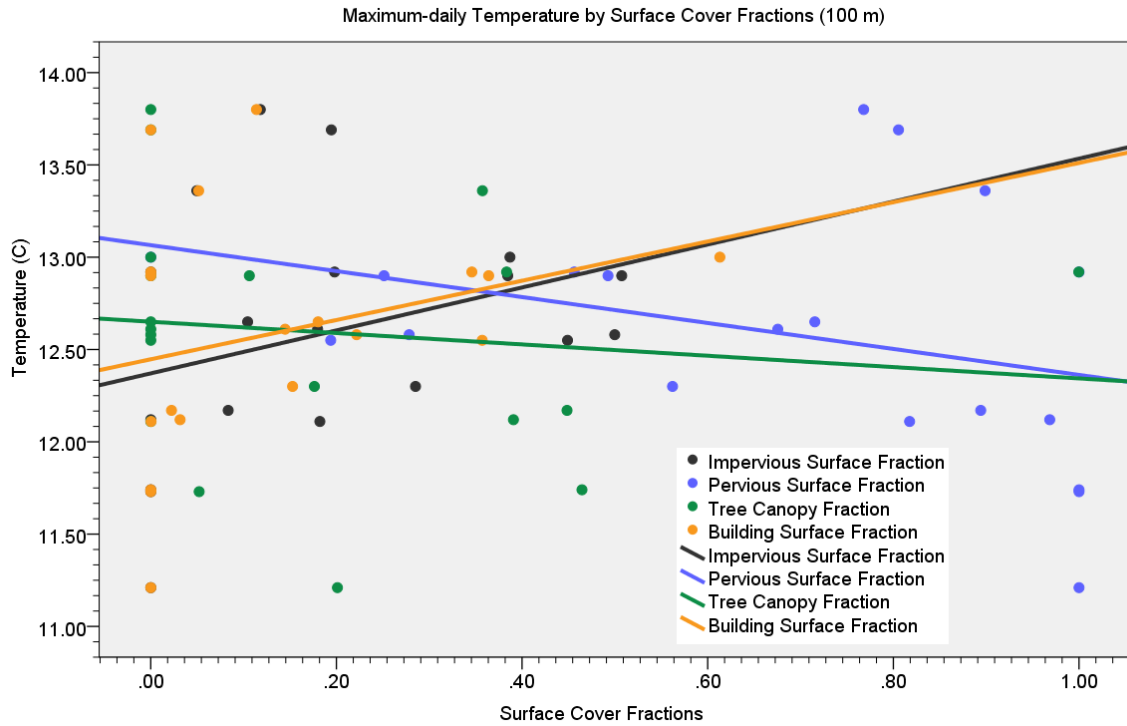


Figure A13: Scatterplot of Tmax against impervious, pervious, building surface and tree canopy fraction at the one-hundred metre radius thermal source zone.

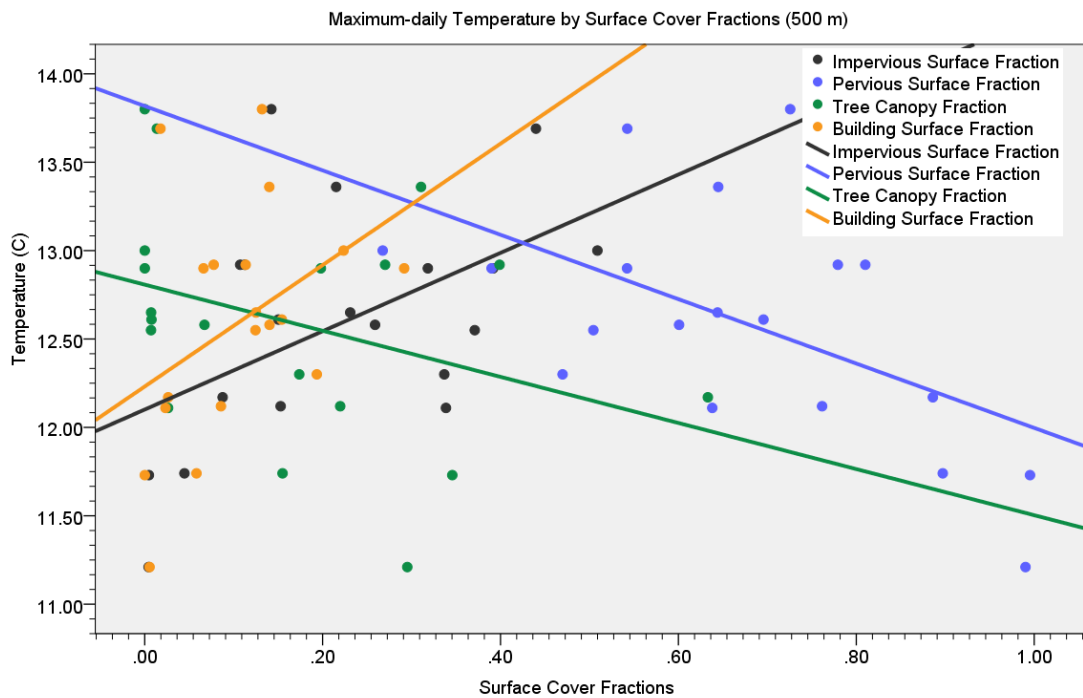


Figure A14: Scatterplot of Tmax against impervious, pervious, building surface and tree canopy fraction at the five-hundred metre radius thermal source zone.

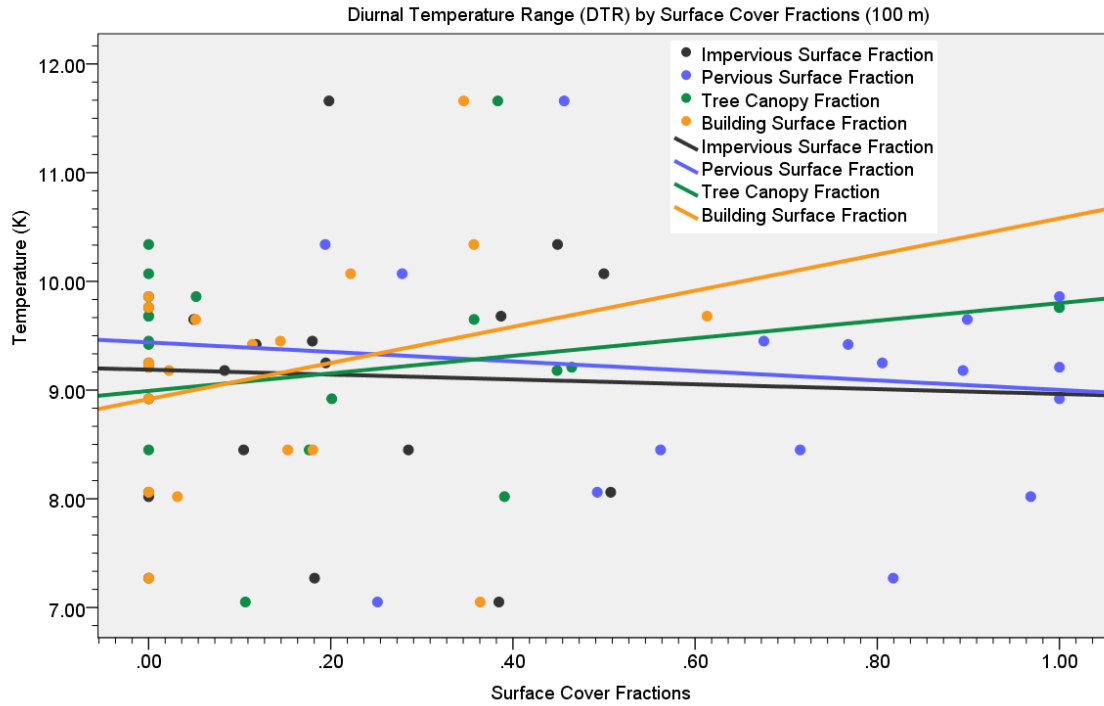


Figure A15: Scatterplot of diurnal temperature range against impervious, pervious, building surface and tree canopy fraction at the one-hundred metre radius thermal source zone.

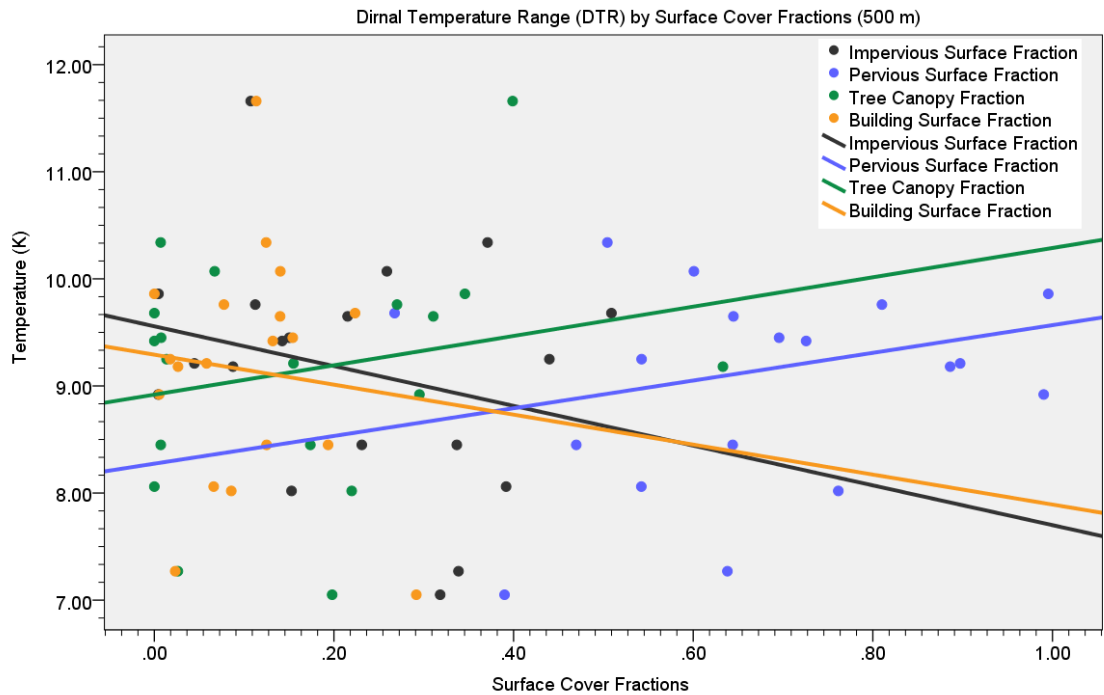


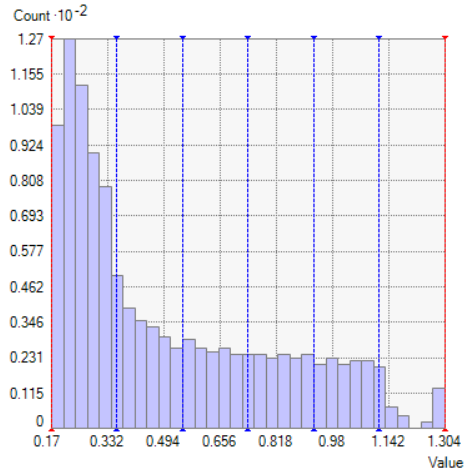
Figure A16: Scatterplot of diurnal temperature range against impervious, pervious, building surface and tree canopy fraction at the five-hundred metre radius thermal source zone.

Table A10: Model parameters and validations results for ordinary Kriging of \bar{T} , T_{\min} , T_{\max} .

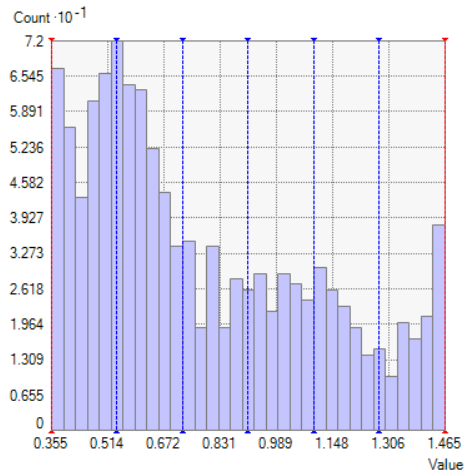
Temperature (N = 19)	SIM Method	Model Parameters								Validation				
		Nugget	Sill	Range (min)	Range (maj)	Anisotropy Factor	Anisotropy	Lag Size	# of Lags	Mean (small)	RMS E (small)	Mean Std (0)	RMS E Std (1)	Average Std Err (0)
Mean	OK (Default)	0.117	0.411	31443.51	31443.51	1	0	3533	12	0.03	0.57	0.04	1.03	0.54
Mean	OK	0.2	0.697	100404	52453.28	0.522	320	8367	12	0.03	0.55	0.03	1.01	0.55
Mean	OK	0.197	0.85	120252.2	54690	0.455	320	8367	15	0.02	0.53	0.01	1.00	0.54
Minimum	OK (Default)	0.8891	0.7196	40289.41	40289.41	1	0	5920	12	0.04	1.06	0.03	0.92	1.14
Minimum	OK	0.8862	0.5845	32914.33	35048.8	0.9391	275	8367	12	0.04	1.09	0.03	0.94	1.14
Minimum	OK	0.8008	0.8873	31729.76	94784.39	2.9872	33	8367	12	0.08	1.07	0.05	1.00	1.06
Minimum	OK	0.7922	0.9017	31729.8	94784.4	2.9872	33	8367	12	0.08	1.07	0.05	1.00	1.06
Minimum	OK	0.7896	0.9228	31729.8	94784.4	2.9872	35	8367	18	0.06	1.05	0.04	0.99	1.06
Minimum	OK	0.8005	0.9089	31951.01	95344.41	2.9841	35	8367	15	0.06	1.05	0.04	0.98	1.06
Maximum	OK (Default)	0.1117	0.8858	125323.8	125323.8	1	0	10443	12	0.01	0.39	0.01	1.01	0.40
Maximum	OK	0	0.2346	78500.45	26278.6	0.3348	325	8367	12	-0.01	0.40	-0.02	0.94	0.42
Maximum	OK	0.0991	0.6058	156654.7	83549.18	0.5333	33	10443	15	0.01	0.38	0.01	1.04	0.38
Maximum	OK	0.0699	0.3752	156654.7	83549.18	0.5333	33	10443	12	0.00	0.40	0.00	0.99	0.42
Maximum	OK	0.0991	0.6058	83549.18	83549.18	1	0	10443	12	0.00	0.38	-0.01	1.02	0.40
Maximum	OK (Optomized) consant trend removed	0.0314	0.1053	16657.63	16657.63	1	0	2082	12	-0.02	0.39	-0.05	1.00	0.39

Table A11: Model parameters and validations results for ordinary co-Kriging of \bar{T} , T_{\min} , T_{\max} .

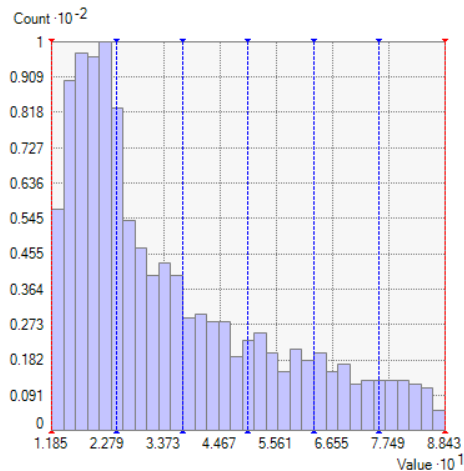
Temperature (N=19)	Model Parameters																	Validation	RMS E (small)	Secondary Dataset
	Nugget (0,0)	Nugget (1,1)	Nugget (2,2)	Nugget (3,3)	Sill (0,0)	Sill (0,1)	Sill (1,1)	Sill (0,2)	Sill (1,2)	Sill (2,2)	Sill (0,3)	Sill (1,3)	Sill (2,3)	Sill (3,3)	Range (maj)	Lag Size	# of Lags	Mean (small)		
Mean	0.129	0.01			0.365	0.05	0.009								31546	8000	12	0.002	0.538	ISF500
Mean	0.129	0.01			0.365	0.05	0.009								31546	3943	20	0.022	0.514	ISF500
Mean	0.119	0.01			0.421	0.036	0.003								32085	3580	12	0.032	0.514	ISF1000
Mean	0	0.006			0.391	0.048	0.008								16658	2082	12	0.027	0.466	ISF1000
Mean	0	0			0.425	-0.08	0.04								19827	2478	12	0.02	0.445	PSF1000
Mean	0.129	0.021	0.009		0.366	-0.05	0.012	0.041	-0.01	0.008					31645	3969	12	0.033	0.489	PSF1000, ISF1000
Mean	0	0	0		0.461	-0.07	0.035	0.05	-0.02	0.016					30941	3868	12	0.003	0.434	PSF1000, ISF1000
Mean	0.064	0.012	0.006	0.005	0.642	-0.04	0.026	0.03	-0.01	0.014	0.013	-0	0.003	9E-04	71613	8173	12	0.003	0.469	PSF1000, ISF1000, BSF1000
Mean	0	0.007	0.001	0.003	0.451	-0.07	0.025	0.049	-0.02	0.015	0.025	-0.01	0.005	0.003	34085	4261	12	0.008	0.42	PSF1000, ISF1000, BSF1000
Min	0.873	0.02	0.009	0.005	0.734	-0.06	0.015	0.041	-0.01	0.009	0.02	-0.01	0.004	0.002	39457	5844	12	0.046	0.997	PSF1000, ISF1000, BSF1000
Min	0.783	0.02	0.009	0.006	0.771	-0.07	0.015	0.048	-0.01	0.009	0.021	-0	0.003	0.001	33866	4233	12	0.082	0.965	PSF1000, ISF1000, BSF1000
Max	0.103	0.017	0.009	0.005	0.217	-0.05	0.017	0.033	-0.01	0.009	0.014	-0	0.003	0.001	49507	5622	12	-0.012	0.351	PSF1000, ISF1000, BSF1000
Max	0.066	0.018	0.007	0.005	0.289	-0.06	0.017	0.041	-0.01	0.01	0.018	-0.01	0.004	0.002	45564	5695	12	-0.012	0.324	PSF1000, ISF1000, BSF1000



Statistics
 Count 1147
 Minimum 0.17037517755988538
 Maximum 1.3038488952663763
 Mean 0.50830229053516
 StdDev 0.2989652552249177
 Skewness 0.7955762578833933
 Kurtosis 2.400350136950764
 Quartile1 0.2547748180054499
 Median 0.3895942843412215
 Quartile3 0.7354839243194972
 Prediction Error (OK Mean)

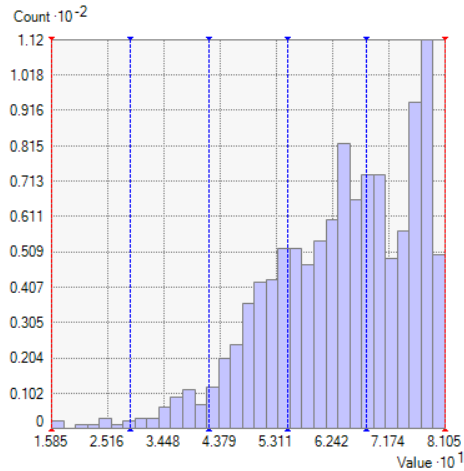


Statistics
 Count 1147
 Minimum 0.35544128099385214
 Maximum 1.464625257278874
 Mean 0.7786662197945905
 StdDev 0.3166591704581502
 Skewness 0.61807412707209
 Kurtosis 2.2078778909155234
 Quartile1 0.5216031757800246
 Median 0.683153875482972
 Quartile3 1.0253550680899988
 Prediction Error (OK Min)

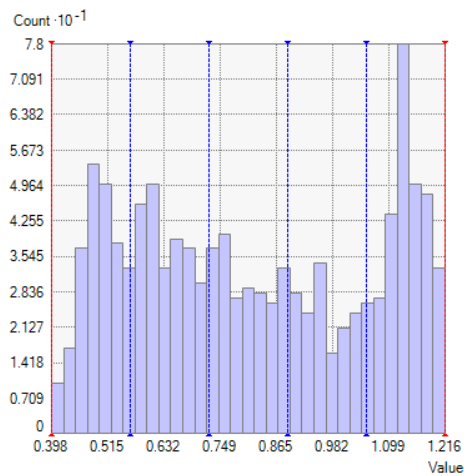


Statistics
 Count 1147
 Minimum 0.11853588892636756
 Maximum 0.8842703265197858
 Mean 0.3501381132343982
 StdDev 0.19481870039058882
 Skewness 0.9742354583042943
 Kurtosis 2.889877573083709
 Quartile1 0.20013734297729552
 Median 0.28015423379441995
 Quartile3 0.4651170898573216
 Prediction Error (OK Max)

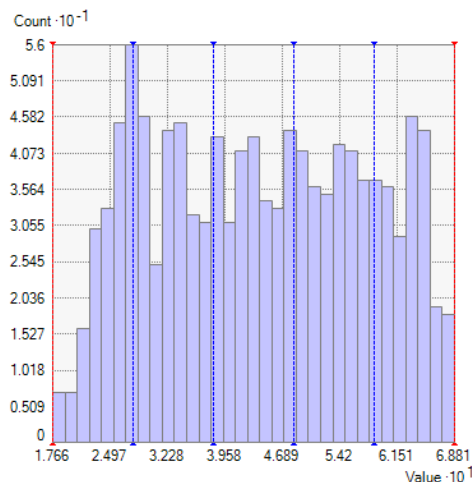
Figure A17: Prediction Error statistics using ordinary Kriging to interpolate mean-daily, minimum-daily and Tmax s.



Statistics
 Count 1147
 Minimum 0.1584917511845845
 Maximum 0.8105183739992214
 Mean 0.6382821800395294
 StdDev 0.11837454456080623
 Skewness -0.7329862465549965
 Kurtosis 3.268581682104862
 Quartile1 0.5581810828050327
 Median 0.65299916262868
 Quartile3 0.7413390698858104
 Prediction Error (OCK Mean)



Statistics
 Count 1147
 Minimum 0.39819971255998504
 Maximum 1.2156196305696798
 Mean 0.8145888642620811
 StdDev 0.24309435103438903
 Skewness 0.09585529826566382
 Kurtosis 1.6335477955258242
 Quartile1 0.5972064285199448
 Median 0.7887869612116267
 Quartile3 1.061026679277037
 Prediction Error (OCK Min)



Statistics
 Count 1147
 Minimum 0.17663090552598998
 Maximum 0.688128313733467
 Mean 0.44114275008456844
 StdDev 0.13476610575888162
 Skewness 0.01572668535265957
 Kurtosis 1.813804568975376
 Quartile1 0.3227466609418668
 Median 0.4395770530601943
 Quartile3 0.5555511940254791
 Prediction Error (OCK – Max)

Figure A18: Prediction Error statistics using ordinary co-Kriging to interpolate mean-daily, minimum-daily and Tmax s.

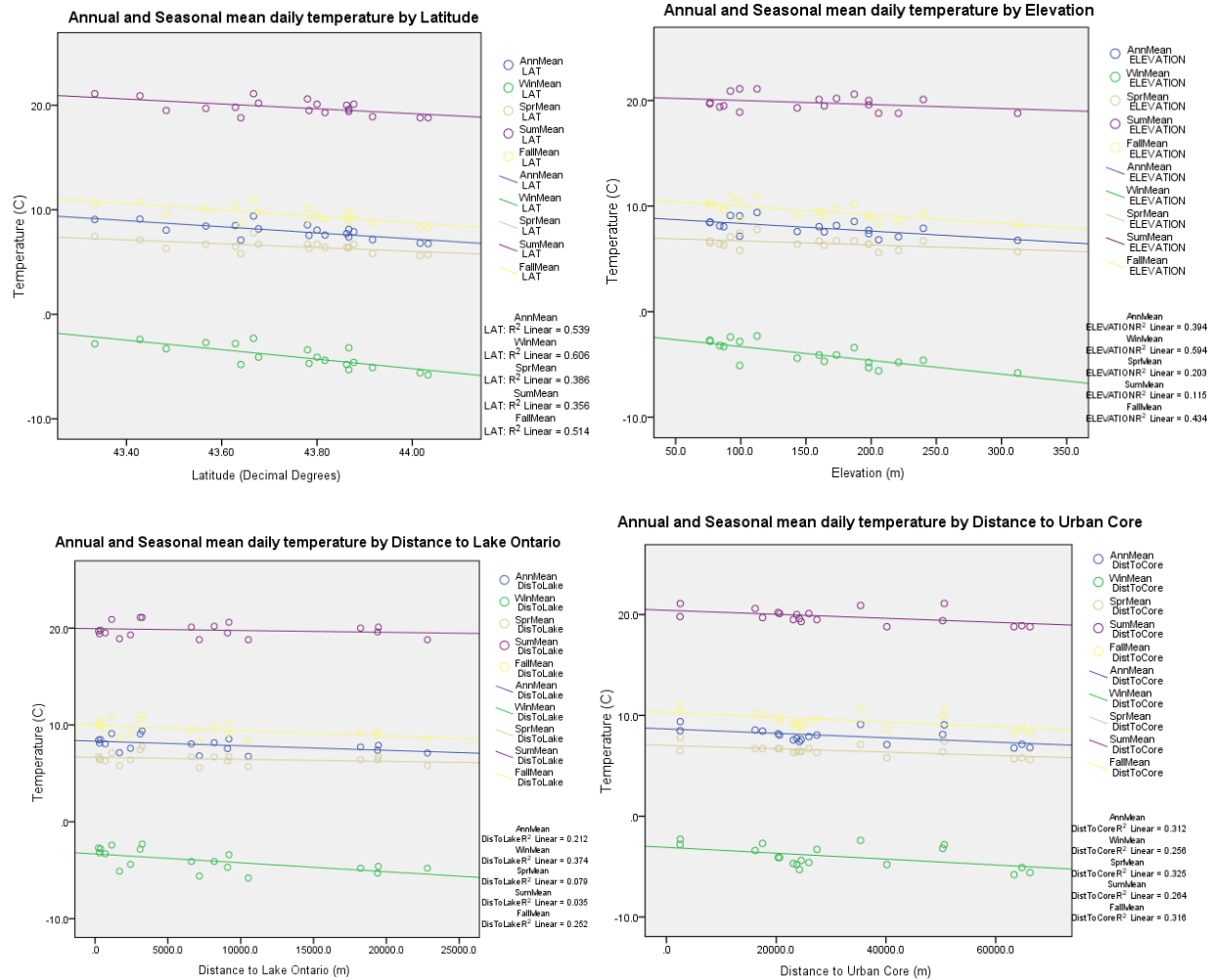


Figure A19: Correlation between climatic factors and temperature parameters

Table A12: The \bar{T} , T_{\min} , T_{\max} by surface cover fractions.

Mean-daily, Maximum-daily, Minimum-daily Air Temperatures and Diurnal Teemperature Range (DTR) by Surface Cover Fractions (500 m and 1000 m)											
Dependent Variable	Independent Variable	500 metres			1000 metres			500		1000	
		Slope (β) and SE	r^2	r	Slope (β) and SE	r^2	r	JB Stat	p-value	JB Stat	p-value
Mean-daily Temperature	ISF	2.64 (\pm 1.05)*	0.27	0.521*	3.19 (\pm 1.2)*	0.3	0.543*	1.07	0.58	1.55	0.46
	PSF	-2.24 (\pm 0.76)*	0.34	-0.581**	- 2.58 (\pm 0.82)	0.37	-0.606**	1.05	0.59	1.46	0.48
	BSF	4.54 (\pm 2.09)*	0.22	0.466*	5.61 (\pm 2.16)*	0.28	0.532*	1.34	0.51	1.04	0.59
	TCF	- 1.66 (\pm 0.96)	0.15	-0.387	- 2.23 (\pm 1.08)	0.2	-0.448	0.79	0.67	1.2	0.54
Maximum-daily Temperature	ISF	2.22 (\pm 0.93)*	0.25	0.500*	3.11 (\pm 0.99)**	0.37	0.607**	1.38	0.5	1.03	0.59
	PSF	- 1.82 (\pm 0.69)*	0.29	-0.540*	- 2.36 (\pm 0.69)**	0.41	-0.637**	1.9	0.39	1.24	0.53
	BSF	3.43 (\pm 1.89)	0.16	0.404	4.58 (\pm 1.94)*	0.25	0.497*	1.47	0.48	0.96	0.61
	TCF	- 1.30 (\pm 0.85)	0.12	-0.349	- 2.06 (\pm 0.93)*	0.22	-0.474*	0.41	0.81	0.77	0.68
Minimum-daily Temperature	ISF	4.07 (\pm 1.63)*	0.27	0.518*	4.21 (\pm 1.96)*	0.21	0.462*	0.21	0.9	0.13	0.93
	PSF	- 3.11 (\pm 1.24)	0.27	-0.521*	- 3.33 (\pm 1.38)*	0.25	-0.505*	0.99	0.61	0.24	0.88
	BSF	4.83 (\pm 3.47)	0.1	0.32	6.93 (\pm 3.59)	0.18	0.424	0.52	0.77	0.26	0.87
	TCF	- 2.67 (\pm 1.47)	0.16	-0.403	- 3.09 (\pm 1.72)	0.16	-0.4	0.33	0.84	0.24	0.88
Diurnal Temperature Range (DTR)	ISF	- 1.86 (\pm 1.72)	0.06	-0.254	- 1.10 (\pm 2.04)	0.02	-0.129	0.11	0.94	0.009	0.99
	PSF	1.29 (\pm 1.31)	0.05	0.233	0.96 (\pm 1.47)	0.02	0.157	0.14	0.92	0.03	0.98
	BSF	- 1.40 (\pm 3.39)	0.009	-0.1	- 2.36 (\pm 3.64)	0.02	-0.155	0.04	0.97	0.13	0.94
	TCF	1.37 (\pm 1.46)	0.05	0.222	1.03 (\pm 1.72)	0.02	0.143	0.07	0.96	1.13	0.57

References

- Apaydin, H., Sonmez, F. K., & Yildirim, Y. E. (2004, December). Spatial interpolation technique for climate data in the GAP region in Turkey. *Climate Research*, 28, 31-40.
- Allen, M. P. (1997). *Understanding Regression Analysis*. New York: Plenum Publishing.
- Arnfield, A. J. (2003). Two Decades of Urban Climate Research: A Review of Turbulance, Exchanges of Energy, Water and the Urban Heat Island. *International Journal of CLimatology*, 23, 1-26.
- Arnold, Jr., C. L., & Gibbons, C. J. (1996). Impervious Surface Coverage: The Emergence of a Key Environmental Indicator. *Journal of the American Planning Association*, 62(2), 243-258.
- Auer, A. H. (1976, April). Observations of an Industrial Cumulus. *Journal of Applied Meteorology*, 15, 406-413.
- Auer, A. H. (1978). Correlation of Land Use and Cover with Meteorological Anomalies. *Journal of Applied Meteorology*, 17, 636-643.
- Auer, A. H., & Dirks, R. A. (1974, February). Contributions to an urban meteorological studyL METROMEX. *Bulletin of the American Meteorological Society*, 55(2), 106-110.
- Bailey, T. C., & Gatrell, A. C. (1995). *Interactive Spatial Data Analysis*. Essex: Pearson Education Limited.
- Balchin, W. G., & Pye, N. (1947). A Micro-Climatological Investigation of Bath and the Surrounding Area. *Quarterly Journal of the Royal Meteorological Society*, 73(317-318), 297-323.
- Baldwin, D. J., Deslodes, J. R., & Band, L. E. (2000). Physical Geography of Ontario. In A. H. Perera, D. L. Euler, & I. D. Thompson, *Ecology of a Managed Terrestrial Landscape: Patterns and Processes of Forest Landscape in Ontario*. UBC Press.
- Balling, R. C., & Cervený, R. S. (1986). Long-Term Association between Wind Speed and the Urban Heat Island of Phoenix, Arizona. *Journal of Climate and Applied Meteorology*, 26, 712-716.
- Bechtel, B., Langkamp, T., Bohner, J., Daneke, C., Obenbrugge, J., & Schempp, S. (2012). Classification and Modelling of Urban Micro-Climates using Multisensoral and

- Multitemporal remote sensing data. *International Archives of Photogrammetry, Remote Sensing and Spatial Information Sciences*, (pp. 463-468). Melbourne.
- Blake, M. (2013). *The Potential for Perennial Vines to Mitigate Summer Warming of an Urban Microclimate*. Ryerson University, Department of Geography. Toronto: Ryerson University Digital Commons.
- Bornstein, R. D. (1968, August). Observations of the Urban Heat Island Effect in New York City. *Journal of Applied Meteorology*, 7, 575-582.
- Brown, D. M., McKay, G. A., & Chapman, L. J. (1980). *The Climate of Southern Ontario: Climatological studies number 5*. Government of Canada, Environment Canada: Atmospheric Environment Service. Hull: Canadian Government Publishing Centre.
- Buhler, O., Kristoffersen, P., & Larsen, S. U. (2007). Growth of Street Trees in Copenhagen with Amphasis on the Effect of Different Establishment Concepts. *Arboriculture & Urban Forestry*, 33(5), 330-337.
- Burrough, P. A. (1986). *Principles of Geogrphical Information System for Land Resource Assessment*. Toronto: Oxford University Press.
- Cadot, E., Rodwin, V. G., & Spira, A. (2007). In the Heat of the Summer. *Journal of Urban Health*, 84(4), 466-468.
- Chandler, T. (1964). City Growth and Urban Climates. *Weather*, 19, 170-171.
- Chandler, T. (1965). *The Climate of London*. London: Hutchinson of London.
- Chang, K.-t. (2010). *Introduction to Geographic Information Systems* (5th ed.). New York: McGraw-Hill.
- Changnon Jr., S. A. (1978, May). Urban Effects on Severe Local Storms at St. Louis. *Journal of Applied Meteorology*, 17, 578-586.
- Chen, D., & Chen, H. W. (2013). Using the Koppen classification to quantify climate variation and change: An example for 1901-2010. *Environmental Development*, 6, 69-79.
- Chuang, W.-C., Gober, P., Chow, W. T., & Golden, J. (2013). Sensitivity to heat: A comparative study of Phoenix, Arizona and Chicago, Illinois (2003 - 2006). *Urban Climate*, 5, 1-18.
- City of Toronto. (2009). *Forests and Land Cover - Parks and recreation Data Catalogue*. Retrieved December 3, 2013, from City of Toronto: <http://www1.toronto.ca/wps/portal/contentonly?vgnextoid=1a66e03bb8d1e310VgnVCM10000071d60f89RCRD>

- Coutts, A., Beringer, J., & Tapper, N. (2010). Changing Urban Climate and CO2 Emissions: Implications for the development of Policies for Sustainable Cities. *Urban Policy and Research*, 28(1), 27-47.
- Cui, L., & Shi, J. (2012). Urbanization and its Environmental effects in Shanghai, China. *Urban Climate*, 2, 1-15.
- Davidson, K., Guttman, N., Ropelewski, C., Canfield, N., Spackman, E., & Gullett, D. (1989). *Calculation of Monthly and Annual 30-Year Standard Normals*. Washington: World Meteorological Organization.
- DBx GEOMATICS Inc. (2012). *Directory of Federal Real Property (DFRP) - Mapping Framework Documentation*. Treasury Board of Canada Secretariat. Ottawa: Treasury Board of Canada Secretariat.
- De Schiller, S., & Evans, J. M. (1996a). Training Architects and Planners to design with urban microclimates. *Atmospheric Environment*, 30(3), 449-454.
- de Smith, M., Longley, P., & Goodchild, M. (2015). *Geospatial Analysis - A Comprehensive Guide*. Retrieved June 1, 2015, from Spatial Analysis Online: <http://www.spatialanalysisonline.com/HTML/index.html>
- Diaz, H. F., & Eischeid, J. K. (2007). Disappearing "apline tundra" Koppen climate type in the western United States. *Geophysical Research Letters*, 34(18), L18707.
- DMTI Spatial Inc. (2011). CanMap RouteLogistics-Land Use (LUR). *Generated by Lesley Gloin*.
- Dobesch, H., Dumolard, P., & Dyras, I. (2007). *Spatial Interpolation of Climate Data: The Use of GIS in Climatology and Meteorology*. London: ISTE Ltd.
- Eliasson, I., & Svensson, M. K. (2003). Spatial air temperature variation and urban land use - a statistical approach. *Meteorological Applications*, 10, 135-149.
- Ellefsen, R. (1991). Mapping and Measuring Buildings in the Canopy Boundary Layer in Ten U.S. Cities. *Energy and Buildings*, 15, 1025-1049.
- Emmanuel, R., & Johansson, E. (2006). Influence of urban morphology and sea breeze on hot humid microclimates: the case of Colombo, Sri Lanka. *Climate Research*, 30(3), 189-200.

- Environment Canada. (2013a). *Calculation of the 1981 to 2010 Climate Normals*. Downsview: Environment Canada. Retrieved December 23, 2013, from Climate Normals: http://climate.weather.gc.ca/climate_normals/index_e.html
- Environment Canada. (2013b). *Climate Normals Read Me File*. Downsview: Environment Canada. Retrieved December 23, 2013, from Climate Normals: http://climate.weather.gc.ca/climate_normals/index_e.html
- Environment Canada. (2014, February 19). *Corporate Profile- About EC - Environment Canada*. Retrieved April 1, 2015, from Environment Canada: <http://www.ec.gc.ca/default.asp?lang=En&n=BD3CE17D-1>
- Environmental Commissioner of Ontario. (2015). *Planning to Conserve: 2014 Annual Energy Conservation Report*. Toronto: Environmental Commissioner of Ontario.
- Environmental Systems Research Insititute. (2010). Geostatistical Analyst Tutorial. *ArcGIS* ESRI help.arcgis.com/.../pdf/geostatistical-analyst-tutorial.pdf
- Environmental Systems Research Insititute. (2014). ArcGIS Resrouce. *ArcGIS Desktop Help 10.2.2*. ESRI.
- Erell, E. (2008). The Application of Urban Climate Research in the Design of Cities. *Advances in Building Research*, 2(1), 95-121.
- Evans, J. M., & De Schiller, S. (1996). Application of microclimate studies in town planning: A new capitol city, an existing urban district and urban river ron development. *Atmospheric Environment*, 30(3), 361-361.
- Fenner, D., Meier, F., Scherer, D., & Polze, A. (2014). Spatial and temporal air temperature variability in Berlin, Germany, during the years 2001-2010. *Urban Climate*, 10, 308-331.
- Forkes, J. (2010). *Urban Heat Island Mitigation in Canadian Communities*. Toronto: Clean Air Partnership.
- Gaugh, W. A., & Rozanov, Y. (2001). Aspect of Toronto's climate: heat island and Lake Breeze. *Canadian Meteorological Oceanographic Society Bulletin*(29), 67-71.
- Geiger, R. (1965). *The Climate Near the Ground* (2nd ed.). Cambridge: Harvard University Press.
- Golden, J. S. (2004). The Built Environment Induced Urban Heat Island Effect in Rapidly Urbanizing Arid Regions - A Sustainable Urban Engineering complexity. *Environmental Sciences*, 1(4), 321-349.

- Gower, S., Mee, C., & Campbell, M. (2011). *Protecting Vulnerable People from Health Impacts of Extreme Heat*. Toronto: Toronto Public Health.
- Grimmond, C. S. (2007). Urbanization and global environmental change: local effects of urban warming. *The Geographical Journal*, 173(1), 83-88.
- Grimmond, C. S., Roth, M., Oke, T. R., Au, Y. C., Best, M., Betts, R. *et al.* (2010). Climate and More Sustainable Cities: Climate Information for Improved Planning and Management of Cities (Producers/Capabilities Perspective). *Procedia Environmental Sciences*, 1, 247-274.
- Hajat, S., O'Connor, M., & Kosatsky, T. (2010). Health effects of hot weather: from awareness of risk factors to effective health protection. *Lancet*, 375, 856-863.
- Harlan, S. L., Brazel, A. J., Prashad, L., Stefanov, W. L., & Larsen, L. (2006). Neighbourhood microclimates and vulnerability to heat stress. *Social Science & Medicine*, 63, 2847-2863.
- Hengl, T., Heuvelink, G. B., & Rossiter, D. G. (2007). About regression-kriging: From equations to case studies. *Computers & Geosciences*, 33, 1301-1315.
- Hidore, J. J. (1966, February). An Introduction to the Classification of Climates. *Journal of Geography*, 65(2), pp. 52-57.
- Holdaway, M. R. (1996). Spatial modeling and interpolation of monthly temperature using kriging. *Climate Research*, 6, 215-225.
- Howard, L. (1833). *The Climate of London*. London.
- Imhoff, M. L., Zhang, P., Wolfe, R. E., & Bounous, L. (2010). Remote sensing of the urban heat island effect across biomes in the continental USA. *Remote Sensing of Environment*, 114, 504-513.
- Jarque, C.M., Bera, A.K. (1987). A Test for Normality of Observations and Regression Residuals. *International Statistical Review*, 55, 2, 163-172.
- Johnston, K., Ver Hoef, Jay. M., Krivoruchko, K., Lucas, Neil. (2003). ArcGIS 9: Using ArcGIS Geostatistical Analyst. Environmental Systems Research Institute (ESRI).
- Kalnay, E., & Cai, M. (2003). Impact of Urbanization and Land-use change on Climate. *Nature*, 423, 528-531.
- Karl, T. R., Diaz, H. F., & Kukla, G. (1988, November). Urbanization: Its Detection and Effect in the United States Climate Record. *Journal of Climate*, 1, 1099-1123.

- Kelly, H. F., & Warren, A. (2014). *Emerging Trends in Real Estate 2015*. Washington: Urban Land Institute.
- Kershaw, S. E., & Millward, A. A. (2012). A spatio-temporal index for heat vulnerability. *Environmental Monitoring and Assessment*, 184, 7329-7342.
- Ko, Y. (2013). Urban Form and Residential Energy Use: A Review of Design Principles and Research Findings. *Journal of Planning Literature*, 28(4), 327-351.
- Koenker, R. (2014). *Roger Koenker Econometrics at Illinois*. Retrieved June 1, 2015, from Gaps in the Literature: <http://www.econ.uiuc.edu/~roger/gaps.html>
- Konopacki, S., & Akbari, H. (2001). *Energy Impacts of Heat Island Reductions in the Greater Toronto Area, Canada*. Berkeley: Toronto Atmospheric Fund.
- Kopec, R. J. (1970). Further observations of the urban heat island in a small city. *Bulletin American Meteorological Society*, 51(7), 602-606.
- Kratzer, A. (1956). *The Climate of Cities (Das Stadtklima)*. (A. M. Society, Trans.) Boston: American Meteorological Society.
- Landsberg, H. E. (1970, December). Man-Made Climatic Changes. *Science*, 170(3964), 1265-1274.
- Landsberg, H. E. (1979). Atmospheric Changes in a Growing Community (The Columbia, Maryland Experience). *Urban Ecology*, 4, 53-81.
- Lee, S., & French, S. P. (2009). Regional impervious surface estimation: an urban heat island application. *Journal of Environmental Planning and Management*, 52(4), 47-496.
- Lelovics, E., Gal, T., & Unger, J. (2013). Mapping Local Climate Zones with Vector-based GIS Methods. *Air and Water Components of the Environment* (pp. 423-430). Cluj-Napoca: Air and Water Conference.
- Li, J., & Heap, A. D. (2014). Spatial interpolation methods applied in the environmental sciences: A review. *Environmental Modelling & Software*, 53, 173-189.
- Lloyd, C. D., & Atkinson, P. M. (2001). Assessing uncertainty in estimates with ordinary and indicator kriging. *Computers & Geosciences*, 27, 929-937.
- Longley, P. A., Goodchild, M. F., Maguire, D. J., & Rhind, D. W. (2011). *Geographic Information Systems & Science* (3rd ed.). Danvers: John Wiley and Sons, Inc.

- Loveland, T. R., & Mahmood, R. (2014, October). A Design for a Sustained Assessment of Climate Forcing and Feedbacks Related to Land Use and Land Cover Change. *Bulletin of the American Meteorological Society*, 95(10), 1563-1572.
- Lowry, W. P. (1974, February). Project METROMEX: Its history, status, and future. *Bulletin of the American Meteorological Society*, 55(2), 87-89.
- Lowry, W. P. (1977). Empirical Estimation of Urban Effects on Climate: A Problem Analysis. *Journal of Applied Meteorology*, 16, 129-135.
- Lowry, W. P. (1998). Urban effects on precipitation amount. *Progress in Physical Geography*, 22(4), 477-520.
- Maloley, M. J. (2010). *Thermal Remote Sensing of Urban Heat Island Effects: Greater Toronto Area*. Natural Resources Canada. Natural Resources Canada.
- Mavrogianni, A., Davies, M., Batty, M., Belcher, S. E., Bohnenstengel, S. I., Carruthers, D. *et al.* (2011). The comfort, energy and health implications of London's urban heat island. *Building Services Engineering Research & Technology*, 32(1), 35-52.
- Mayer, H. (1999). Air pollution in cities. *Atmospheric Environment*, 33(24), 4029-4037.
- McCarthy, M. P., Best, M. J., & Betts, R. A. (2010). Climate change in cities due to global warming and urban effects. *Geophysical Research Letters*, 37, L09705.
- McKinney, M. L. (2008). Effect of urbanization on species richness: A review of plants and animals. *Urban Ecosystems*, 11, 161-176.
- McPherson, G., Simpson, J. R., Peper, P. J., Maco, S. E., & Xiao, Q. (2005). Municipal Forest Benefits and Cost in Five US Cities. *Journal of Forestry*, 108(8), 411-416.
- Meehl, G. A., & Tebaldi, C. (2004). More Intense, More Frequent, and Longer Lasting Heat Waves in the 21st Century. *Science*, 305(5686), 994-997.
- Mendenhall, W., Beaver, R.J., Beaver, B.M., Ahmed, S.E. (2011). Introduction to Probability and Statistics. Nelson Education.
- Meng, Q., Liu, Z., & Borders, B. E. (2013). Assessment of regression kriging for spatial interpolation - comparisons of seven GIS interpolation methods. *Cartography and Geographic Information Science*, 40(1), 28-39.
- Millward, A. A., & Sabir, S. (2011). Benefits of a forested urban park: What is the value of Allan Gardens to the city of Toronto, Canada? *Landscape and Urban Planning*, 100, 177-188.

- Middleton, W. K., & Millar, F. G. (1936, September). Temperature Profiles in Toronto. *The Journal of the Royal Astronomical Society of Canada*, 30(7), 265-272.
- Mizuno, M., Nakamura, Y., Murakami, H., & Yamamoto, S. (1991). Effects of Land Use on Urban Horizontal Atmospheric Temperature Distributions. *Energy and Buildings*, 15, 165-176.
- Mohsin, T. (2009). *Greater Toronto Area Urban Heat Island: Analysis of Temperature and Extremes*. PhD Thesis, University of Toronto, Graduate Department of Geography, Toronto.
- Mohsin, T., & Gough, W. A. (2010). Trend Analysis of long-term temperature times series in the Greater Toronto Area (GTA). *Theoretical and Applied Climatology*, 101, 311-327.
- Mohsin, T., & Gough, W. A. (2012). Characterization and estimation of urban heat island at Toronto: impact of the choice of rural sites. *Theoretical and Applied Climatology*, 108, 105-117.
- Mullaney, J., Lucke, T., & Trueman, S. J. (2015). The effect of permeable pavements with an underlying base layer on the growth and nutrients status of urban trees. *Urban Forestry & Urban Greening*, 14, 19-29.
- Munn, R. E., Hirt, M. S., & Findlay, B. F. (1969). A Climatological Study of the Urban Temperature Anomaly in the Lakeshore Environment at Toronto. *Journal of Applied Meteorology*, 8, 411-422.
- Munn, R. E., Thomas, M., & Yap, D. (1999). Climate. In B. I. Roots, D. A. Chant, & C. E. Heidenreich, *Special Places: The Changing Ecosystem of the Toronto Region* (pp. 33-49). Toronto: UBC Press.
- Myrup, L. O. (1969). A Numerical Model of the Urban Heat Island. *Journal of Applied Meteorology*, 8, 908-918.
- Nakamura, R., Mahrt, L. (2005). Air Temperature Errors in Naturally Ventilated Radiation Shield. *Journal of Atmospheric and Ocean Technology*, 22, 1046 - 1058.
- Naughton, M. P., Henderson, A., Mirabelli, M. C., Kaiser, R., Wilhelm, J. L., Kieszak, S. M. *et al.* (2002). Heat-Related Mortality During a 1999 Heat Wave in Chicago. *American Journal of Preventative Medicine*, 22(4), 221-227.
- Oke. (1973). City Size and the Urban Heat Island. *Atmospheric Environment*, 7, 769-779.

- Oke. (1982). The energetic basis of the urban heat island. *Quarterly Journal of the Royal Meteorological Society*, 108(455), 1-24.
- Oke. (1988). The urban energy balance. *Progress in Physical Geography*, 12, 471-508.
- Oke. (1992). *Boundary Layer Climates* (2nd ed.). New York: Routledge.
- Oke. (2004). *Siting and Exposure of Meteorological Instruments at Urban Sites*. Banff: Kluwer.
- Oke. (2006). *Initial Guidance to Obtain Representative Meteorological Observations at Urban Sites*. World Meteorological Organization.
- Oke. (2006). Towards better scientific communication in urban climate. *Theoretical and Applied Climatology*, 84, 179-190.
- Oke, T. R., & Maxwell, G. B. (1975). Urban heat Island Dynamics in Montreal and Vancouver. *Atmospheric Environment*, 9, 191-200.
- Oliver, J. E. (1973). *Climate and Man's Environment: An Introduction to Applied Climatology*. New York: Wiley.
- Organization for Economic Co-operation and Development. (2014). *Cities and Climate Change: National governments enabling local action*. Paris: OECD.
- Owen, T. W., Carlson, T. N., & Gilles, R. R. (1998). An assessment of satellite remotely-sensed land cover parameters in quantitatively describing the climatic effect of urbanization. *International Journal of Remote Sensing*, 19(9), 1663-1681.
- Oxizidis, S., Dudek, A. V., & Aquilina, N. (2007). Typical Weather Years and the Effect of Urban Microclimate on the Energy Behaviour of Buildings and HVAC Systems. *Advances in Building Energy Research*, 1, 89-103.
- Pearson, D., & Burton, I. (2009). *Adapting to Climate Change in Ontario: Towards the Design and Implementation of a Strategy and Action Plan*. Toronto: The Queen's Printer for Ontario.
- Penney, J. (2008). *Climate Change Adaptation in the City of Toronto: Lessons for Great Lake Communities*. Toronto: Clean Air Partnership.
- Perez-Lombard, L., Ortiz, J., & Pout, C. (2008). A review on buildings energy consumption information. *Energy and Buildings*, 40, 394-398.
- Pond, D. (2009, December). Ontario's Greenbelt: Growth Management, Farmland Protection and Regime Change in Southern Ontario. *Canadian Public Policy*, 35(4), 413-432.

- Rinner, C., & Hussain, M. (2011). Toronto's Urban Heat Island - Exploring the Relationship between Land Use and Surface Temperature. *Remote Sensing*, 3, 1251-1265.
- Roth, M. (2013). Urban Heat Island. In H. J. Fernando (Ed.), *Handbook of Enviromental Fluid Dynamics, Volume Two: Systems, Pollution, Modeling, Measurements* (Vol. Volume Two, pp. 143-159). Boca Raton: CRC Press Taylor & Francis Group.
- Sakakibara, Y., & Matsui, E. (2005). Relation between heat island intensity and city size indices/urban canopy characteristics in settlements of Nagano basin, Japan. *Japanese Progress in Climatology*, 65-77.
- Samanta, S., Pal, D. K., Lohar, D., & Pal, B. (2012). Interpolation of climate variables and temperature modeling. *Theoretical and Applied Climatology*, 107, 35-45.
- Sanderson, M. (2004). *Weather and Climate in southern Ontario* (Vol. Publication Series Number 58). (C. Mitchell, Ed.) Waterloo: Department of Geography Publication Series, University of Waterloo.
- Sani, S. (1972). Some aspects of urban micro-climate in Kuala Lumpur West Malaysia. *Akademika*, 85-94.
- Schmid, H. P., Cleugh, H. A., Grimmond, C. B., & Oke, T. R. (1991). Spatial Variability of Energy Fluxes in Suburban Terrain. *Boundary Layer Meteorology*, 54, 249-276.
- Seilheimer, T. S., Wei, A., Chow-Fraser, P., & Eyles, N. (2007). Impact of urbanization on the water quality, fish habitat, and fish community of a Lake Ontario marsh, Frenchman's Bay. *Urban Ecosystem*, 10, 299-319.
- Shashua-Bar, L., & Hoffman, M. E. (2000). Vegetation as a climatic component in the design of an urban street. An empirical model for predicting the cooling effect of urban green areas with trees. *Energy and Buildings*, 31, 221-235.
- Smith, R. (1976). *Climate: Central Waterfront Planning Committee information base*. Toronto: Central Waterfront Planning and Technical Committee.
- Smoyer, K. E., Rainham, D. G., & Hewko, J. N. (2000). Heat-stress-related mortality in five cities in Southern Ontario: 1980-1996. *International Journal of Biometeorology*, 44, 190-197.
- Sofer, S., & Potchter, O. (2006). The urban heat island of a city in an arid zone: the case of Eilat, Israel. *Theoretical and Applied Climatology*, 85, 81-88.

- Soloman, S., Qin, D., Manning, M., Marquis, M., Averyt, K., Tignor, M. M. *et al.* (2007). *Climate Change 2007: The Physical Science Basis. Contribution of Working Group I to the Fourth Assessment Report of the Intergovernmental Panel on Climate Change.* Intergovernmental Panel on Climate Change. New York: Cambridge University Press.
- Souch, C., & Grimmond, S. (2006). Applied Climatology: urban climates. *Progress in Physical Geography*, 30(2), 270-279.
- Stathopoulou, E., Mihalakakou, G., Santamouris, M., & Bagiorgas, H. S. (2008). On the impact of temperature on tropospheric zone concentration levels in urban environments. *Journal of Earth System Science*, 117(3), 227-236.
- Stewart, I. D. (2011a). A systematic review and scientific critique of methodology in modern urban heat island literature. *International Journal of Climatology*, 31, 200-217.
- Stewart, I. D. (2011b). *Redefining the Urban Heat Island*. PhD Thesis, University of British Columbia, Department of Geography, Vancouver.
- Stewart, I. D., & Oke, T. R. (2012). Local Climate Zones for Urban Temperature Studies. *Bulletin of the American Meteorological Society*, 1879-1900.
- Stewart, I. D., Oke, T. R., & Krayenhoff, E. S. (2013). Evaluation of the 'local climate zone' scheme using temperature observations and model simulations. *International Journal of Climatology*.
- Stupart, R. F. (1912). Meteorology In Canada. *The Journal of the Royal Astronomical Society of Canada*, VI(2), 74-87.
- Svensson, M. K., & Eliasson, I. (2002). Diurnal air temperatures in build-up areas in relation to urban planning. *Landscape and Urban Planning*, 61, 37-54.
- Szymanowski, M., Kryza, M., & Spallek, W. (2013). Regression-based air temperature spatial prediction models: an example from Poland. *Meteorologische Zeitschrift*, 22(5), 577-585.
- Tam, B. Y., Gough, W. A., & Mohsin, T. (2015). The impact of urbanization and the urban heat island effect on day to day temperature variation. *Urban Climate*, 12, 1-10.
- Taylor, F. W. (2005). *Elementary Climate Physics*. Toronto: Oxford University Press.
- Thiessen, A. D. (1940). The Founding of the Toronto Magnetic Observatory and the Canadian Meteorological Service. *The Journal of the Royal Astronomical Society of Canada*, 308-348.

- Thomas, M. K. (1970). *A Century of Canadian Meteorology*. Retrieved November 17, 2014, from <http://www.cmos.ca/site/404?url=http://www.cmos.ca/bibliography.html>
- Thomas, M. K. (1971). *History of Canadian Meteorology and Oceanography*. Retrieved November 14, 2014, from Canadian Meteorological and Oceanographic Society: http://cmosarchives.ca/History/CenturyMeteorology1_1971.pdf
- Thornthwaite, C. W. (1933, July). The Climates of the Earth. *Geographical Review*, 23(3), 433-440.
- Thorsson, S., Rocklov, J., Konarska, J., Lindberg, F., Holmer, B., Dousset, B. *et al.* (2014). Mean radiant temperature - A predictor of heat related mortality. *Urban Climate*, 10, 332-345.
- Tveito, O. E., Wegehenkel, M., van der Wel, F., & Dobesch, H. (2006). *The use of Geographics Information Systems in Climatology and Meteorology: Final Report Cost Action 719*. European Cooperation in Science and Technology, Earth Systems Science and Environmental Management. Vienna: COST.
- Unger, J., Lelovics, E., & Gal, T. (2014). Local Climate Zone Mapping using GIS methods in Szeged. *Hungarian Geographical Bulletin*, 63(1), 29-41.
- United Nations Environment Programme. (2012). *Global Environment Outlook (GEO-5)*. United Nations. United Nations Environment Programme.
- Vlahov, D., & Galea, S. (2002). Urbanization, Urbanicity, and Health. *Journal of Urban Health*, 79(4), S1-S12.
- Voogt, J. A., & Oke, T. R. (2003). Thermal remote sensing of urban climates. *Remote Sensing of Environment*, 86(3), 370-384
- Voogt, J. A., & Oke, T. R. (2007). How Researchers Measure Urban Heat Islands. Presentation on the basics of urban heat island and how they are measured and modeled. US EPA, State and Local Branch, Climate Protection Partnership Division. 1-34.
- Walsh, C. J., Roy, A. H., Feminella, J. W., Cottingham, P. D., Groffman, P. M., & Morgan, R. P. (2005). The urban stream syndrome: current knowledge and the search for a cure. *Journal of the North American Benthological Society*, 24(3), 706-723.
- Weatherburn, T. A. (2009). The Urban Heat Island in Toronto: Interpreting Mesoclimates Through Detrended Kriging and Multiple Linear Regression. *MRP*.

- Willmott, C. J. (1982, November). Some Comments on the Evaluation of Model Performance. *Bulletin American Meteorological Society*, 63(11), 1309-1313.
- Yoshino. (1975). *Climate in a Small Area: An Introduction to Local Meteorology*. Tokyo: University of Toyko Press.
- Yoshino, M. (1991). Development of Urban Climatology and Problems Today. *Energy and Buildings*, 15-16, 1-10.
- Yuan, F., & Bauer, M. (2007). Comparison of impervious surface area and normalized difference vegetation index as indicators of surface urban heat island effects in Landsat imagery. *Remote Sensing of Environment*, 106(3), 375-386.
- Zimmerman, D., Pavlik, C., Ruggles, A., & Armstrong, M. P. (1999). An Experimental Comparison of Ordinary and Universal Kriging and Inverse Distance Weighting. *Mathematical Geology*, 31(4), 375-390.